Distributed Coupling and Cold Copper Accelerator Technology and Applications

Emilio Nanni

ESRF Seminar

1/6/2025

Acknowledgements

arXiv > physics > arXiv:2503.20829

Physics > Accelerator Physics

[Submitted on 26 Mar 2025 (v1), last revised 6 Apr 2025 (this version, v2)]

ESPPU INPUT: C^3 within the "Linear Collider Vision"

Matthew B. Andorf, Mei Bai, Pushpalatha Bhat, Valery Borzenets, Martin Breidenbach, Sridhara Dasu, Ankur Dhar, Tristan du Pree, Lindsey Gray, Spencer Gessner, Ryan Herbst, Andrew Haase, Erik Jongewaard, Dongsung Kim, Anoop Nagesh Koushik, Anatoly K. Krasnykh, Zenghai Li, Chao Liu, Jared Maxson, Julian Merrick, Sophia L. Morton, Emilio A. Nanni, Alireza Nassiri, Cho-Kuen Ng, Dimitrios Ntounis, Mohamed A. K. Othman, Marco Oriunno, Dennis Palmer, Michael E. Peskin, Caterina Vernieri, Muhammad Shumail, Evgenya Simakov, Emma Snively, Ann Sy, Harry van der Graaf, Brandon Weatherford, Haoran Xu

The Linear Collider Vision calls for a Linear Collider Facility with a physics reach from a Higgs Factory to the TeV-scale with e^+e^- collisions. One of the technologies under consideration for the accelerator is a cold-copper distributed-coupling linac capable of achieving high gradient. This technology is being pursued by the C^3 collaboration to understand its applicability to future colliders and broader scientific applications. In this input we share the baseline parameters for a C^3 Higgs-factory and the energy reach of up to 3 TeV in the 33 km tunnel foreseen under the Linear Collider Vision. Recent results, near-term plans and future R\&D needs are highlighted.

JINST — PUBLISHED BY IOP PUBLISHING FOR SISSA MEDIALAB

RECEIVED: June 2, 2023
ACCEPTED: August 23, 2023
PUBLISHED: September 28, 2023

SNOWMASS'2021 ACCELERATOR FRONTIER

Status and future plans for C^3 R&D

Perspective | Open Access

Sustainability Strategy for the Cool Copper Collider

Martin Breidenbach, Brendon Bullard, Emilio Alessandro Nanni, Dimitrios Ntounis, and Caterina Vernieri
PRX Energy **2**, 047001 – Published 26 October 2023

Community Events

https://web.slac.stanford.edu/c3/events

https://sites.google.com/view/ec4c3

More Details Here (Follow, Collaborate):
https://web.slac.stanford.edu/c3/

Acknowledgments

SLAC
Brandon Weatherford
Sami Tantawi
Zenghai Li
Chris Nantista
Emma Snively
Mohamed Othman
Muhammad Shumail
Annika Gabriel
Dennis Palmer
Valery Dolgashev
Mamdouh Nasr
Ankur Dhar
Caterina Vernieri
Jeffrey Neilson
Xueying Lu
Marco Oriunno
Julian Merrick
Gordon Bowden
Ann Sy
Andy Haase
Gregory Le Sage
Mitchell Schneider
Matt Boyce
Valery Borzenets
Galen Aymar
Martin Breidenbach

Stanford University
Billy W. Loo Jr.

Indiana University
Peter Maxim

Loma Linda University
Reinhard Schulte

UCSF
Bruce Faddegon
Jose Mendez

Varian
Eric Abel
Matthew Murphy

General Atomics
B. Coriton
Leo D. Holland

University of Illinois at Chicago
Andreas Schroeder

L3Harris Applied Technologies
M. Boyle
P. Laurence

University of Chicago
Young-Kee Kim
Sergei Nagaitsev

Special thanks to the members of the COLD project

Particle Accelerators Drive Scientific Discovery

Coherent X-rays from LCLS (2009)

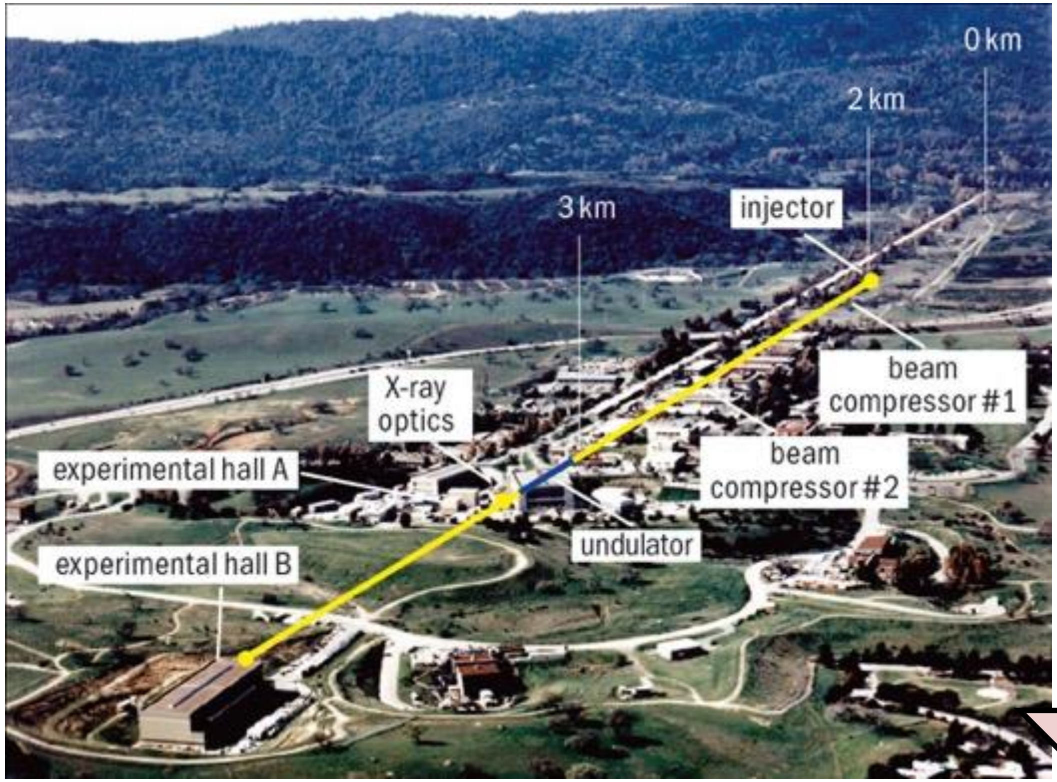

Ultrafast Electron Diffraction (2015)

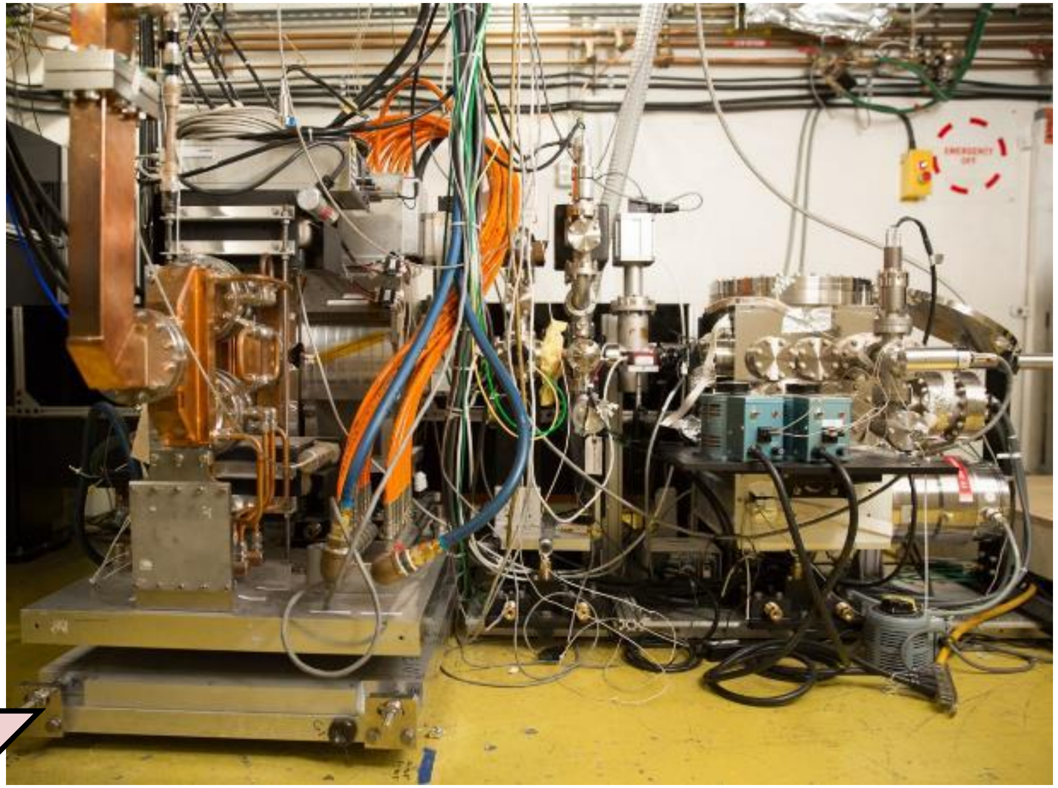

What new science is enabled by the next generation of accelerator technology?

Integrated Vision for RF Accelerator R&D

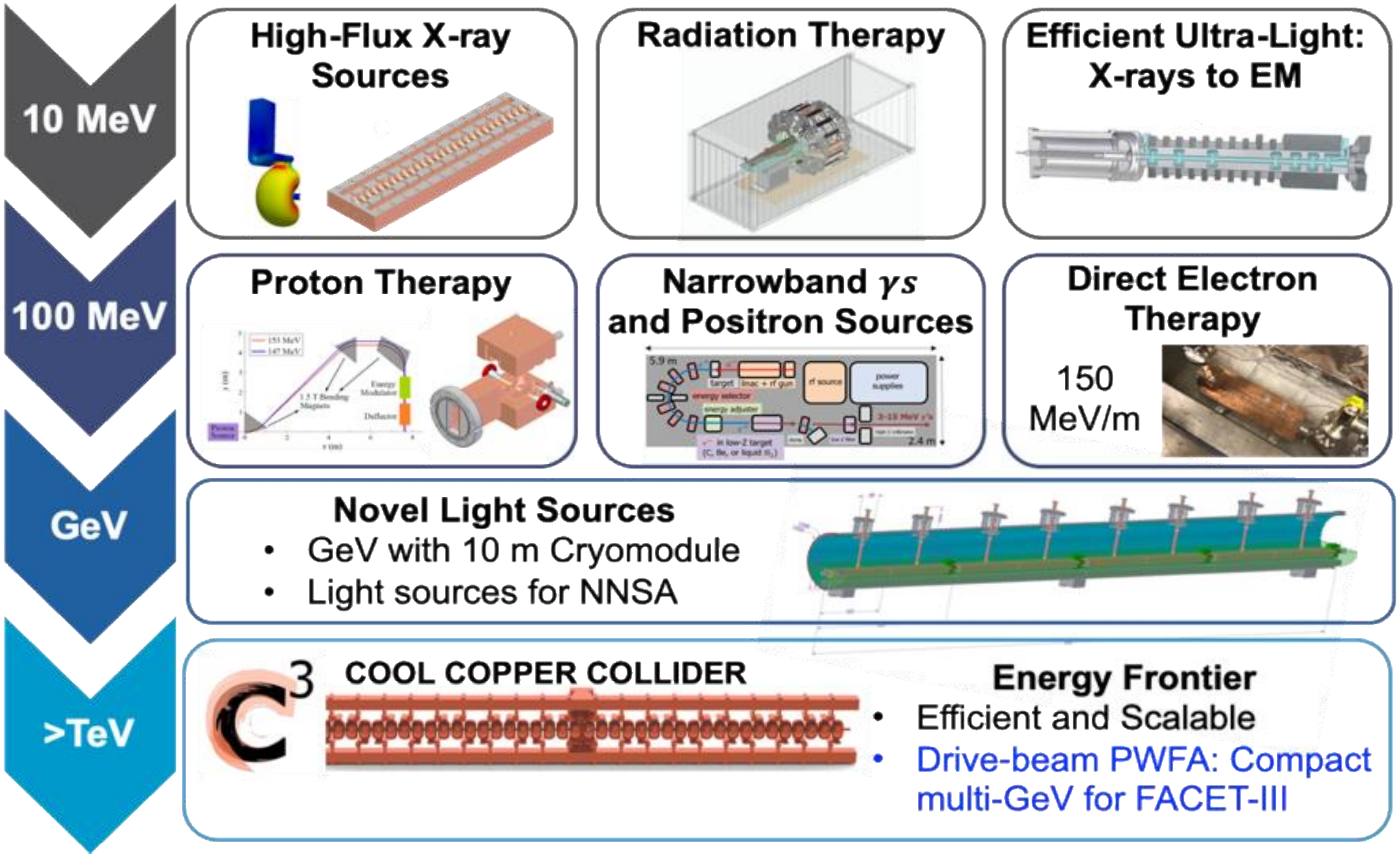

- Technology development that transitions smoothly in energy
- Broad base of scientific and non-scientific applications

Development of Distributed Coupling and Cold-Copper as a Platform for Accelerators

What Defines the Optimal Accelerator Cavity Geometry?

Performance depends on beam aperture which is driven by the bunch charge
Charge particle radiate wakefields that set the limit

Advanced Optimization Tools

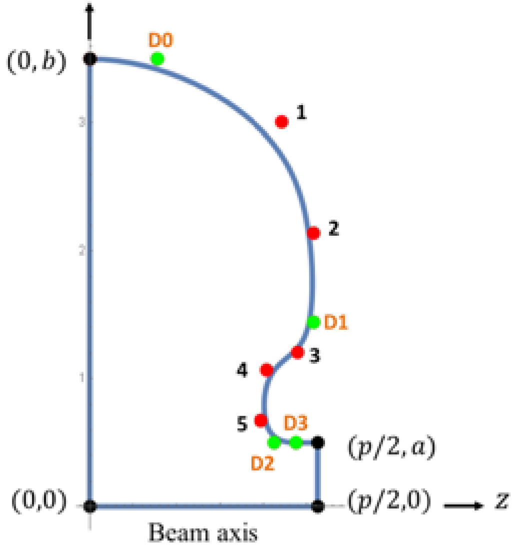

Variable control points for splines define the cavity shape.

M. Nasr et al., IPAC'18

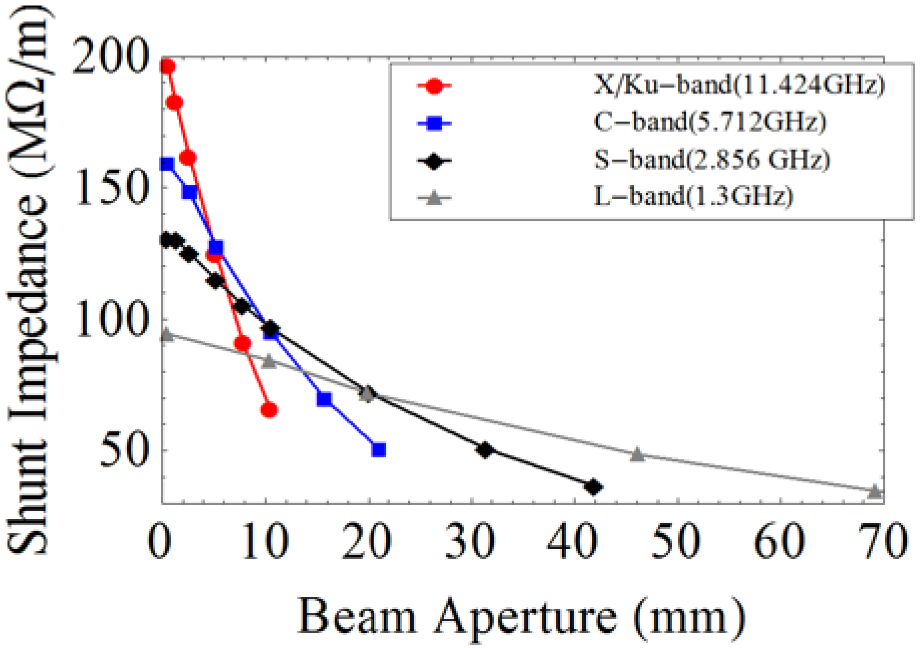

20% reduction in surface electric field for same shunt impedance

New Scaling Laws Determine the Best Performance for Accelerating Structures

Optimized Cavity Geometries for Standing Wave Linac

Small aperture for reduced phase achieves exceptional Rs
Cryogenic operation: Increased Rs, reduced pulse heating

Frequency	a/λ	Phase Adv.	Rs (MΩ/m) 300K	Rs (MΩ/m) – 77K
C-band (5.712 GHz)	0.05	π	121	272
C-band (5.712 GHz)	0.05	2π/3	133	300
X-band (11.424 GHz)	0.1	π	133	300

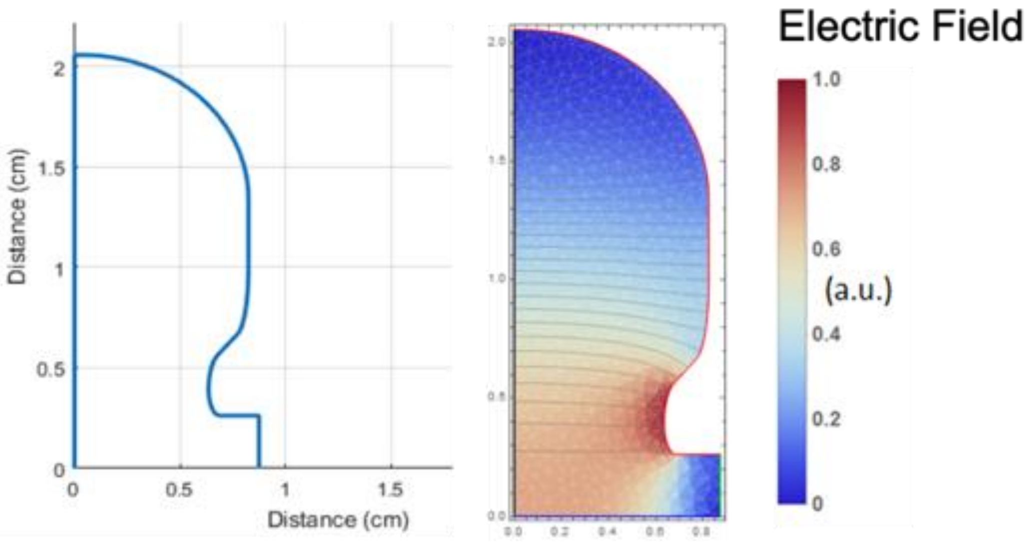

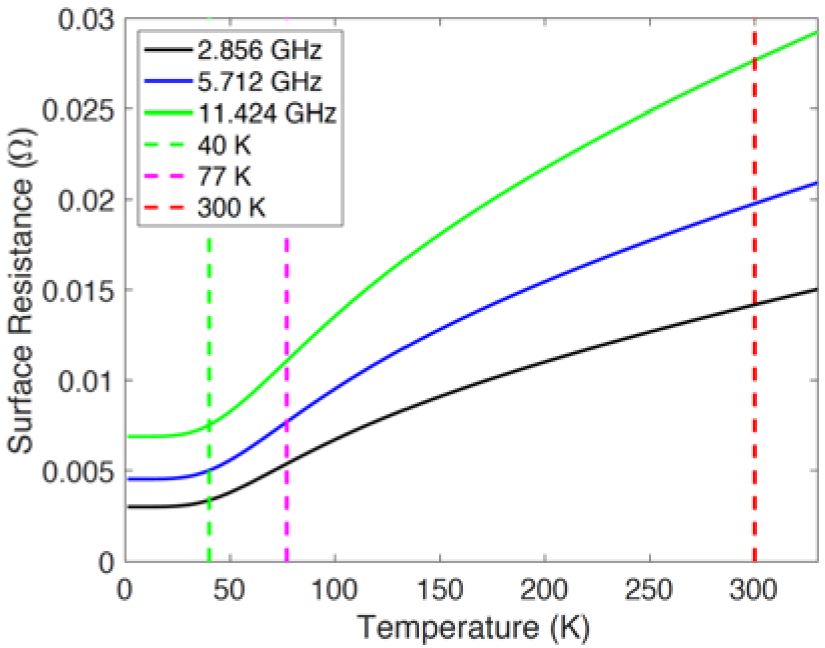

Breakthrough in the Performance of RF Accelerators

RF power coupled to each cell – no on-axis coupling

Full system design requires modern virtual prototyping

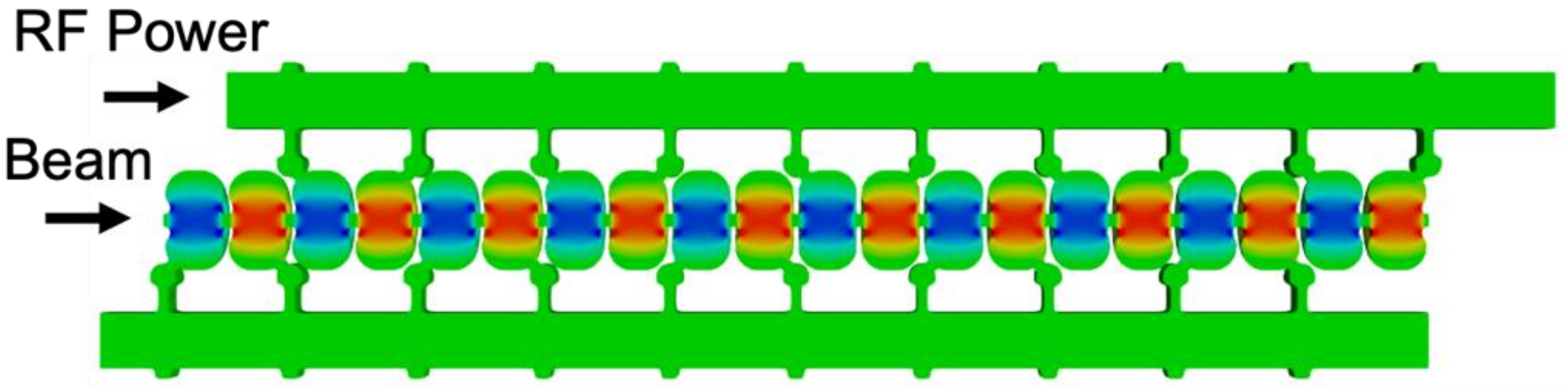

Electric field magnitude produced when RF manifold feeds alternating cells equally

Optimization of cell for efficiency (shunt impedance) $R_s = G^2/P$ [MΩ/m]

- Control peak surface electric and magnetic fields

Key to high gradient operation

Cryo-Copper: Enabling Efficient High-Gradient Operation

Cryogenic temperature elevates performance in gradient

- Material strength is key factor
- Impact of high fields for a high brightness injector may eliminate need for one damping ring

Operation at 77 K with liquid nitrogen is simple and practical

- Large-scale production, large heat capacity, simple handling
- Small impact on electrical efficiency

$$\eta_{cp} = LN\ Cryoplant$$
$$\eta_{cs} = Cryogenic\ Structure$$
$$\eta_k = RF\ Source$$

$$\frac{\eta_{cs}}{\eta_k}\eta_{cp} \approx \frac{2.5}{0.5}[0.15] \approx 0.75$$

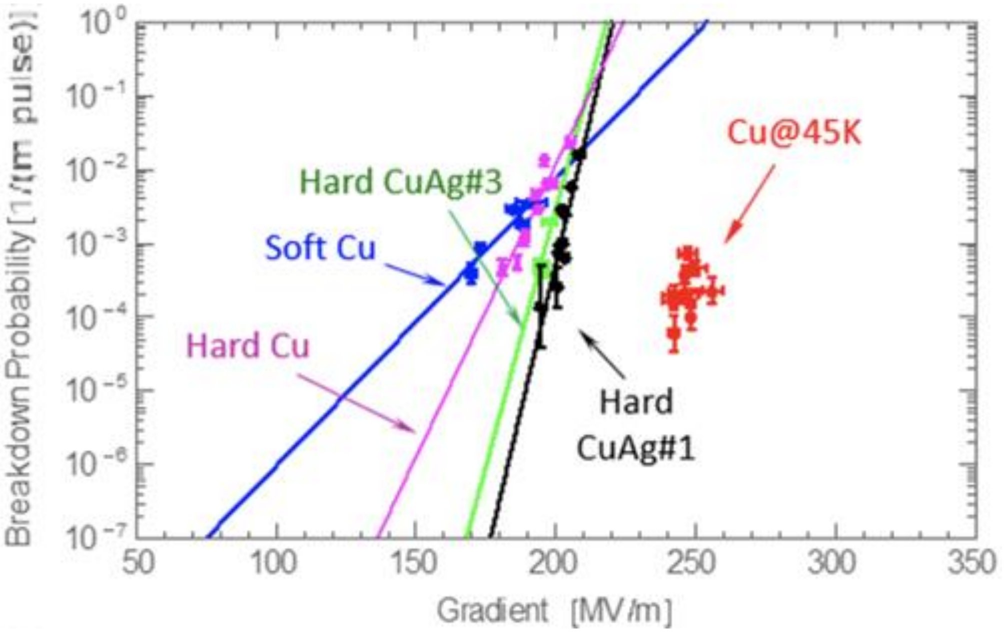

Cahill, A. D., et al. *PRAB* 21.10 (2018): 102002.

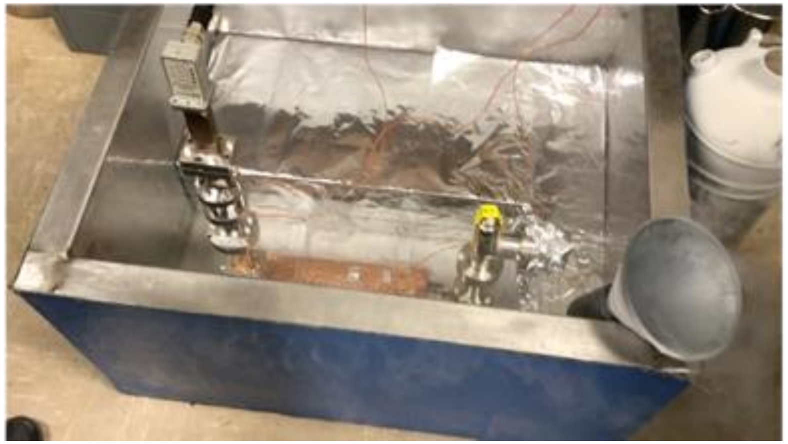

RF Power Requirements

70 MeV/m 250 ns Flattop (extendible to >100 ns)
~1 microsecond rf pulse, ~30 MW/m
Conservative 2.3X enhancement from cryo

- No pulse compression

Ramp power to reduce reflected power
Flip phase at output to reduce thermals

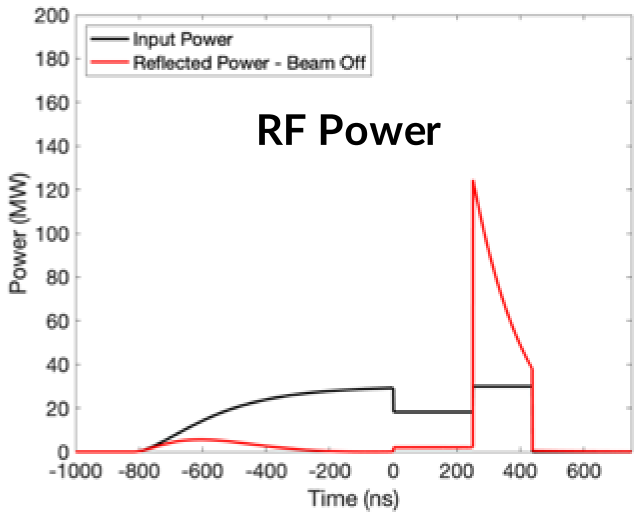

One 65 MW klystron every two meters -> Matches CLIC-k rf module power

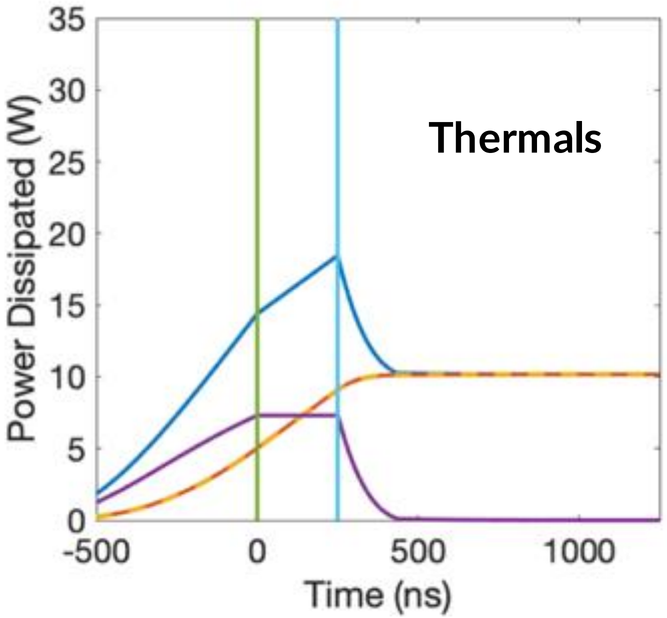

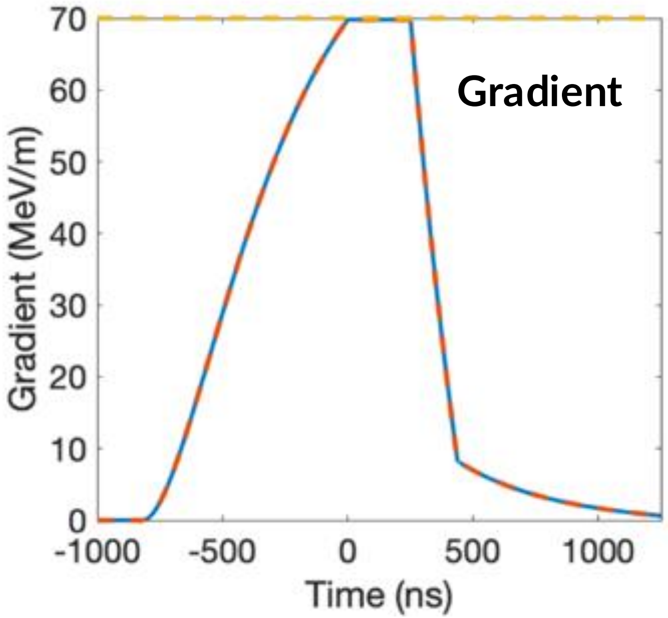

High Gradient Performance of D.C. and Cold-Copper

C^3 is based on a new rf technology
- Dramatically improving efficiency and breakdown rate

Distributed power to each cavity from a common RF manifold

Operation at cryogenic temperatures (LN_2 ~80 K)

Robust operations at high gradient: 120 MeV/m

Scalable to multi-TeV operation

C^3 Prototype One Meter Structure

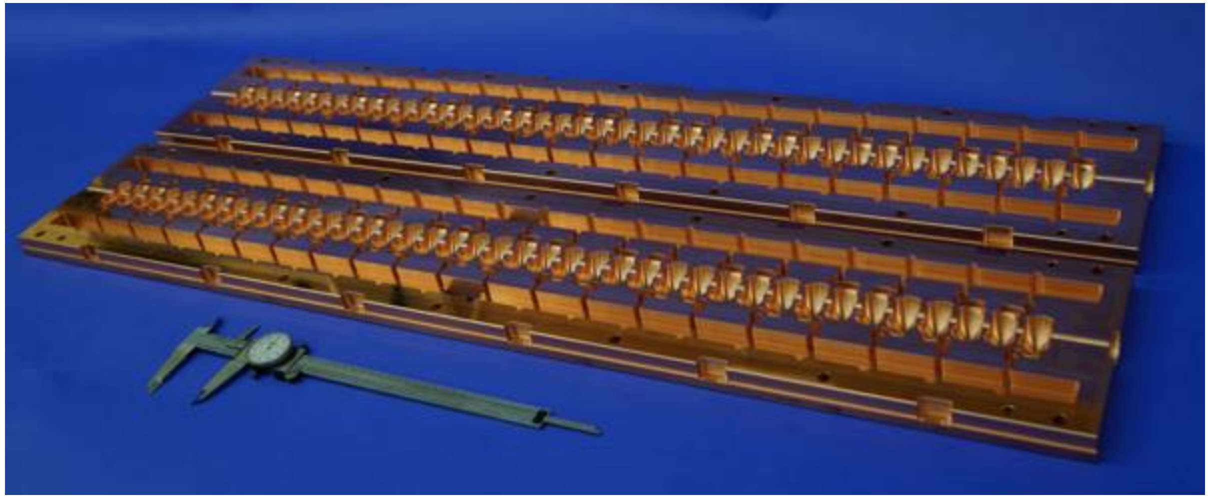

High Gradient Operation at 150 MV/m

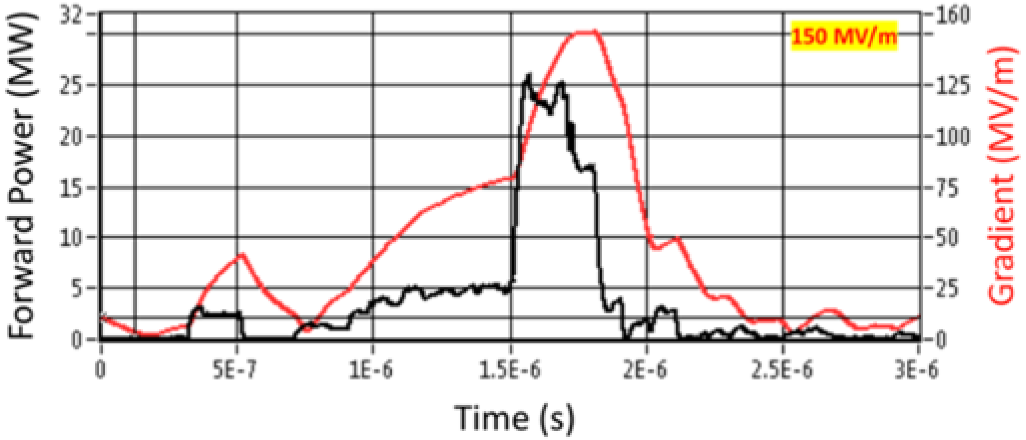

Cryogenic Operation at X-band

High power Test at Radiabeam

Two Cell Assembly for High Power Test

SLAC **Radiabeam**

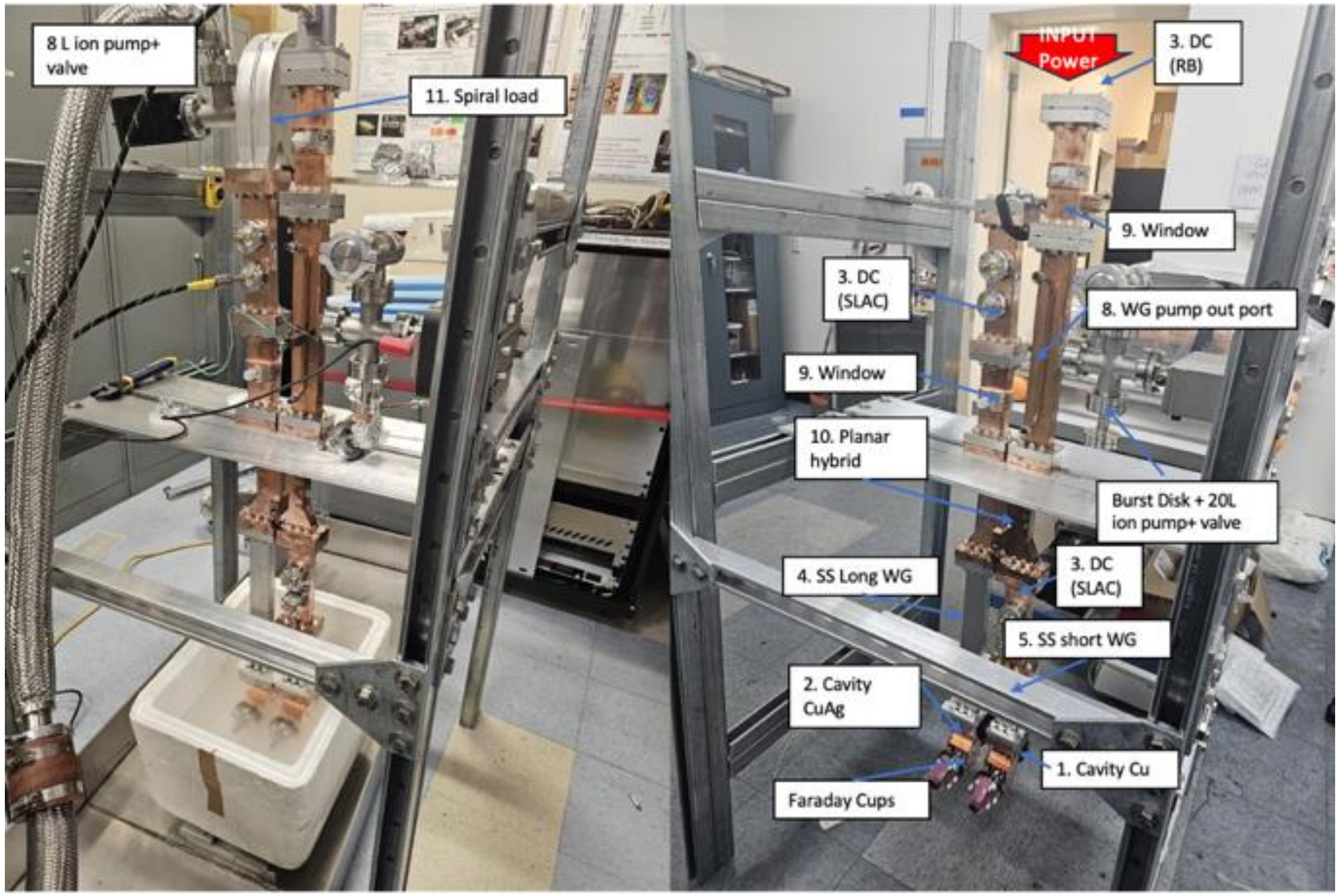

Exceeding Gradients and Pulse Lengths Required for C^3

- Measured and modeled response for CuAg Cavity

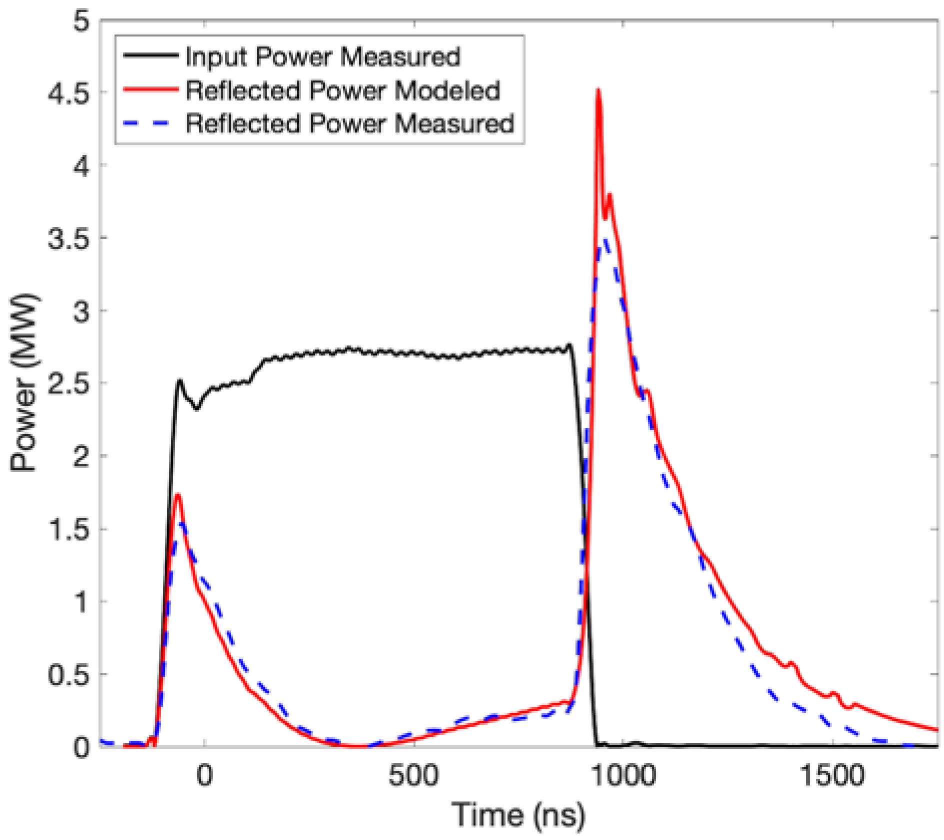

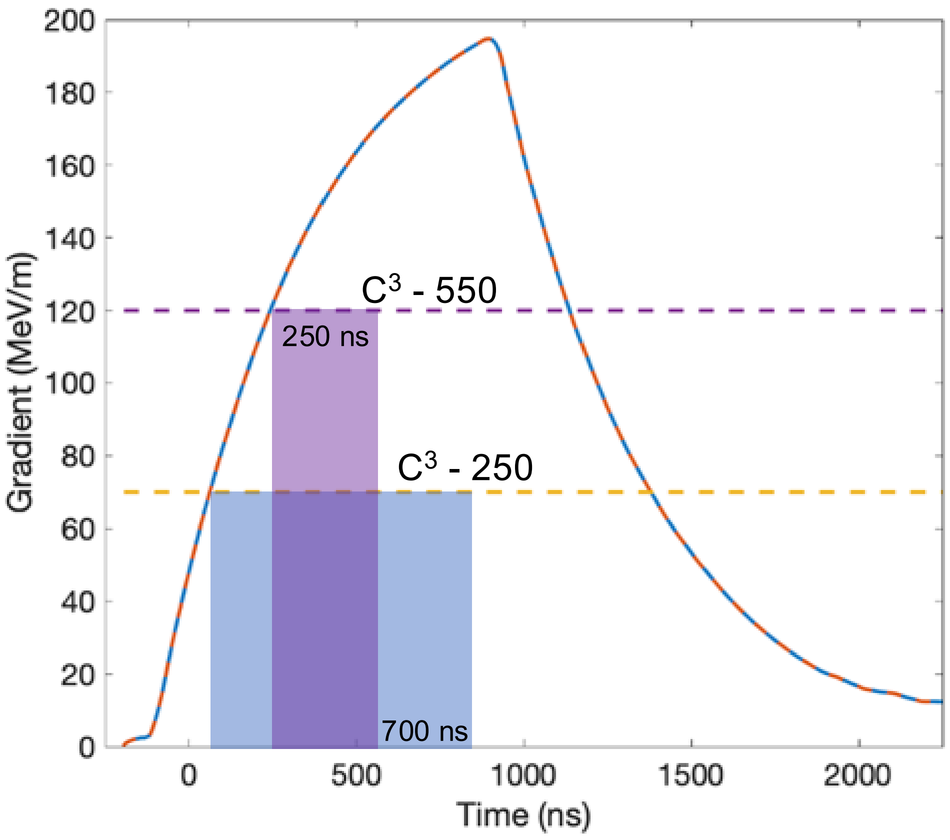

Single Cell Cryogenic High Gradient Tests

- ~20M Pulses (two weeks)
- Increased pulse length – 400 ns, 700 ns, 1 microsecond

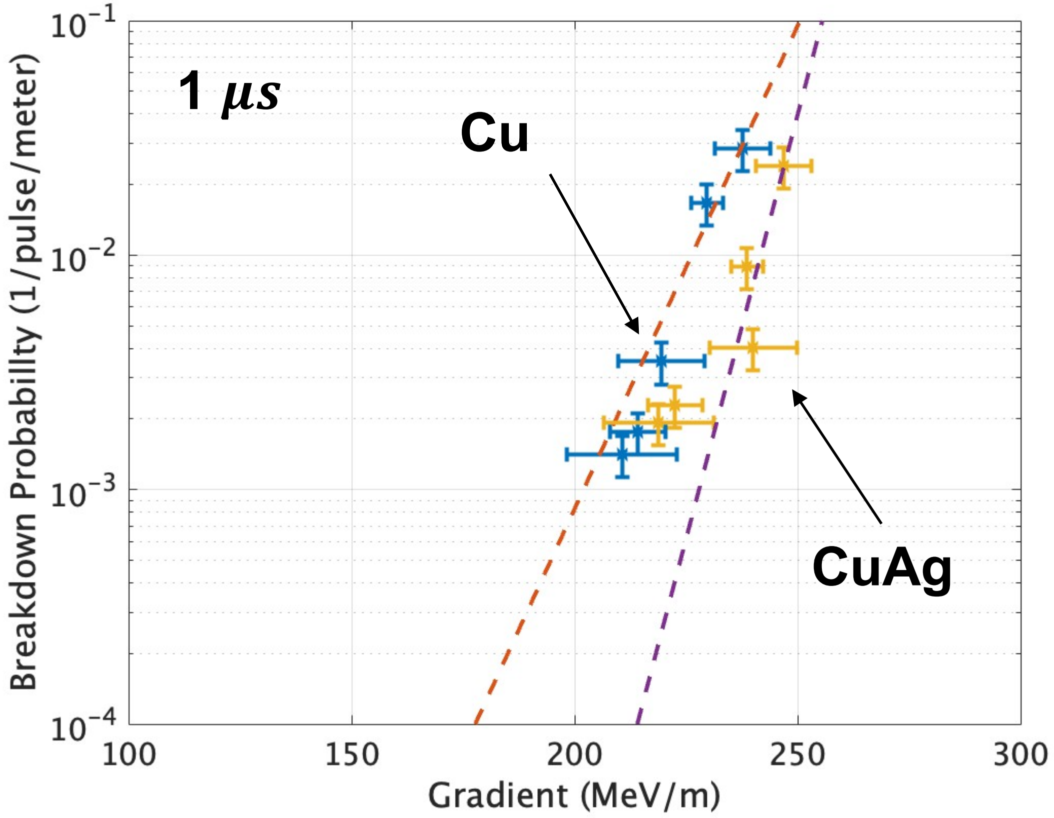

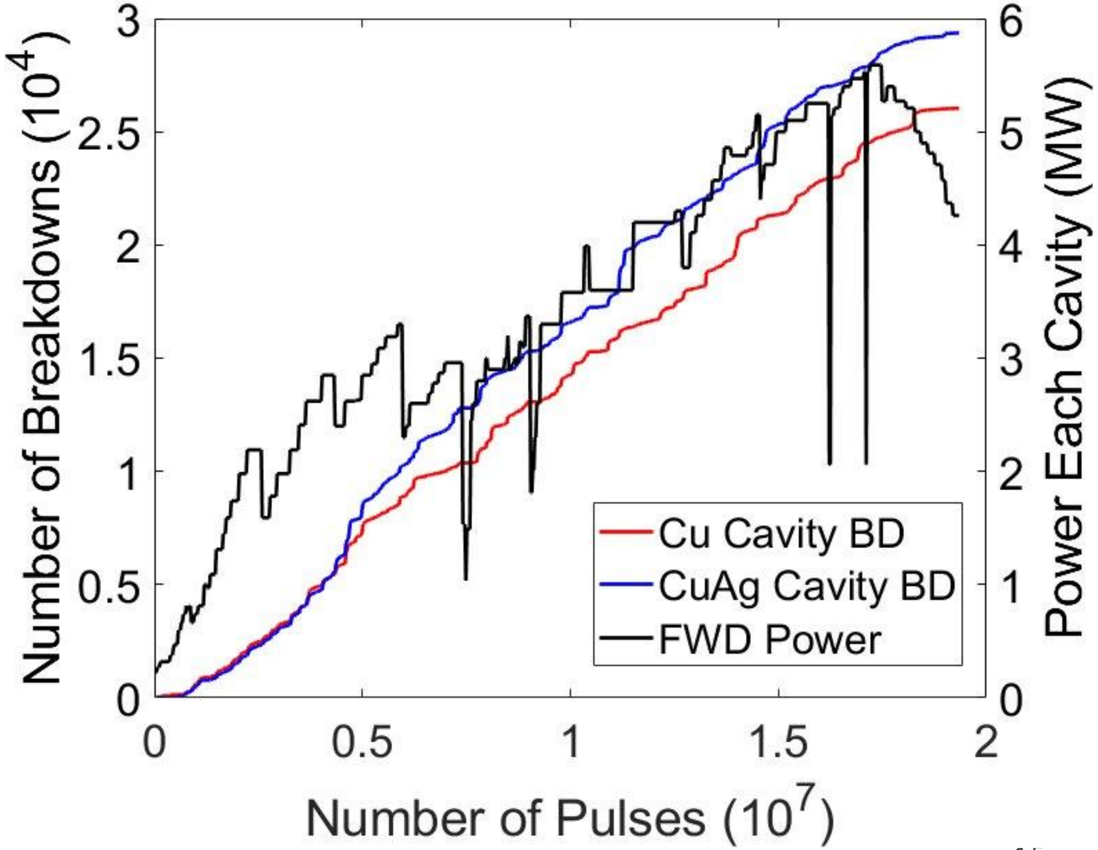

A. Diego, M. Schneider, M. Boyce and A. Dhar

Exploring the Energy Frontier…

What's Next for the Energy Frontier?

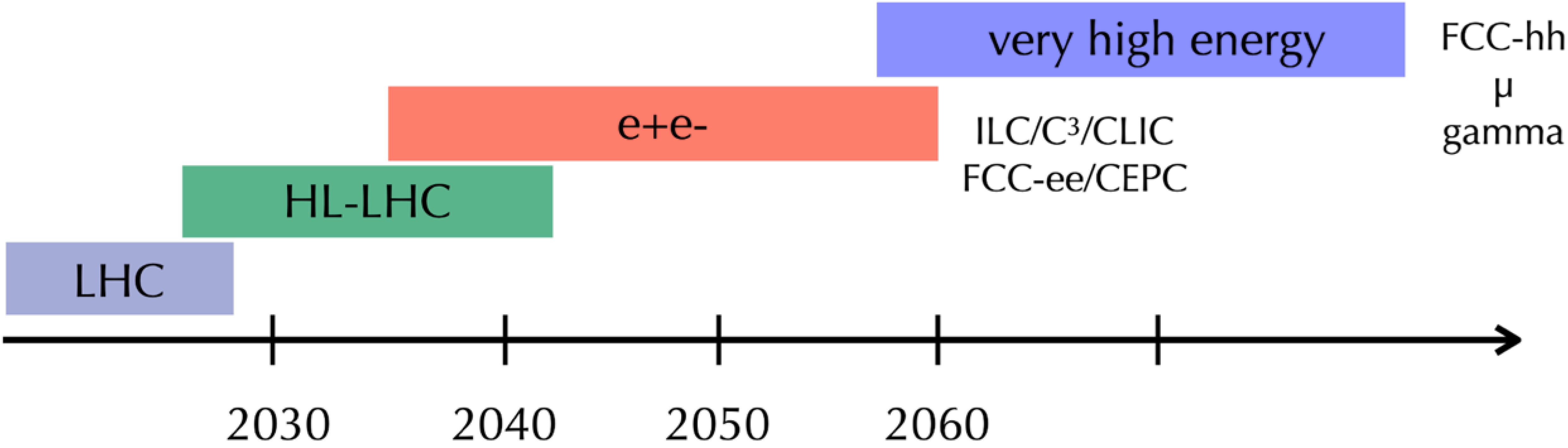

Wish list beyond HL-LHC:

1. Establish Yukawa couplings to light flavor ⟹ needs precision
2. Establish self-coupling ⟹ needs high energy

For the next e+e- Linear Collider

1. 5X the Beam Energy
2. 1000X the Luminosity (Effectively Beam Power Density)

Higgs Production at e^+e^-

ZH is dominant at **250 GeV**

Above **500 GeV**

- Hvv dominates
- ttH opens up
- HH production accessible with ZHH

Full Higgs physics program capable of a validated discovery requires reaching into the TeV range

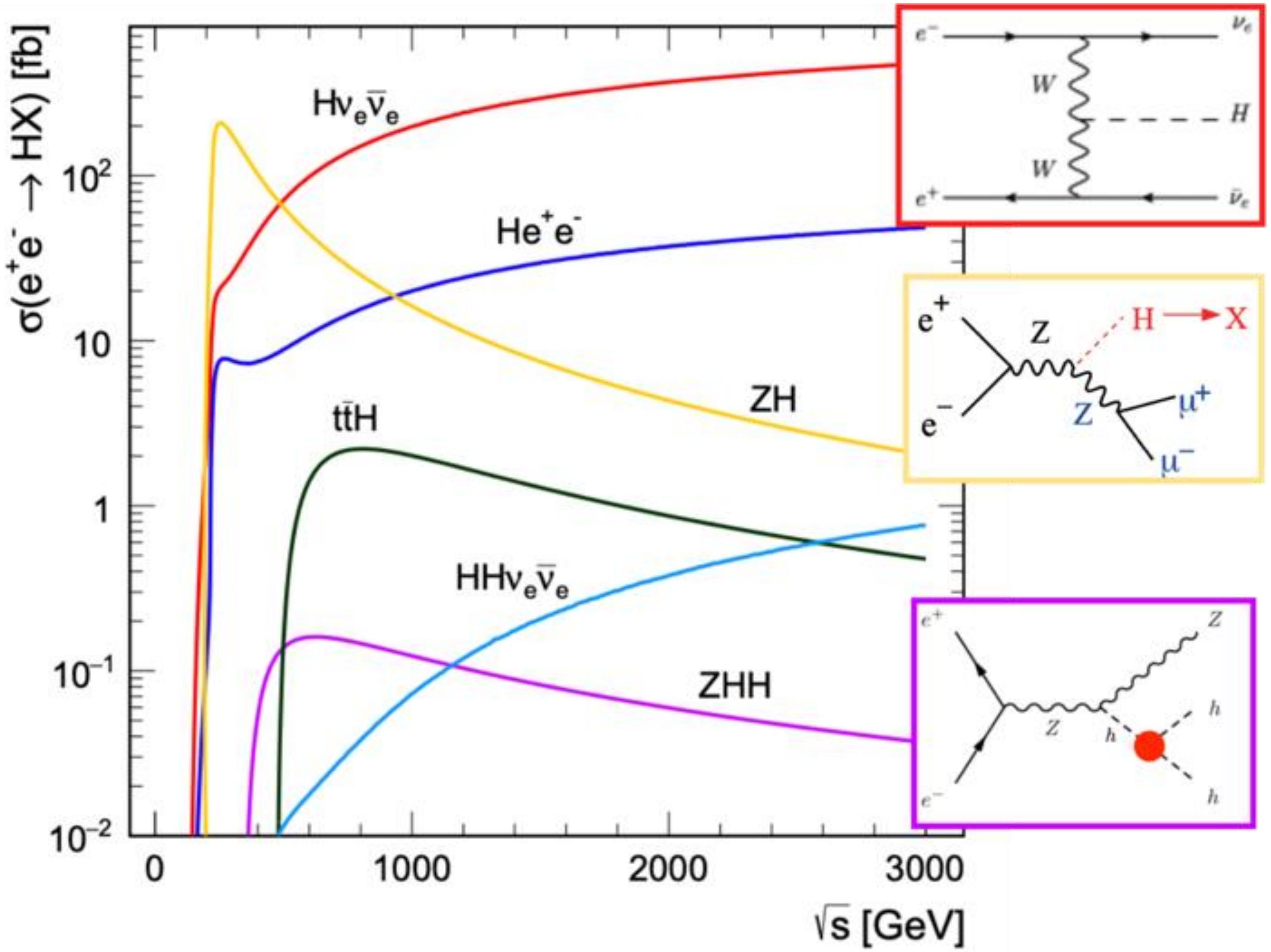

A novel route to a linear e^+e^- collider…

Requirements for a High Energy e^+e^- Linear Collider

Using established collider designs to inform initial parameters

Quantifying impact of wakes requires detailed studies

- Most important terms – aperture, bunch charge (and their scaling with frequency)

Target initial stage design at 250 GeV CoM

- 2 MW single beam power

Machine	CLIC	NLC	C^3
Freq (GHz)	12.0	11.4	5.7
a (mm)	2.75	3.9	2.6
Charge (nC)	0.6	1.4	1
Spacing (λ)	6	16	30/20
# of bunches	312	90	133/75

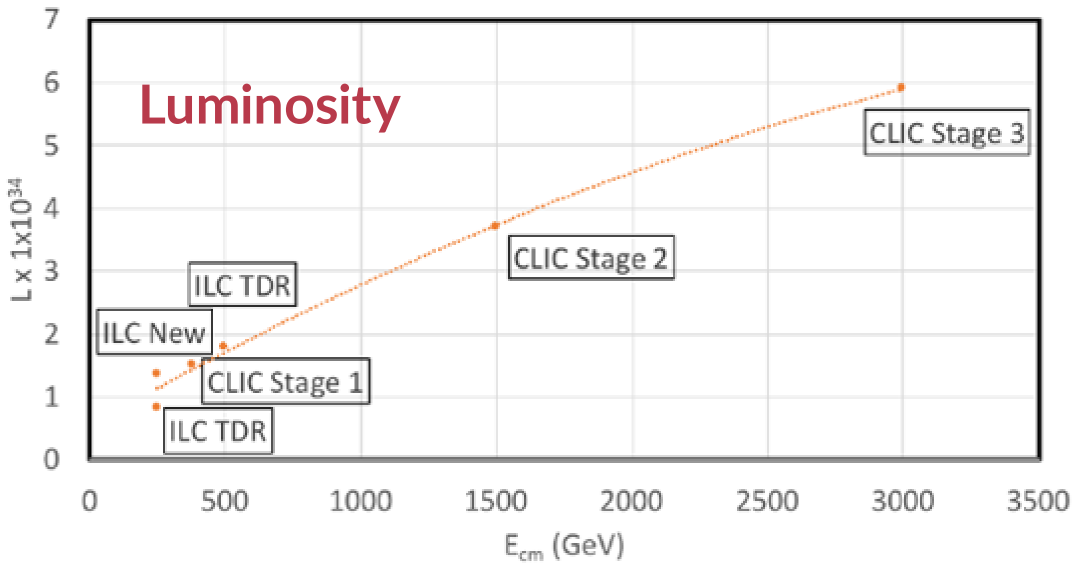

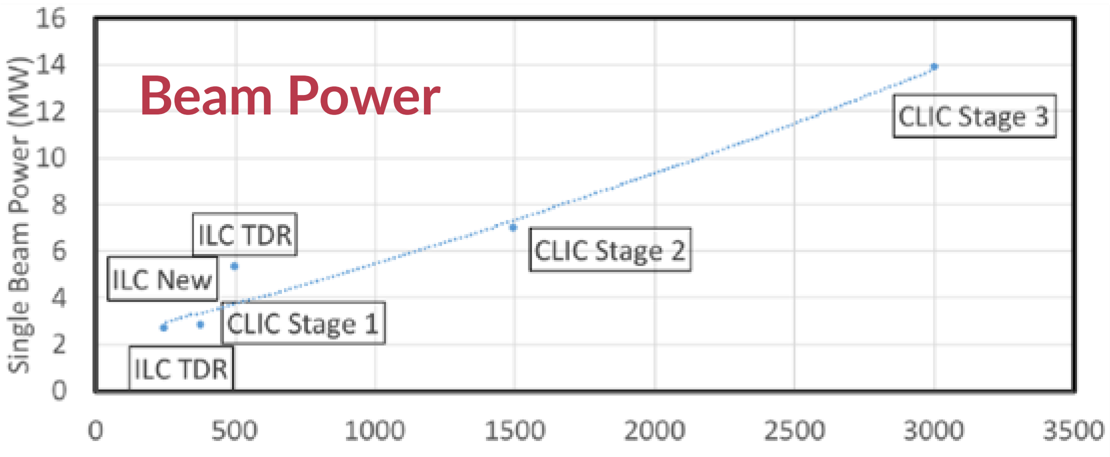

https://clic-meeting.web.cern.ch/clic-meeting/clictable2010.html

NLC, ZDR Tbl. 1.3,8.3

Accelerator Complex

8 km footprint for 250/550 GeV CoM ⟹ 70/120 MeV/m

Large portions of accelerator complex are compatible between LC technologies

- Beam delivery and IP modified from ILC (1.5 km for 550 GeV CoM)
- Damping rings and injectors to be optimized with CLIC as baseline
- Costing studies use LC estimates as inputs

C^3 - Investigation of Beam Delivery (Adapted from ILC/NLC)

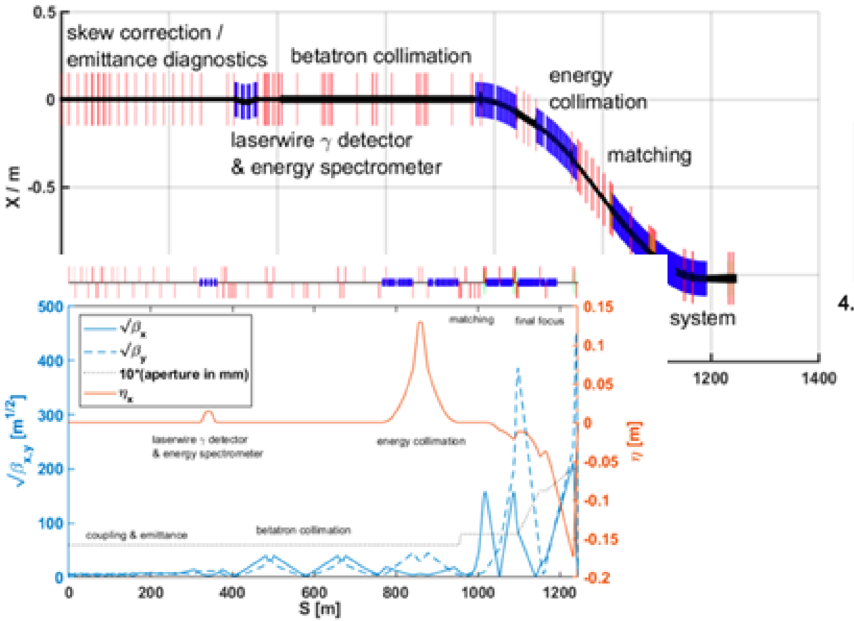

C^3 - 8 km Footprint for 250/550 GeV

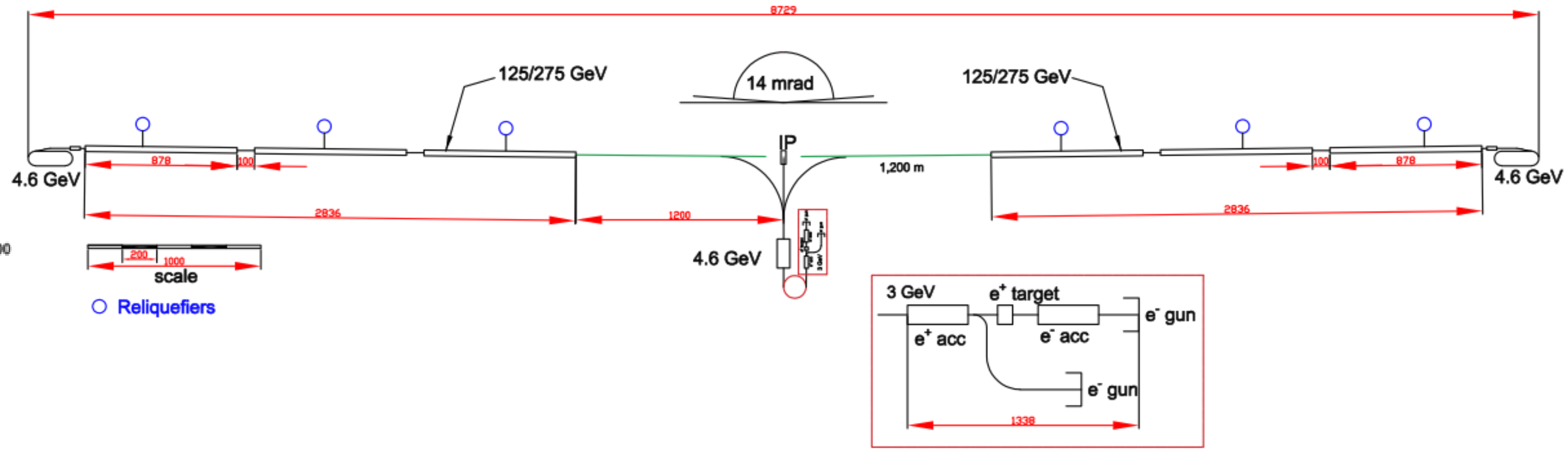

Table of Parameters

- Updated parameters for ESPPU 2025, based on luminosity* + BIB studies (Tu 10:20 MDI)

Scenario	C^3-250 s.u.	C^3-550 s.u.	C^3-250 high lumi	C^3-550 high lumi
Luminosity [$x10^{34} cm^{-2} s^{-1}$]	1.3	2.4	7.6	4.8
Gradient [MeV/m]	70	120	70	120
Effective Gradient [MeV/m]	63	108	63	108
Num. Bunches per Train	266	150	532	300
Train Rep. Rate [Hz]	60	60	120	60
Bunch Spacing [ns]	2.65	1.75	2.65	1.75
Single Beam Power [MW]	2	2.45	8	4.9
Site Power [MW]	$\sim$110	$\sim$125	$\sim$180	$\sim$180
Parameter Set [6]	PS1	PS2	PS2	PS2

*Ntounis, et al., *Phys. Rev. Accel. Beams* **27**, 061001, 2024

Quarter Cryomodule (QCM)

- Vacuum insulation, raft length up to 2.5 m
- First step into realizing Stage 2 goals
- Outfit for alignment and vibration testing
- Follow-on experiments with structures at high gradient and beam acceleration

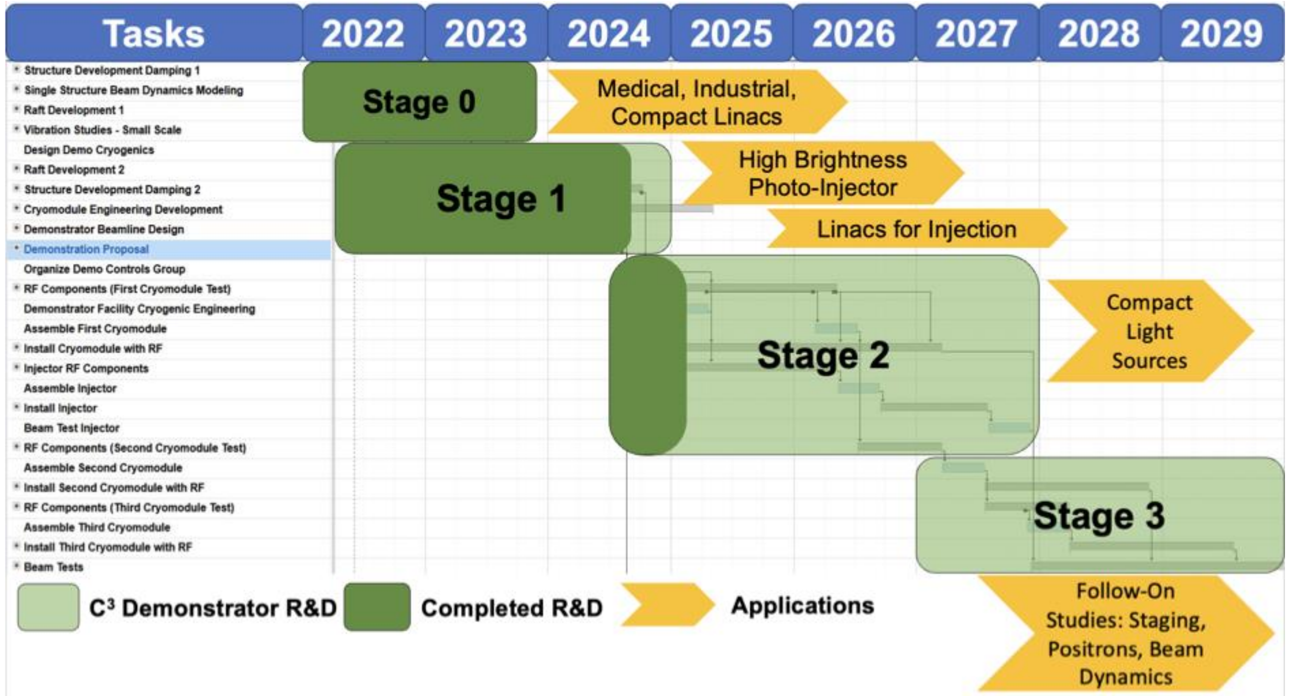

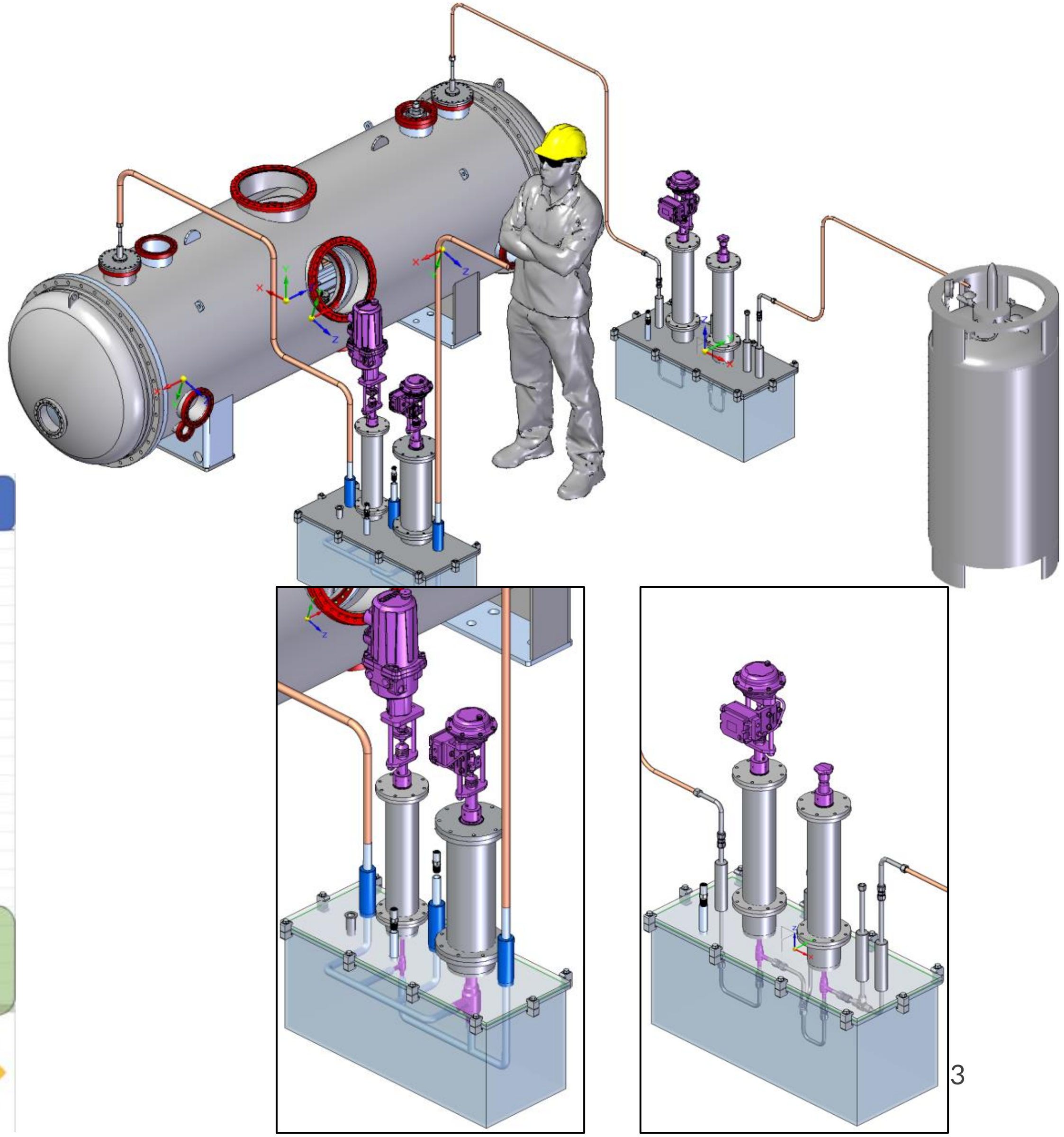

Synergies with Future Colliders

RF Accelerator Technology Essential for All Near-Term Collider Concepts

C^3 Demo is positioned to contribute synergistically or directly to all near-term collider concepts

- CLIC - components, damping, fabrication techniques
- ILC - options for electron driven positron source based C^3 technology
- Muon Collider - high gradient cryogenic copper cavities in cooling channel, alternative linac for acceleration after cooling
- AAC - C^3 Demo utilized for staging, C^3 facility multi-TeV energy upgrade reutilizing tunnel, $\gamma\gamma$ colliders
- FCC-ee - common electron and positron injector linac from 6 to 20 GeV
  - **reduce length 3.5X OR reduce rf power 3.5X**

Wide Aperture S-band Injector Linac
$a/\lambda = 0.125$

- Planned test at Argonne
- Tracking with Lucretia includes longitudinal and transverse wakes, chromatic effects etc
- Error study is 100 seeds, 100 μm element offsets, 300 μrad element rolls (rms)
  - No corrections applied

90% seeds < 8 um-rad with lattice errors

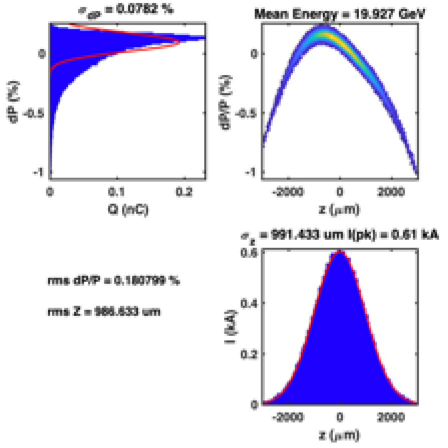

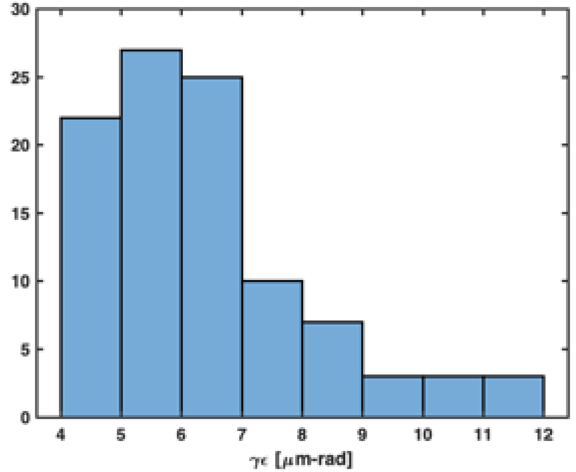

Vibrant International Community for Future Colliders is Essential

Ongoing R&D

Auxiliary Systems: LLRF and Alignment

- NG-LLRF in development based on RFSoC
- Demonstrated C3 requirements in high power test
- Initial thoughts to system implementation

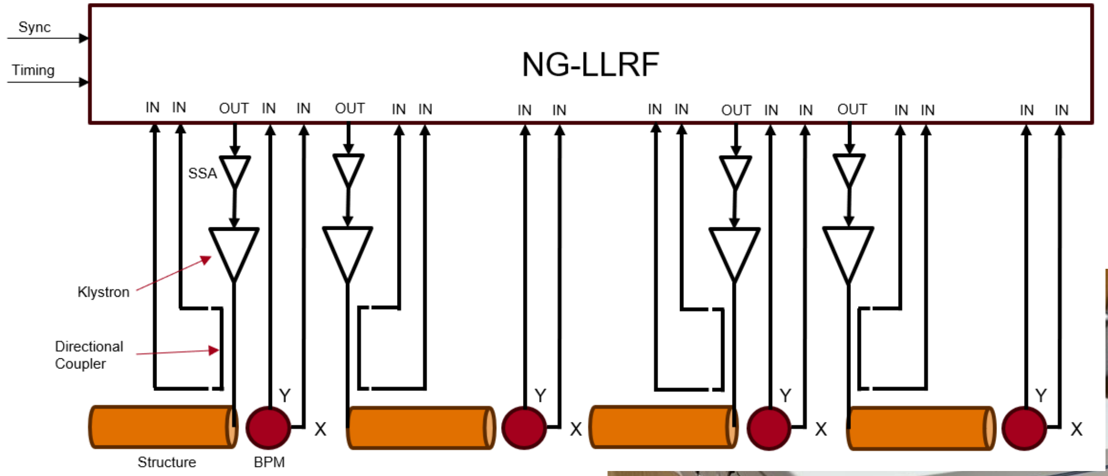

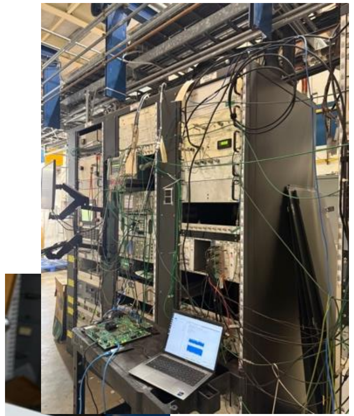

W 9:00 NCRF

- Rasnik alignment system

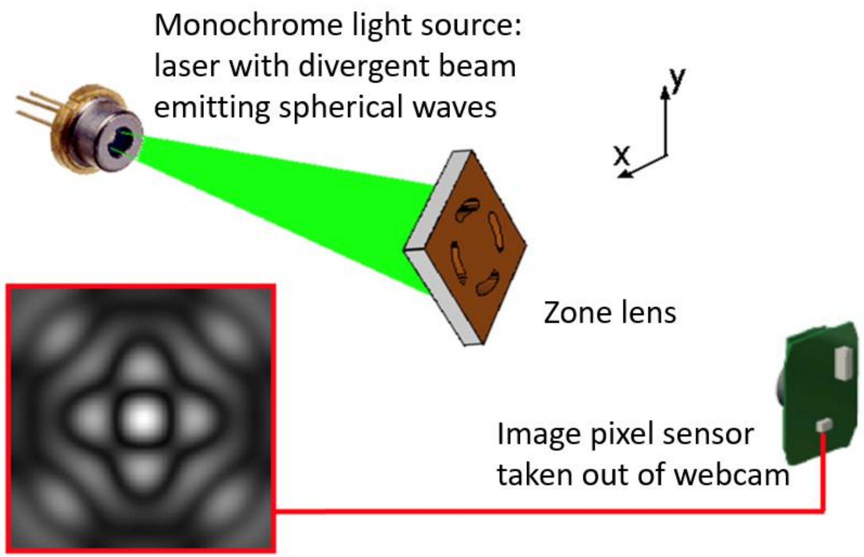

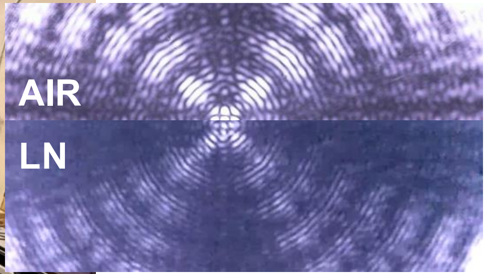

W 9:40 NCRF

Alignment and Vibrations for Collider Quality Beams

System level optimization essential for achieving performance

RF Structure Optimization

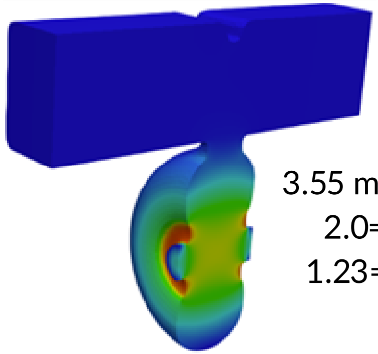

3.55 mm iris radius
$2.0 = E_{max}/E_{acc}$
$1.23 = H_{coup}/H_{wall}$

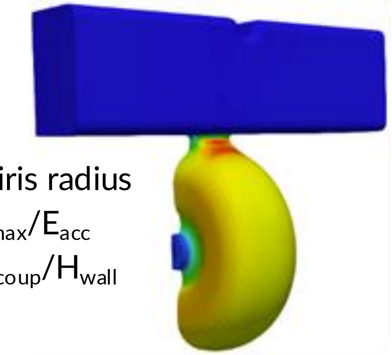

Electric Field

Magnetic Field

M. Shumail, Z. Li

Vibration Measurements and Analysis

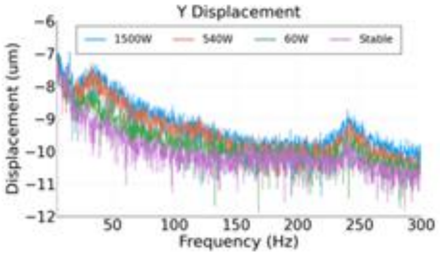

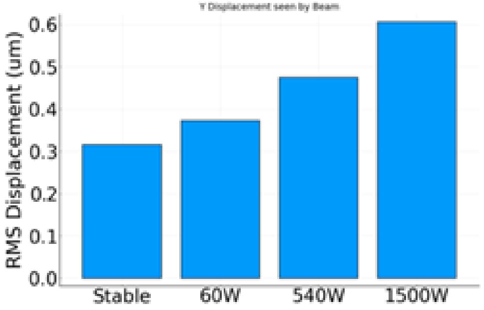

RadiaBeam

Z. George, V. Borzenets, A. Dhar, D. Palmer

Two-Phase Fluid Simulations

FAMU-FSU College of Engineering

K. Shoele

Main Linac Beam Dynamics

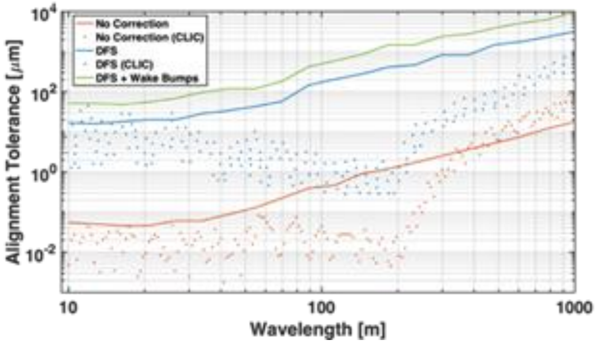

White (C³), Schulte (CLIC)

Alignment Parameters	Units	Value
Raft Components	µm	5
Short Range (~10m)	µm	30
Long Range (>200m)	µm	1000
Structure Vert. Vibration	µm	9
Quad Vert. Vibration	nm	15
BPM Resolution	µm	0.1
BPM-Quad Alignment	µm	2

Precision Short and Long Range Alignment

H. Van Der Graaf

Nikhef

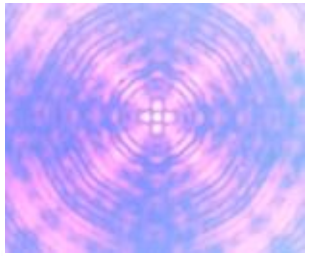

100 nm resolution
Approved effort to test cold

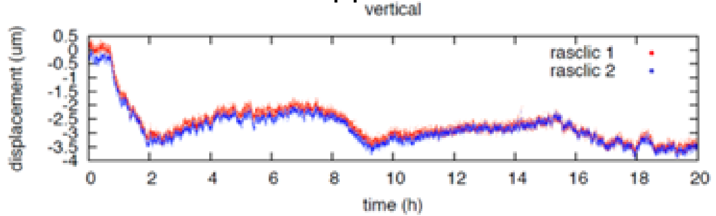

https://arxiv.org/pdf/2307.07981.pdf

Meter-long Linac Cryogenic High Gradient Tests

Conditioned Linac at Radiabeam up to 20 MW, 60 Hz, and 1 µs

- Conditioning limited by klystron, not structure
- Accelerometer measurements at max power showed sub-micron displacements, even with mechanical propagation from outside the bunker

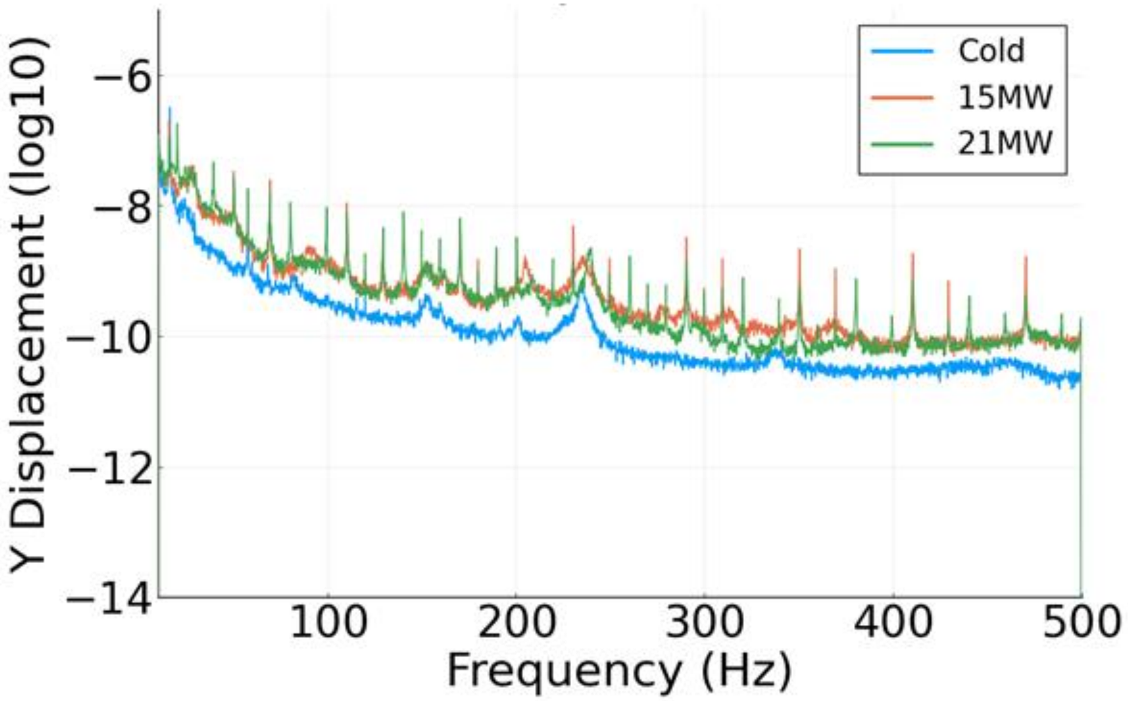

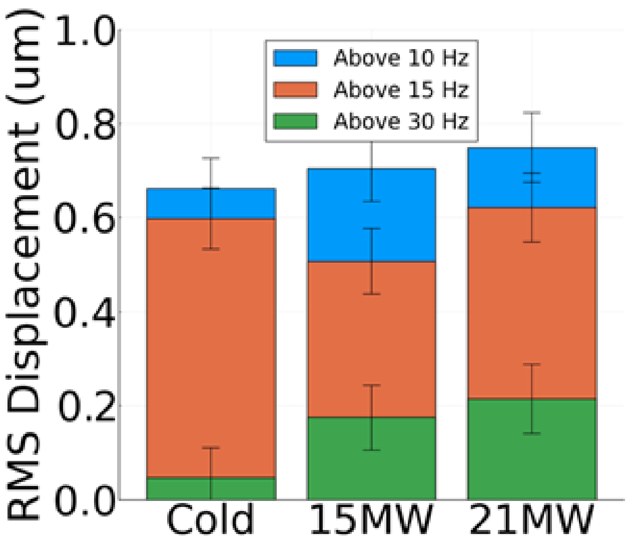

Main Linac Beam Dynamics Studies

Studies needed to guide accelerator design and alignment tolerances with novel structures

- Test Case: C^3 is a cryogenic-cooled e^+e^- collider concept with a distributed coupling accelerator structure
- Multi-bunch simulation studies were conducted to identify long-range HOMs that deteriorate beam’s quality
- Single bunch studies also used for studying alignment tolerances

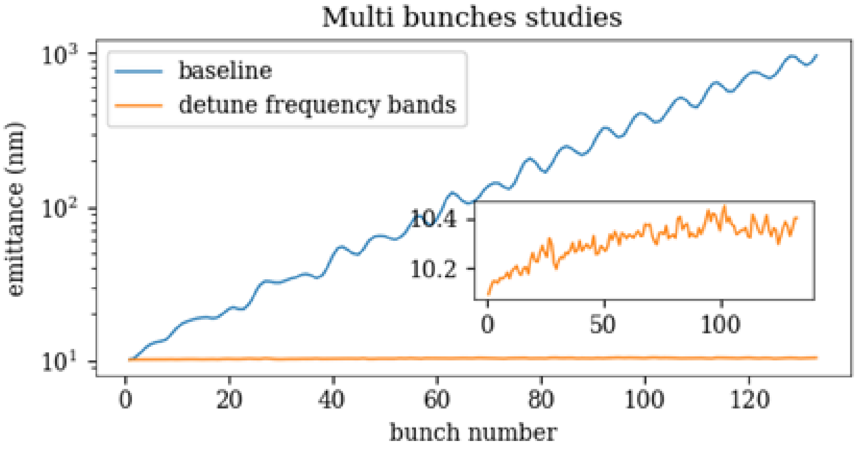

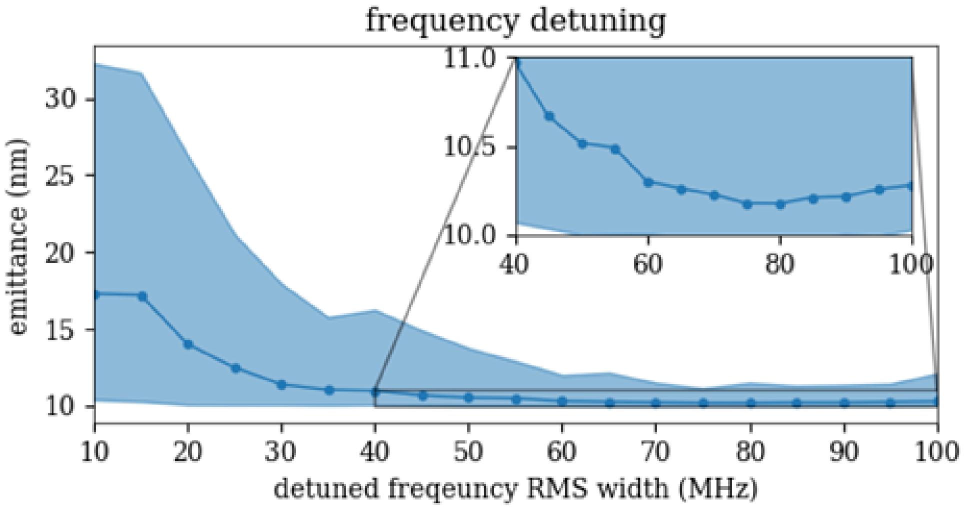

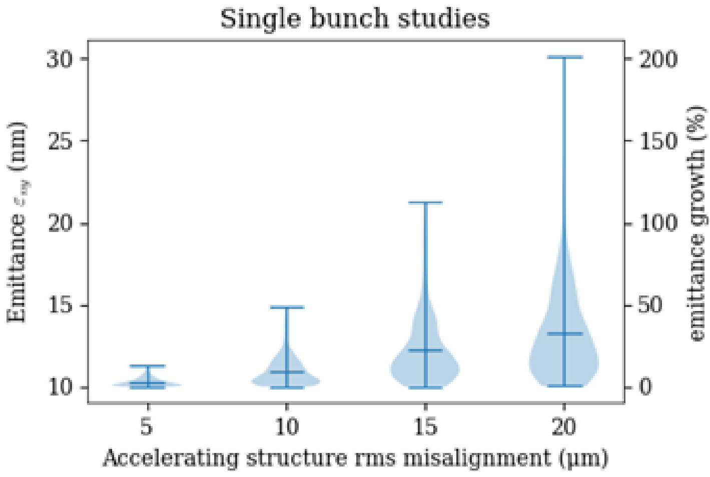

Gaussian Detuning Provides Required 1st Band Dipole Suppression for Subsequent Bunch, Damping Also Needed

Dipole mode wakefields immediate concern for bunch train

4σ Gaussian detuning of 80 cells for dipole mode (1st band) at f_c=9.5 GHz, w/ $\Delta f/f_c$=5.6%

First subsequent bunch s = 1m, full train ~75 m in length

- Damping needed to suppress re-coherence

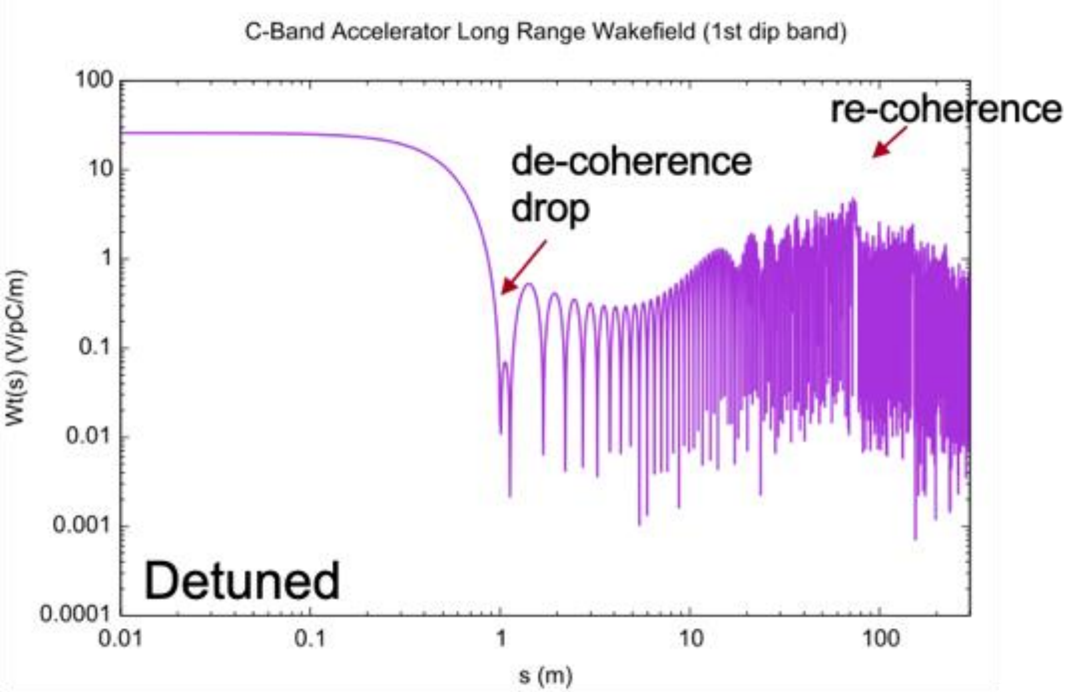

(Only copper surface loss damping included)

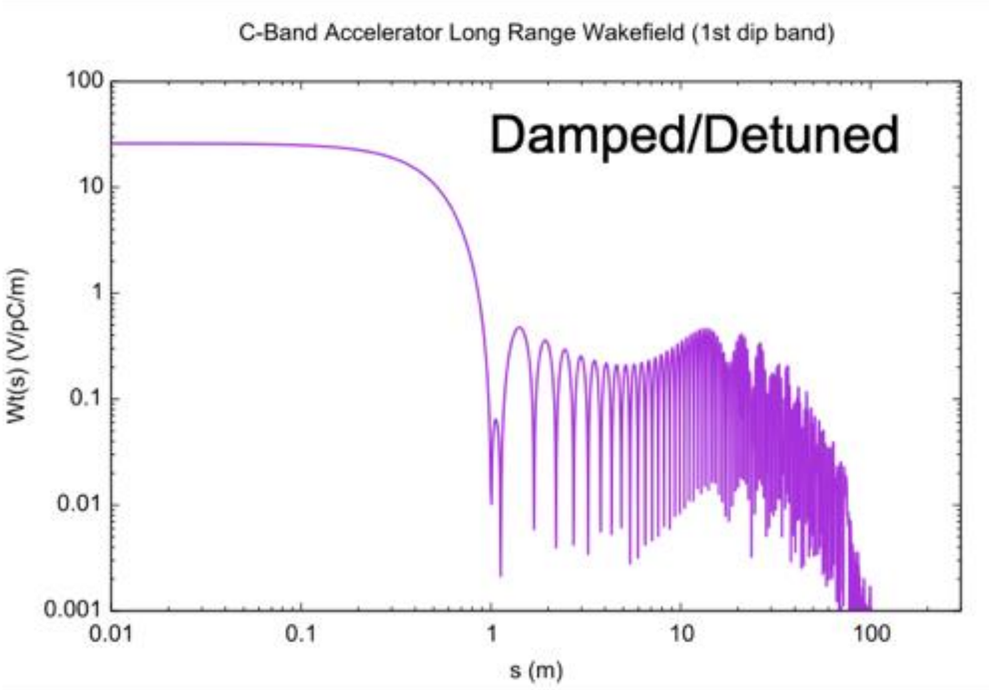

(1.0e3 Q total HOM damping included)

Distributed Coupling Structures Provide Natural Path to Implement Detuning and Damping of Higher Order Modes

Individual cell feeds necessitate adoption of split-block assembly
Perturbation due to joint does not couple to accelerating mode
Exploring gaps in quadrature to damp higher order mode

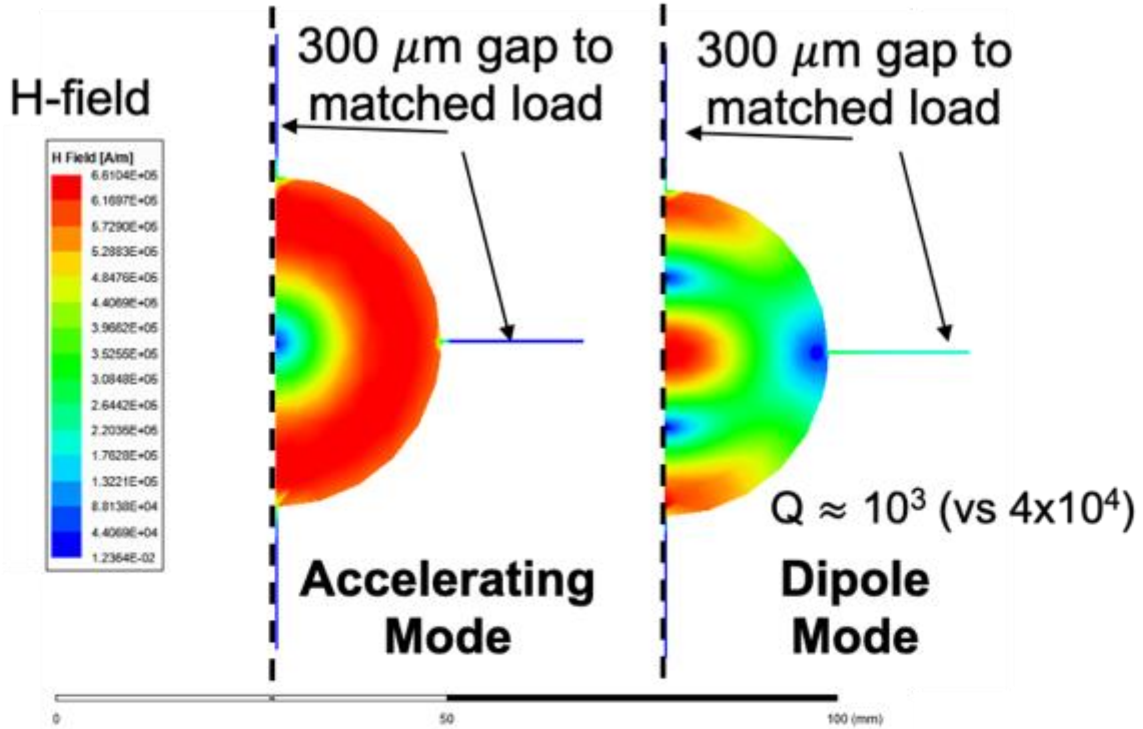

Detuned Cavity Designs

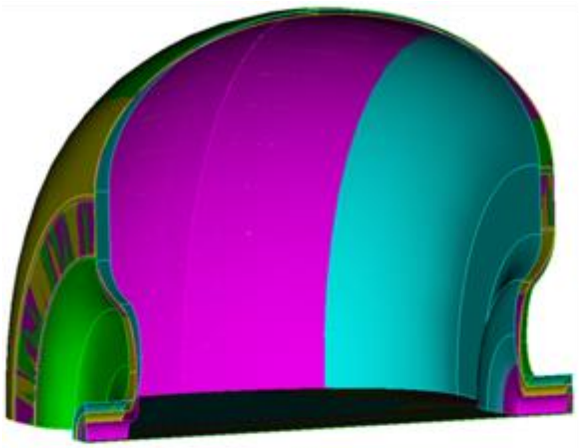

Quadrant Structure

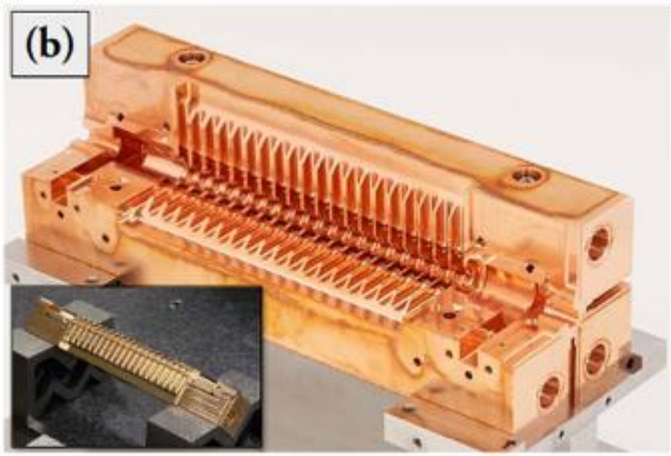

Abe et al., PASJ, 2017, WEP039

HOM Damping and Detuning

Detuning through nose cone profiles, damping through lossy thin slits

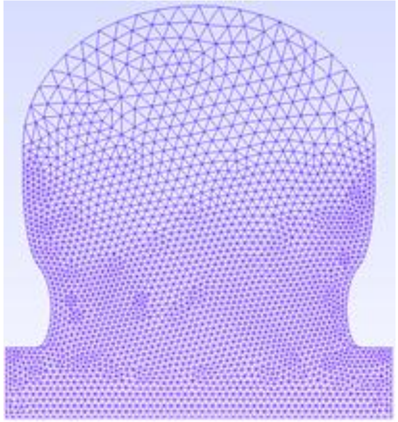

Frontend cell:
Gap1
R=113.67 MΩ/m

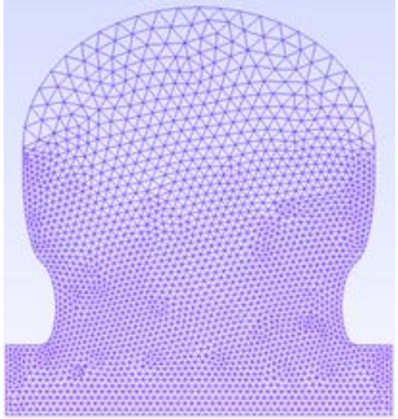

Middle cell:
Gap1-0.5mm
R=114.32 MΩ/m

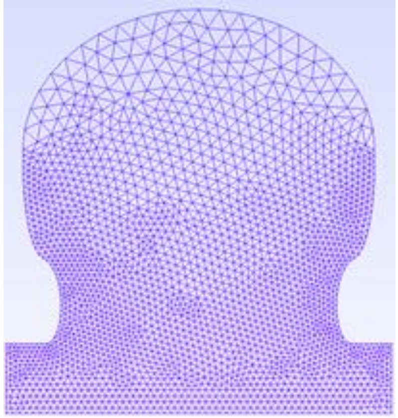

Backend cell:
Gap1-1mm
R=114.38 MΩ/m

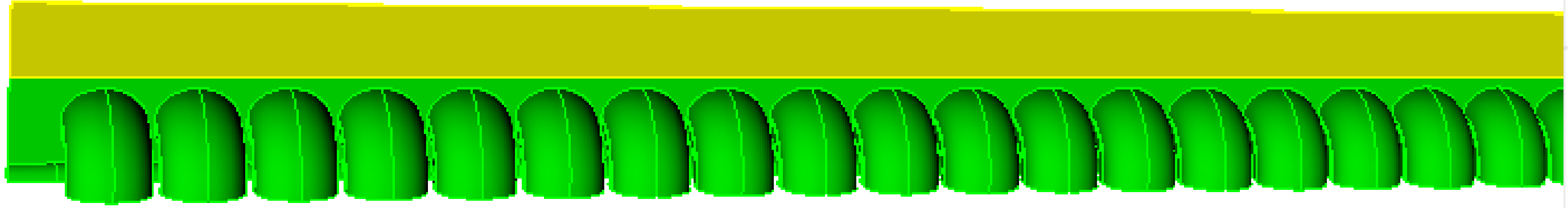

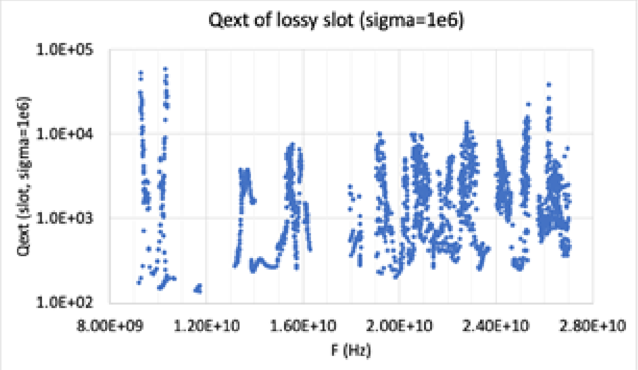

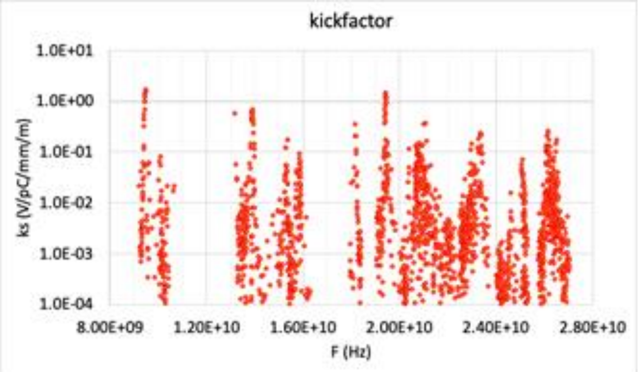

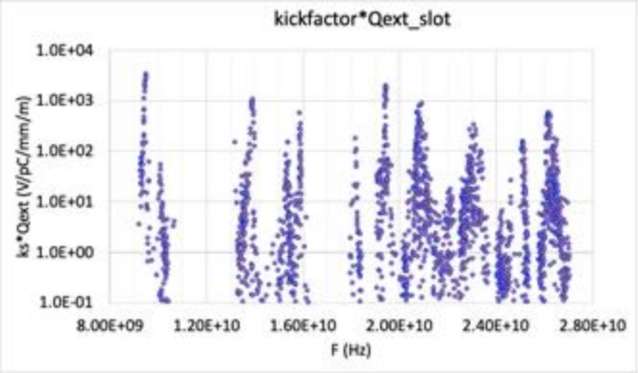

SLAC Z. Li

NiCr Deposition Method

NiCr is typically sputtered for thin film applications

- This is not viable for coating large damping slits

Potential solution is to electroplate layers of Ni and Cr and then use a hydrogen furnace to form NiCr

- The RF loss of this fired sample was verified through S11 measurements of a resonant cavity

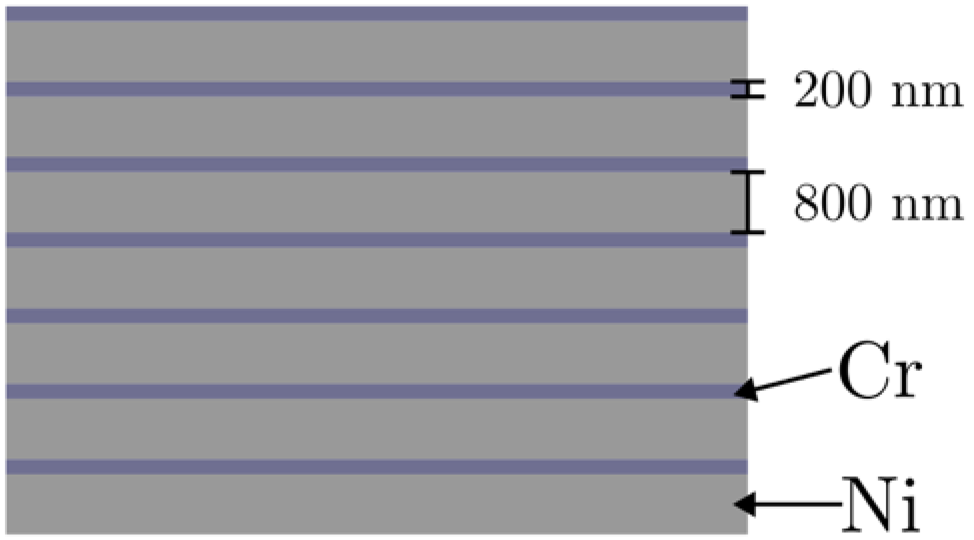

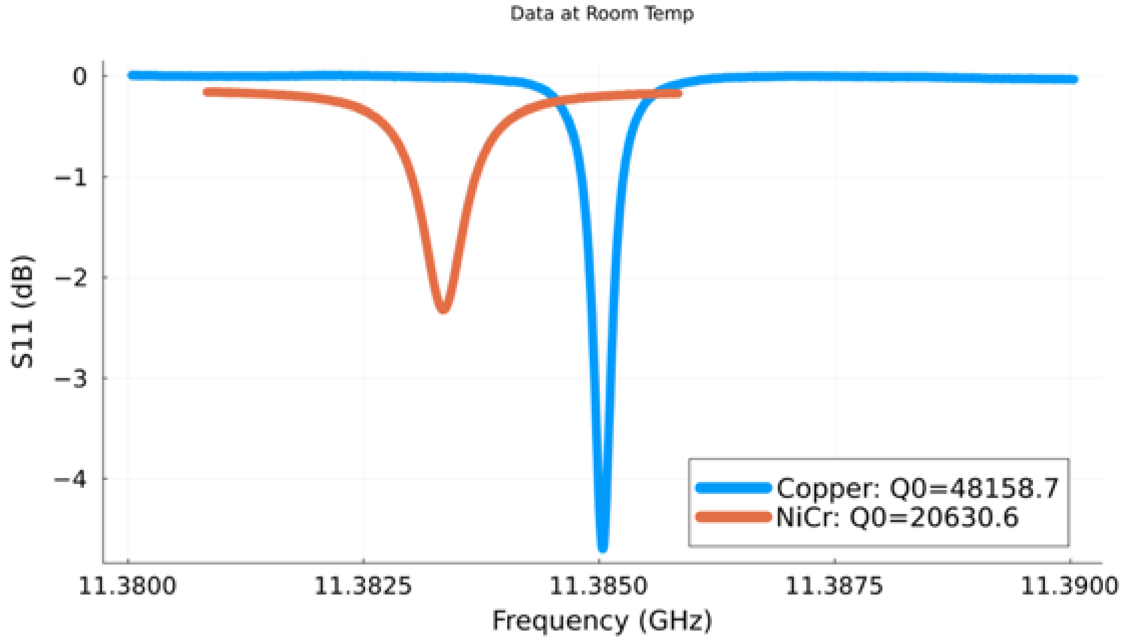

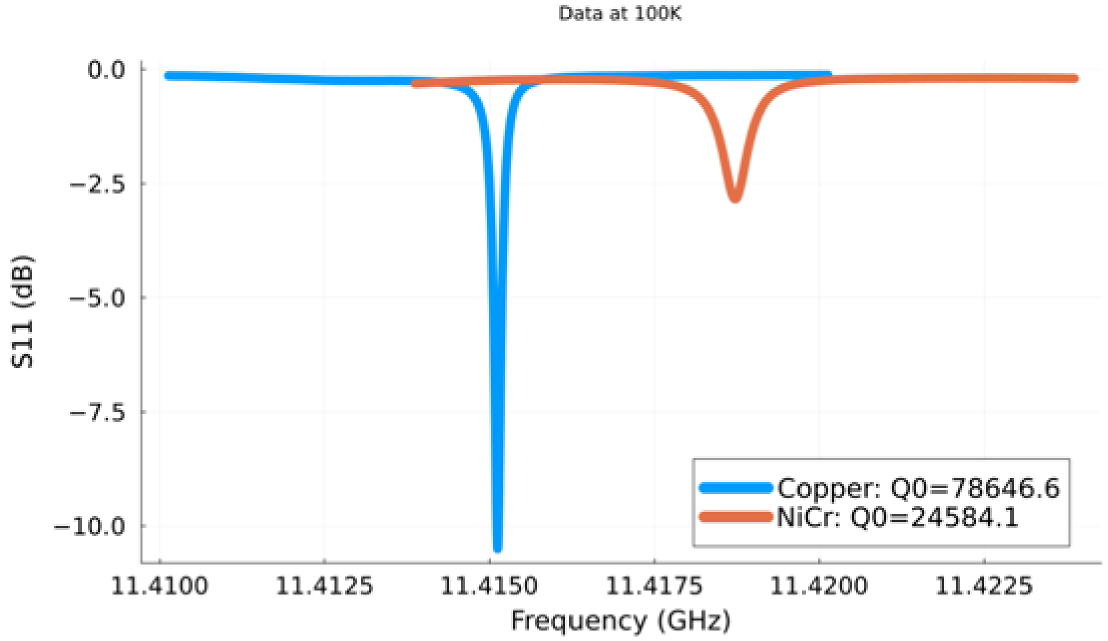

NiCr Application to Main Linac

This electroplating method provides a scalable solution for depositing NiCr on damping slits

- Linac cavities would be rough machined along with slits, waveguides, etc
- Electroplating would cover entire linac
- Final machining removes NiCr layer from unwanted areas, leaving coated slits

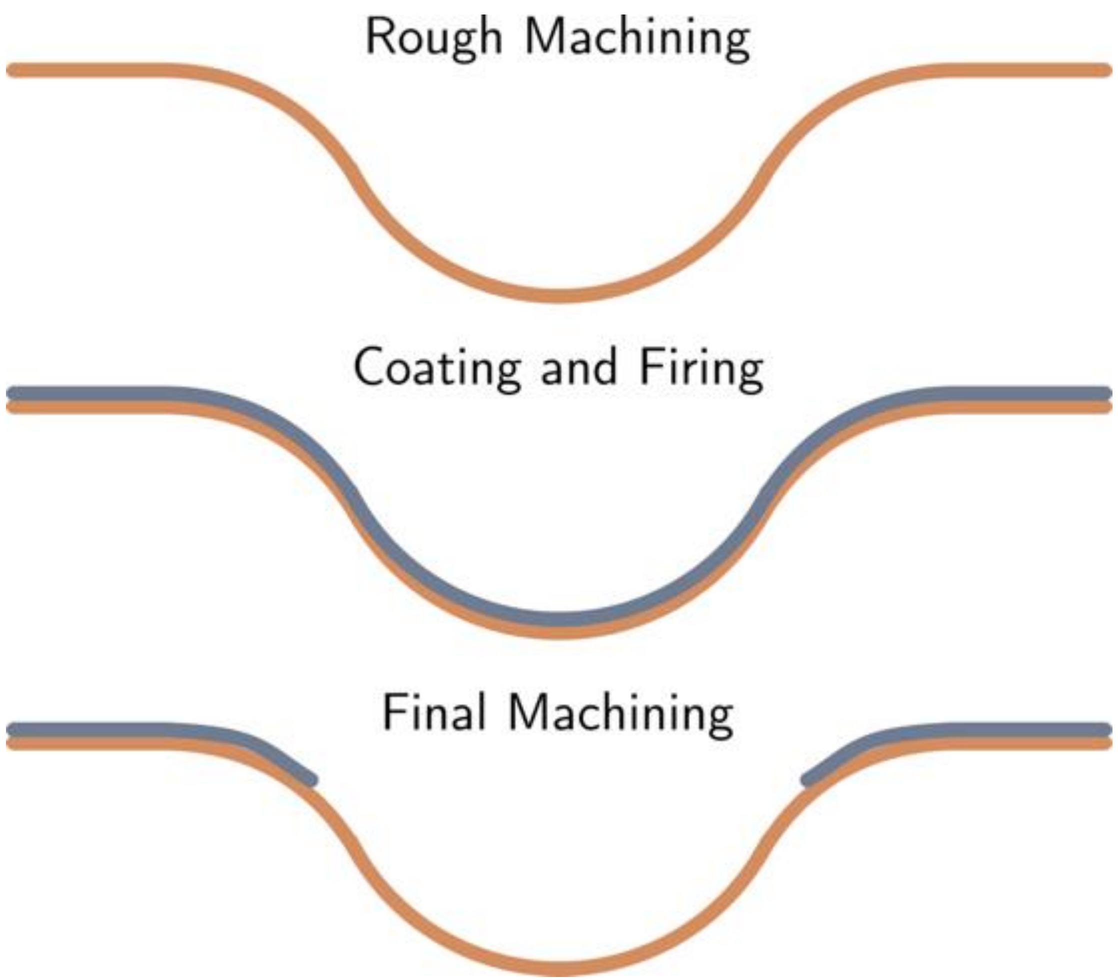

NiChrome High Power Testing

Field emission study using electrodes and breakdown light detection

- NiChrome a promising material for damping slits
- Tested up to 47.5 MV/m, 1 kHz, and 1 microsecond
- TWT tests for high power RF tests to begin soon
- Very promising high power performance so far

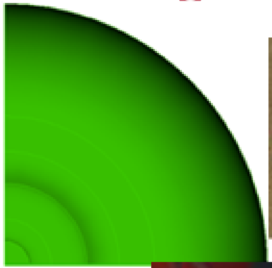

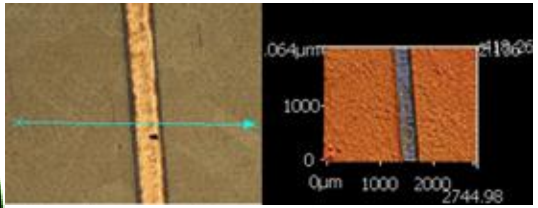

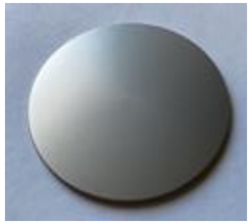

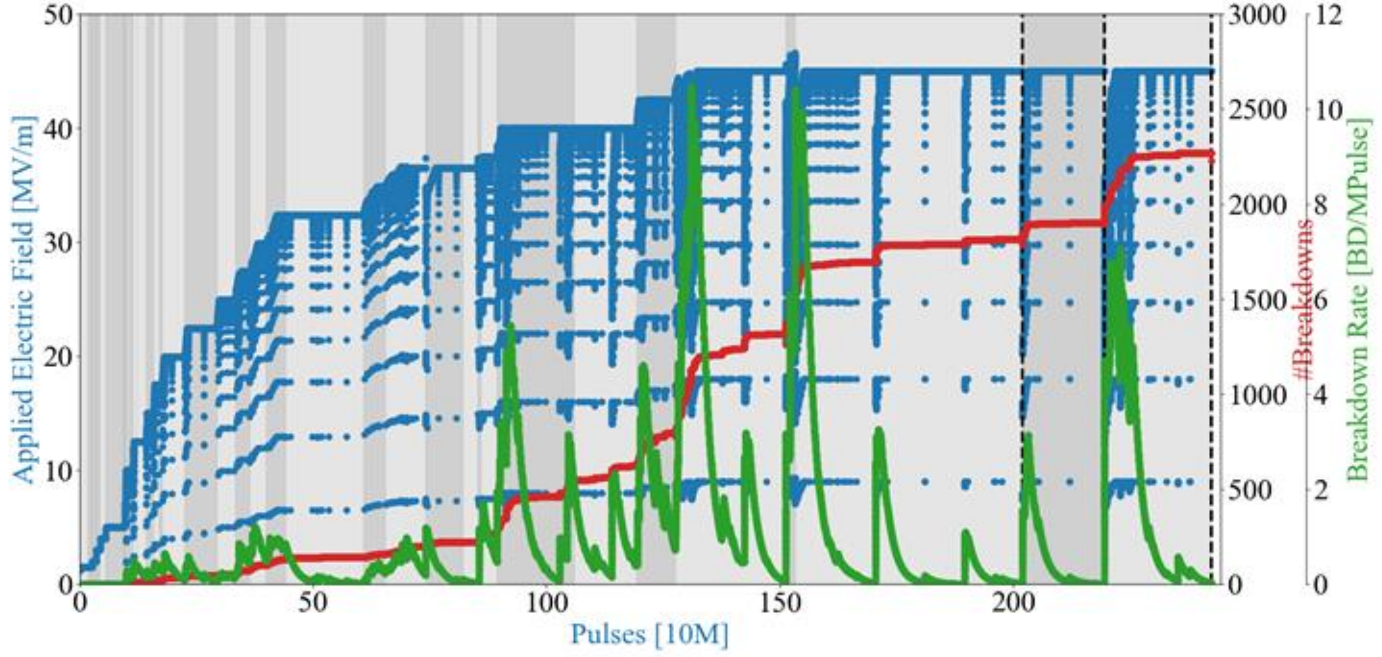

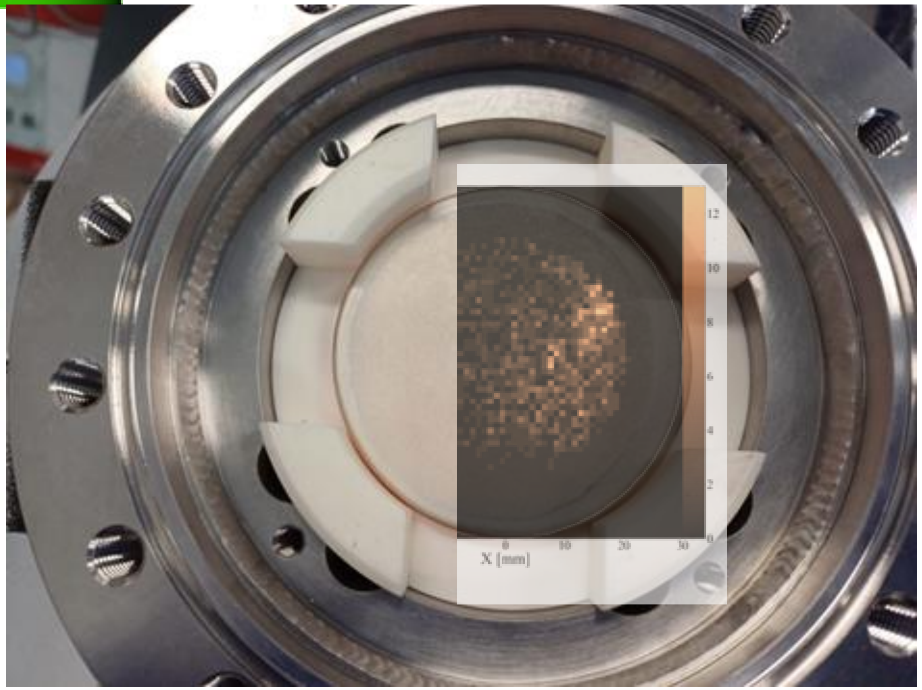

SLAC V. Bjelland, W. Wuensch @ CERN

Future R&D Directions

Max Shunt Impedance with 135 deg Phase Advance

Achieve Same Efficiency with a Larger Aperture (compared with 180 deg cell) (Muhammad Shumail)

Quality factor, aperture size, and gap distance for $R_s = 114\ M\Omega/m$ and $\mathrm{Es/Ea} = 2$

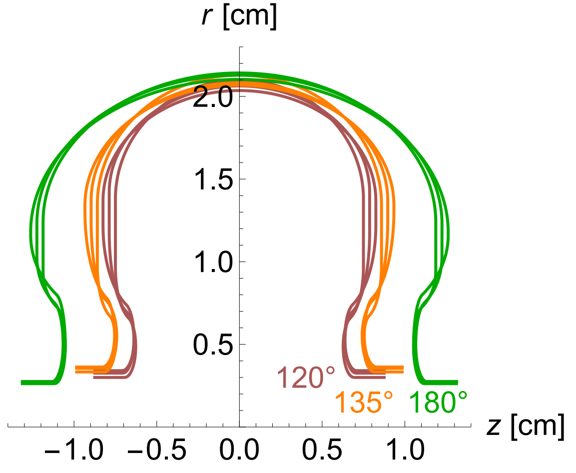

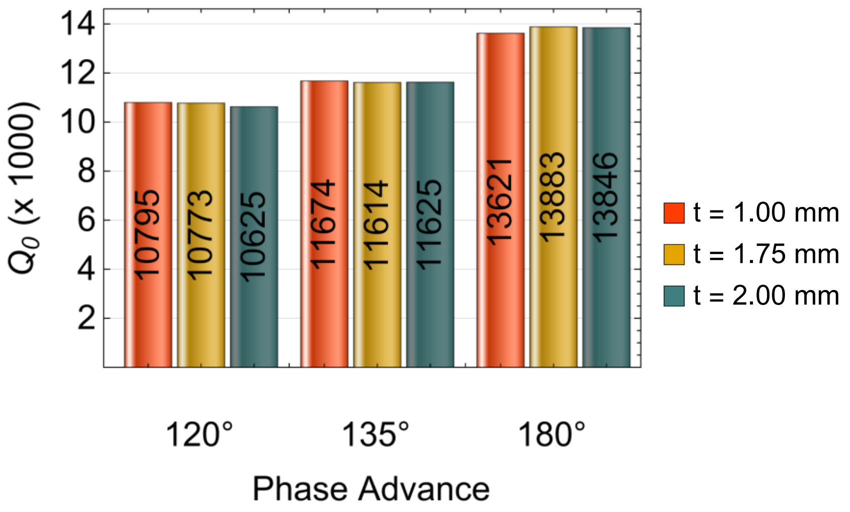

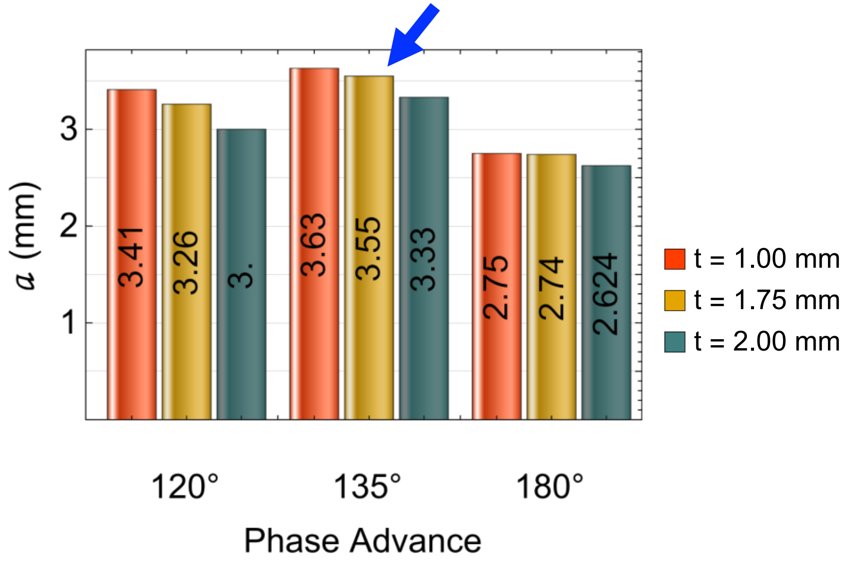

Cavity (with two different coupler implementations) Parameters

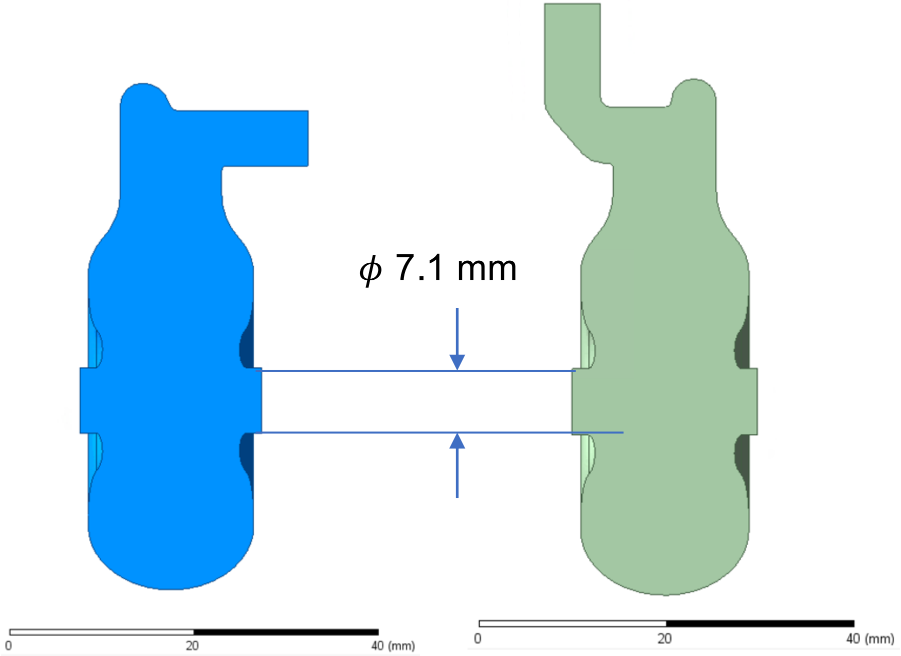

Parameters@ 77 K	Cavity Left	Cavity Right
Resonant Frequency, f_0 (GHz)	5.712	5.712
Coupling Coefficient, β	1.8625	1.8634
Reflection Coefficient, Γ	0.3013	0.3015
Shunt Impedance, r_s (MΩ/m)	317.22	317.22
$\frac{\eta_0 H_{surf_{peak}}}{Gradient}$	1.14	1.14
Quality Factor, Q_0	30124	30122

(Muhammad Shumail)

135/deg vs 180/deg Design

- **3π/4 phase Design**
  - **Aperture radius of 3.55 mm,** same shunt impedance (300 MΩ/m (77K) and the peak E field
  - **With 35% larger aperture**, rf structure is much more resilient to both short-range and long-range wakefield effects.
- **PI phase design**
  - **Aperture radius of 2.624 mm,** shunt impedance 300 MΩ/m (77K)

Distributed coupling for 135 deg Design

Equivalent phases and Feeding Scheme:

Beam Direction

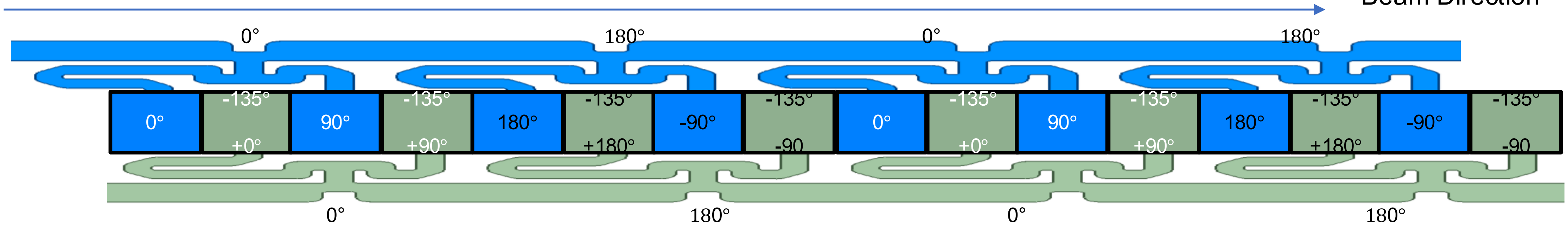

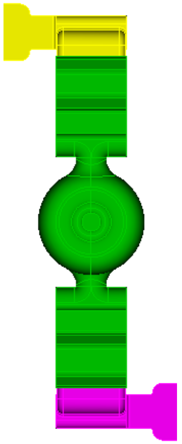

There has to be a phase difference of 135° between the upper and lower rf feeding manifold.

T-junction
with power splitter

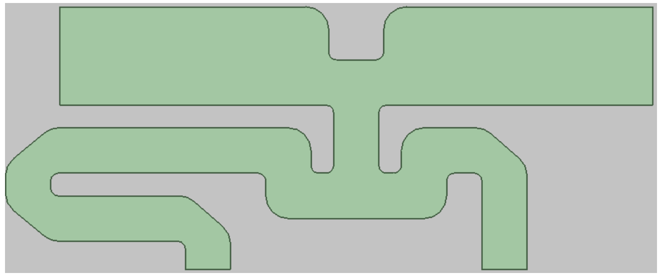

1-period of 135 deg
distributed coupling
structure

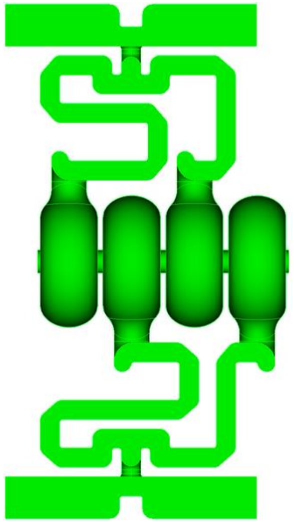

Response of Cavities Through the Manifold for Tuning

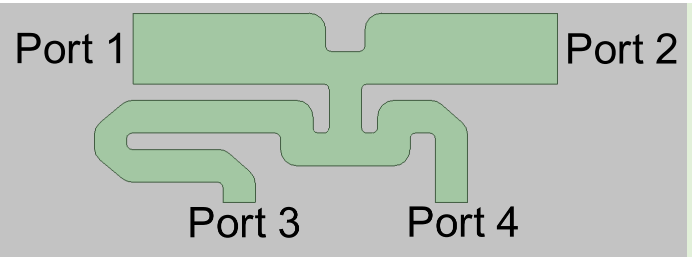

When all cavities in the manifold are detuned except, possibly, those connected to port 3 and/or 4 of one of the four-port unit networks then the reflection coefficient at Port 2 of that network is 1.

The graphs below show the response of the cavities as seen through Port 1 when one or none of them are detuned for various values of ϕ.

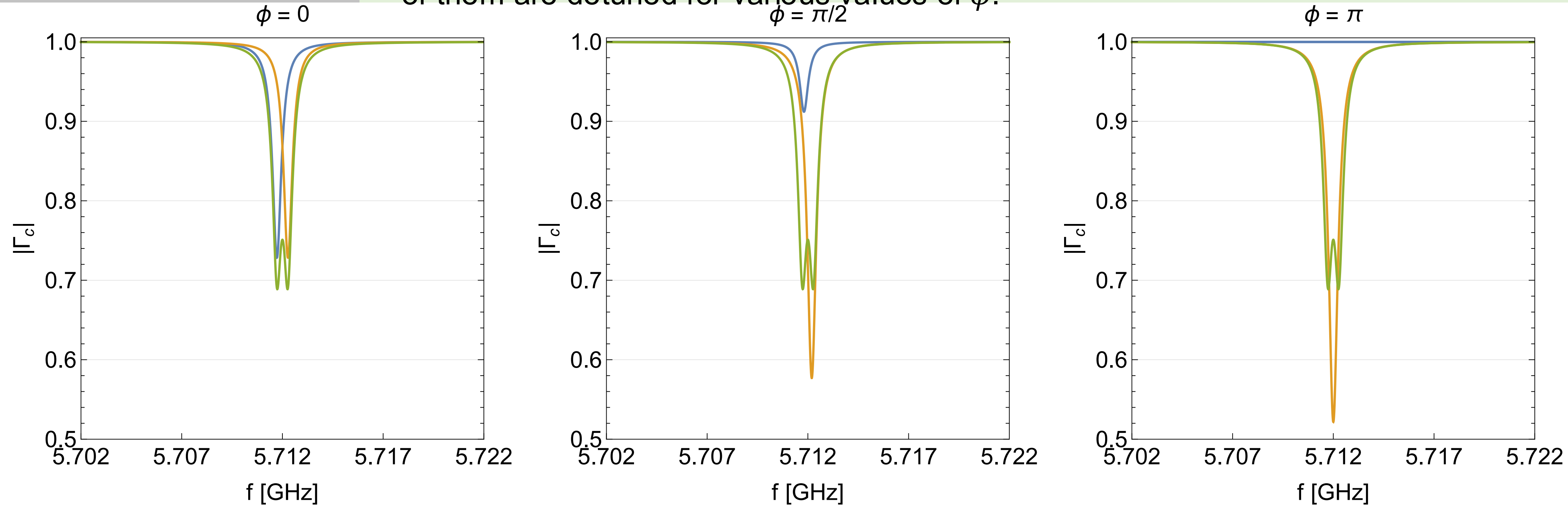

-- Blue: Response of cavity at port 3 when cavity at port 4 is detuned

-- Orange: Response of cavity at port 4 when cavity at port 3 is detuned

-- Green: Response of both cavities at port 3 and port 4

Example of Manifold -> Right Going 7x2

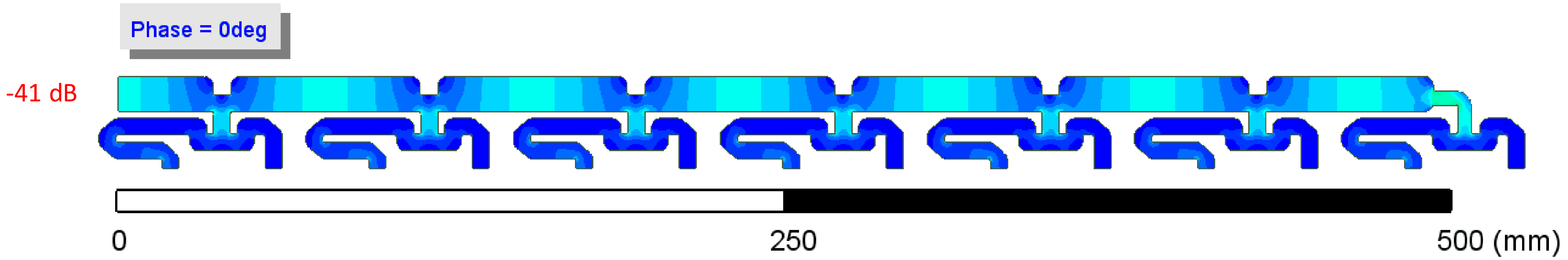

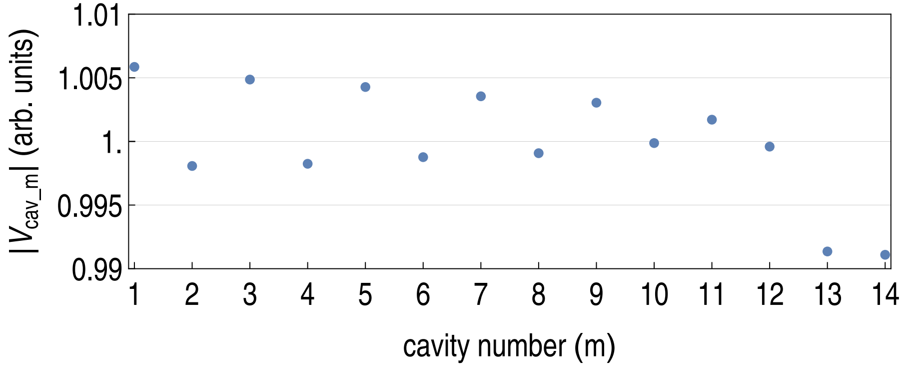

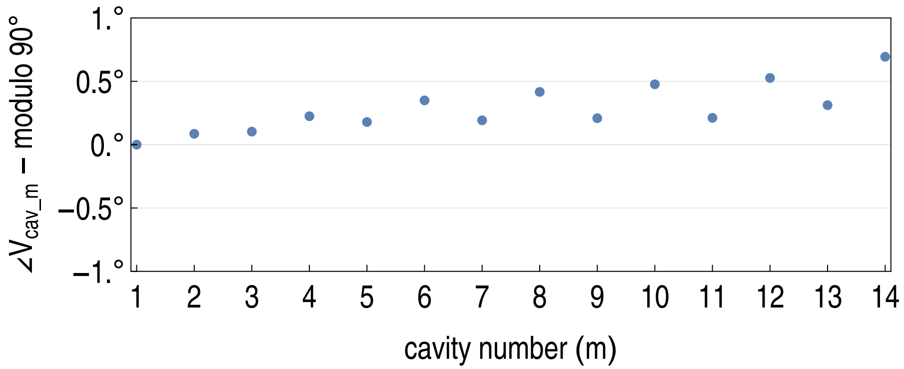

135 deg Standing Wave Structure with 2 Feed Waveguide

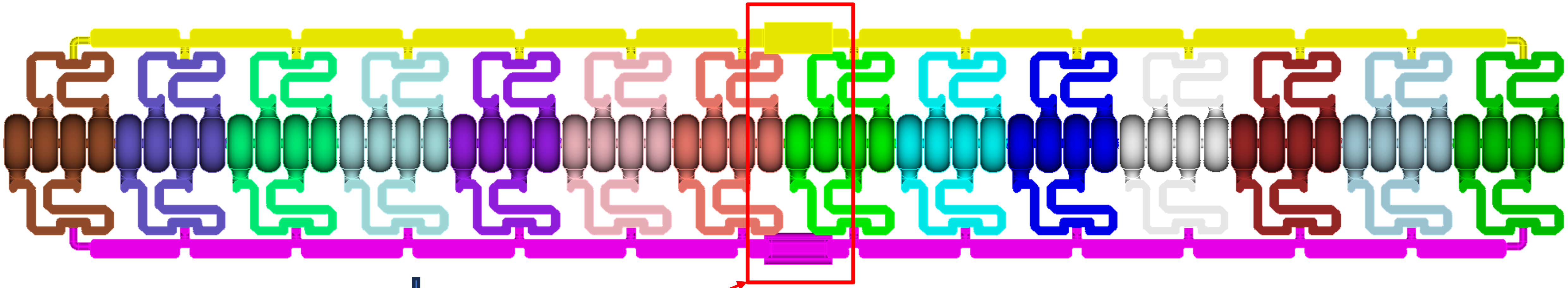

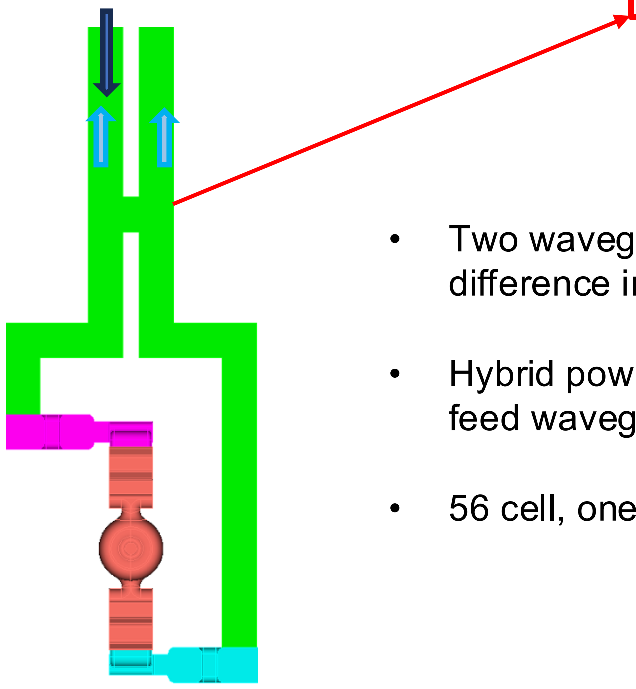

- Two waveguides need to be 135 deg difference in phase
- Hybrid power splitter to isolate the two feed waveguides
- 56 cell, one meter

High Temperature Superconductors with RF

- The main material of choice is Yttrium Barium Copper Oxide (YBCO) though other Rare Earths (REBCO) may be used to similar effect.
- The most mature form of this technology are tapes optimized for high conductivity along one axis, though experiments are ongoing with film growth on other substrates.
- Primarily used for low power high Q applications like axion cavities.

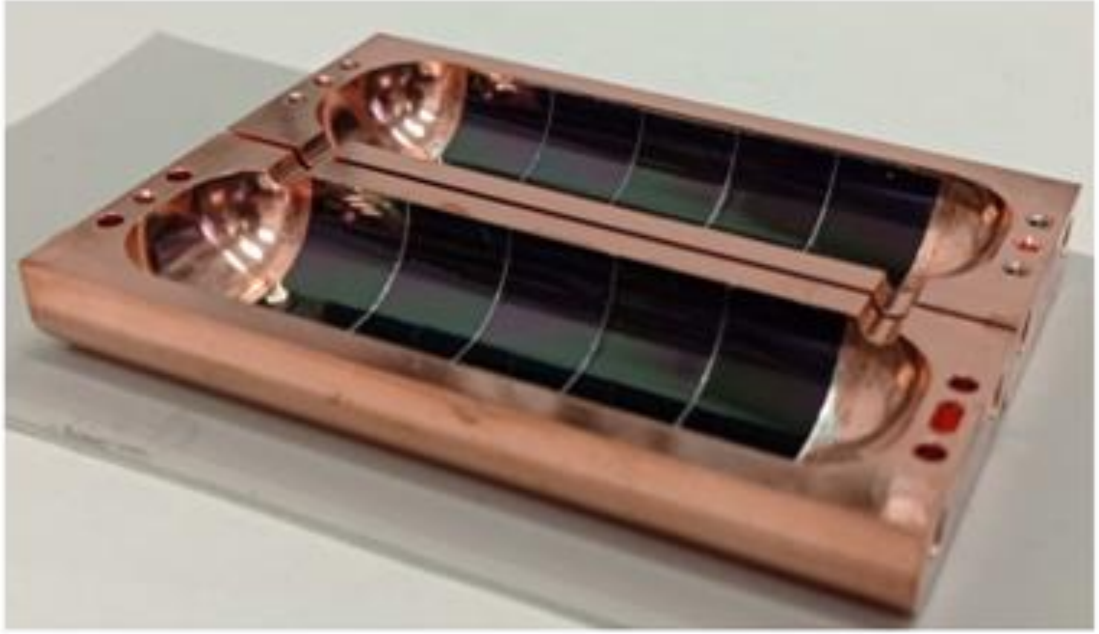

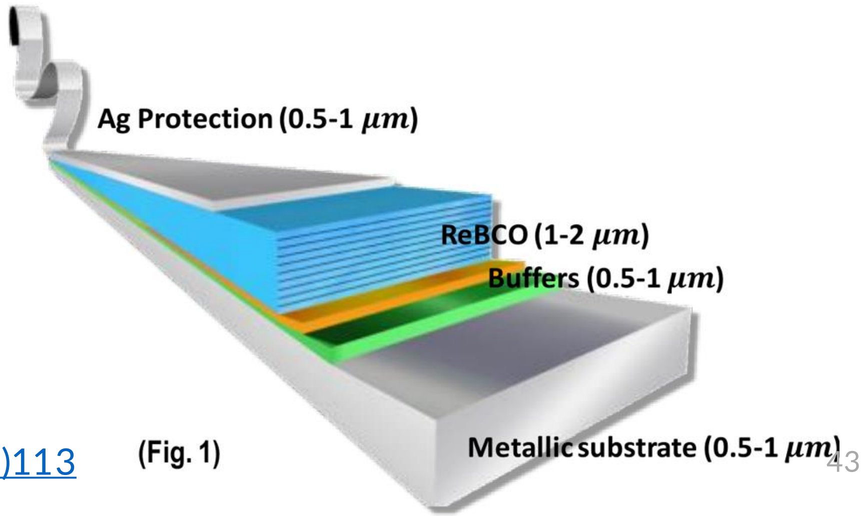

(Fig. 1)

S. Ahyoune et al., *JHEP*, vol. 2025, Apr. 2025, doi: 10.1007/JHEP04(2025)113

Applying HTS to RF design

As a first potential application, a pulse compressor cavity utilizing the TM010 mode has been built. It will be tested in a second cryostat designed for testing accelerator cavities.

This cavity is built from 8 facets with soldered YBCO tapes, allowing surface current to run along the axis of maximum conductivity.

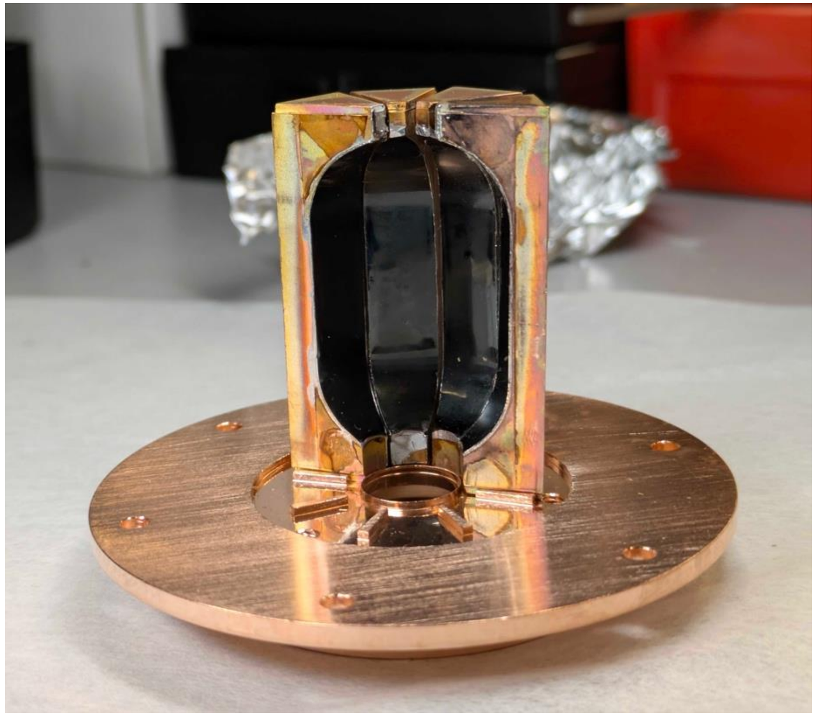

HTS Cavity

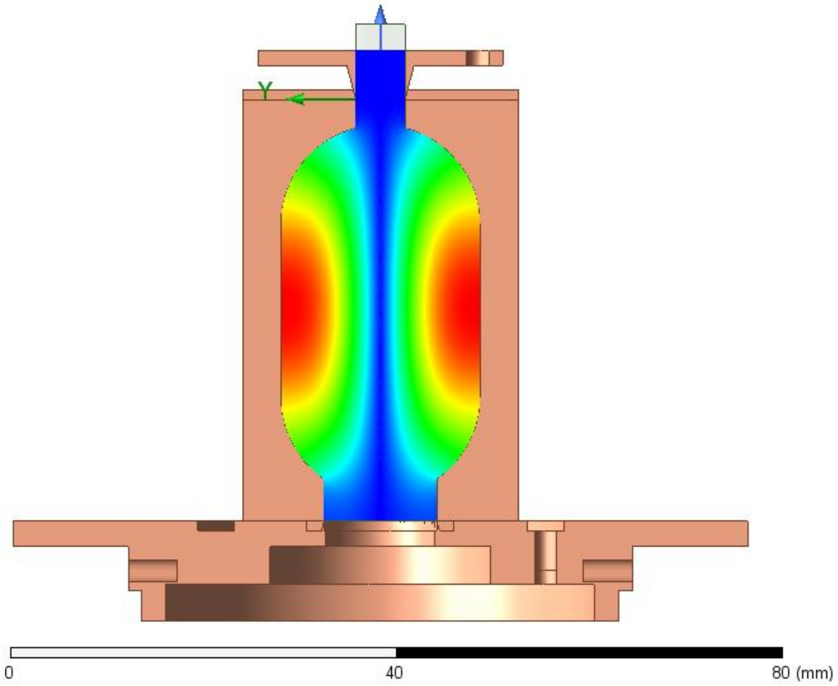

Surface current density

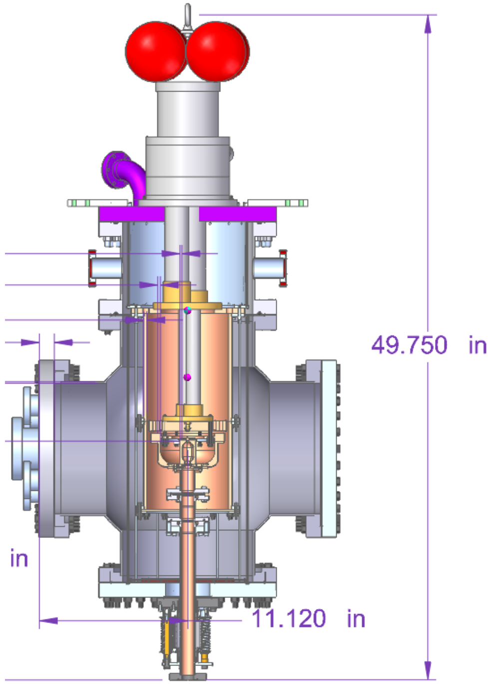

Cryostat for testing cavity

Cryogenic Measurements

Initial measurements of HTS cavity at cryogenic temperatures have been performed

Q_e remains roughly around 60000, with Q_0 rising to over 120k at 80 K

At this temperature, a copper cavity would have a Q_0 of 40k

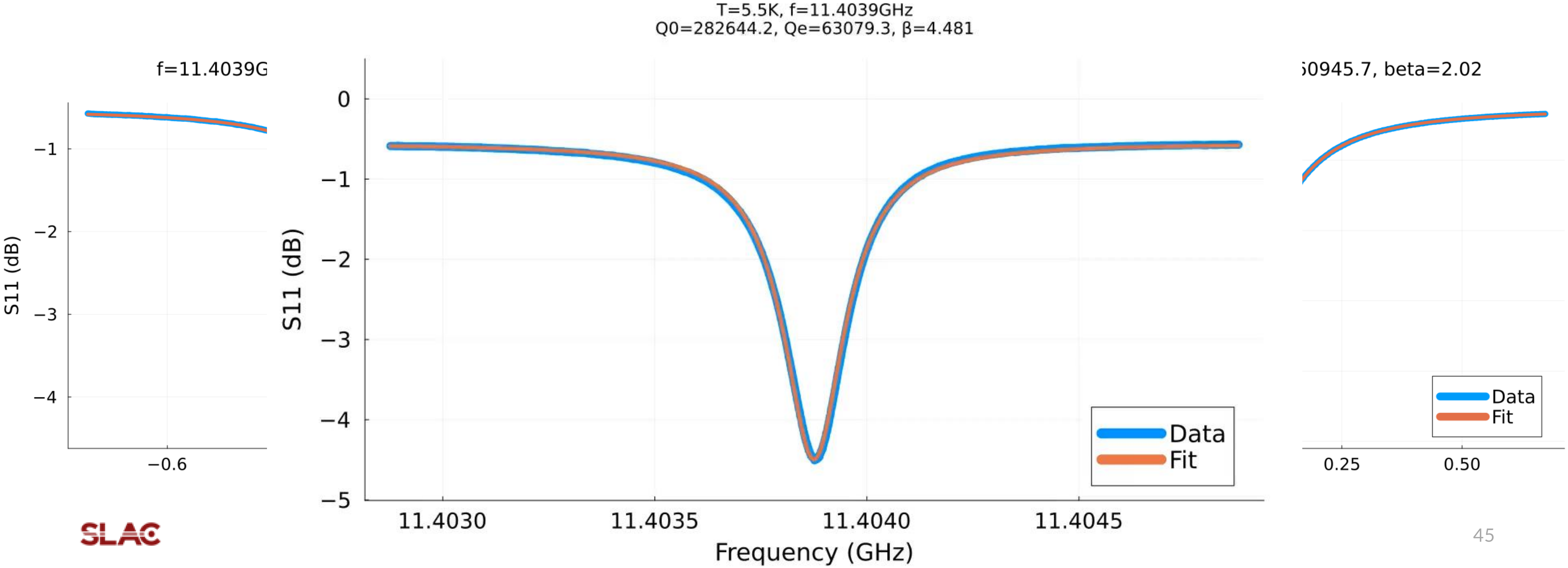

Future Plans

The next stage of our research program will be to understand the transitional dynamics of these HTS materials at MW-scale power.

Both cryostats will in turn be connected to an XL-4 klystron to be driven with up to 2 MW of power.

These measurements should provide foundational knowledge for designing future high power RF cavities.

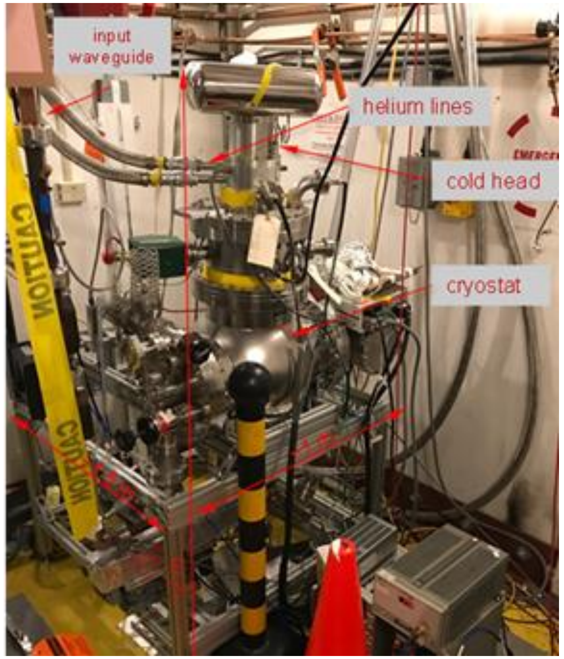

Cavity testing cryostat

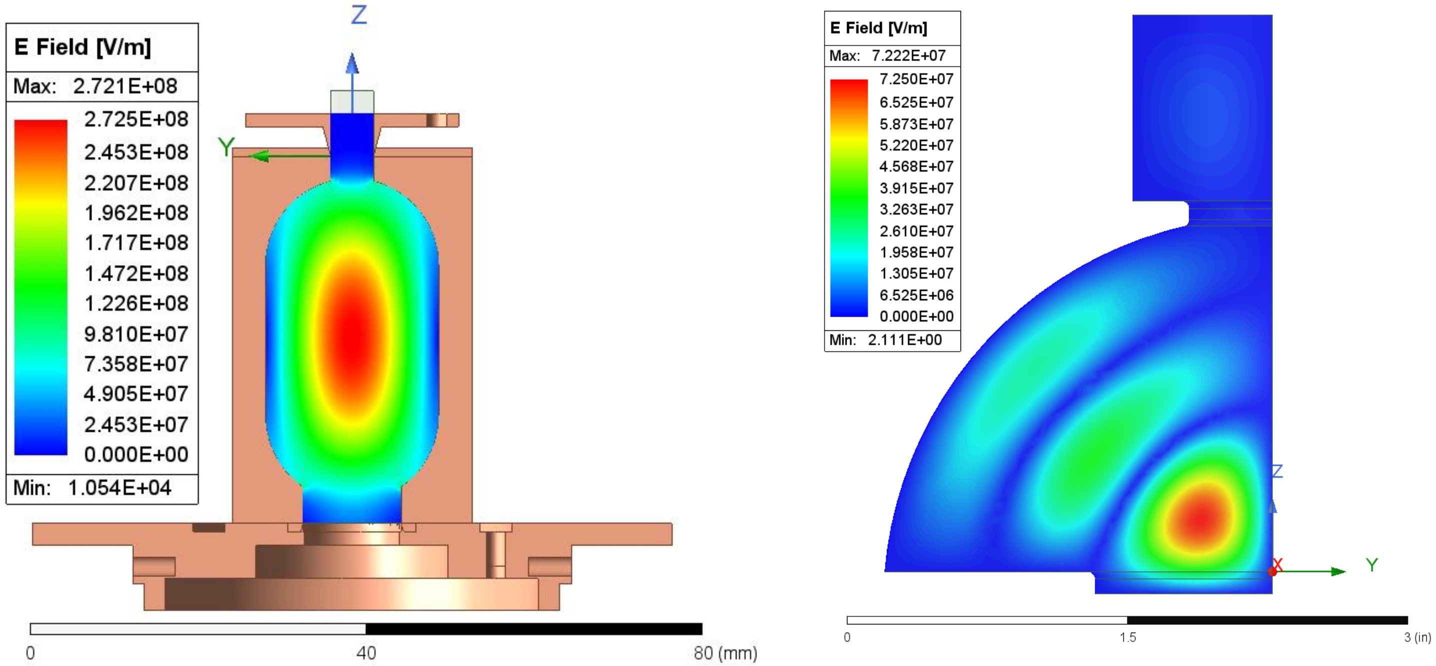

Expected electric fields at 2 MW

Future Designs at Lower Frequencies

Another crucial area of study is how the behavior of these materials scales with frequency

To this end, an S-band (2.856 GHz) cavity of similar shape is being designed

Q0 >380,000 at 80 K, fill time of 3 microseconds

These facets would require 34 mm wide tapes, which should be available in the near future

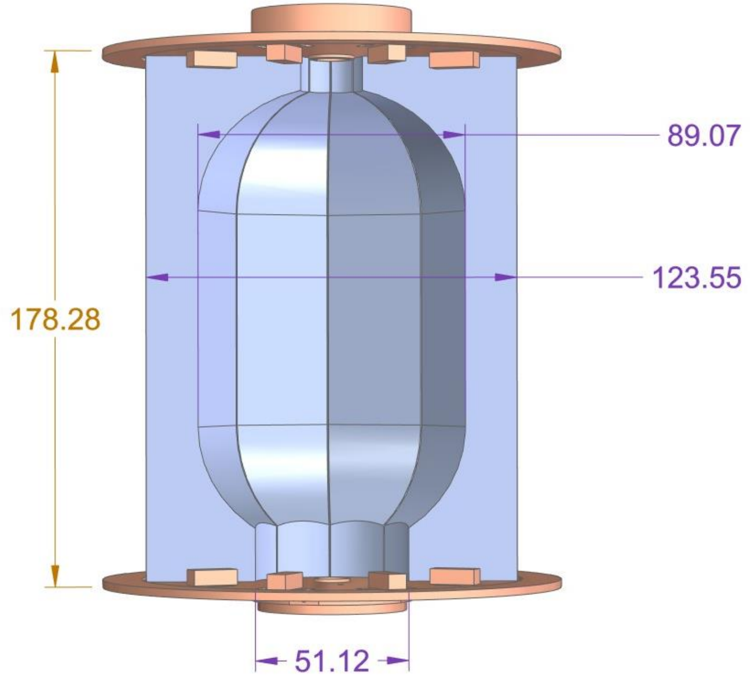

S-band Preliminary Design

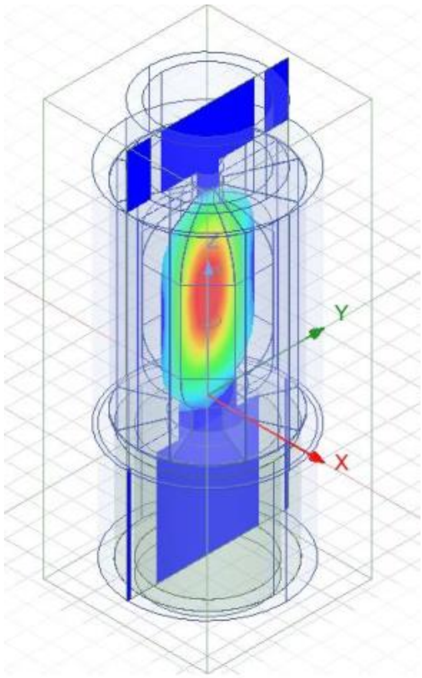

Expected electric fields

SLAC

Near-Term Applications

Medical Accelerators

- Why medical accelerators in the world
- How they feedback with HEP – workhorse accelerators in the commercial sector with stringent requirements on precision and reliability
- Cutting edge research in high dose rate radiation therapy

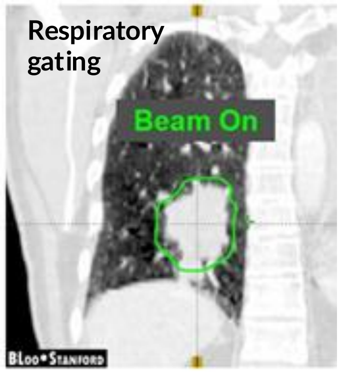

Motion Management

FLASH Therapy

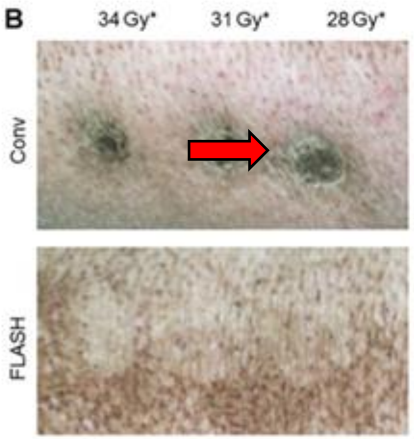

Vozenin, M.C., et al. "The advantage of FLASH radiotherapy confirmed in mini-pig and cat-cancer patients." *Clinical Cancer Research* 25.1 (2019): 35-42.

- Sub-second treatment time appears to improve healthy tissue sparing with comparable tumor control
- Demonstrated in preclinical setting with photons, electrons, and protons
- Requires high dose rate >40 Gy/L/s


Bourhis, Jean, et al. "Treatment of a first patient with FLASH-radiotherapy." *Radiotherapy and oncology* 139 (2019).

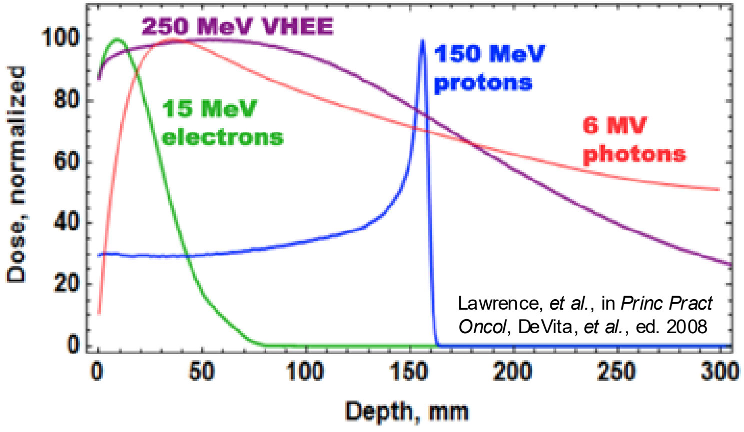

Dose profiles for various particle beams in water (beam widths r = 0.5 cm)

Image courtesy of Varian Medical Systems, Inc. All rights reserved.

Medical Accelerator R&D at SLAC

Meeting the demand for high dose rate FLASH capability

D.O.E. Accelerator Stewardship Program

High Energy Compact Cryogenically Cooled Linac System for Very-High-Energy-Electron Radiation Therapy

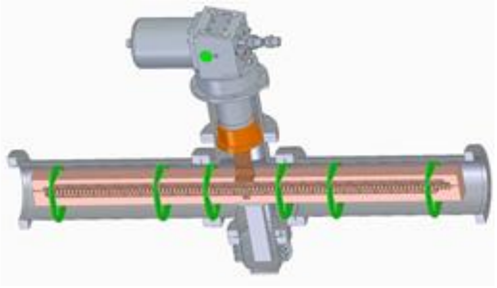

3D High Speed RF Beam Scanner for Hadron Therapy of Cancer

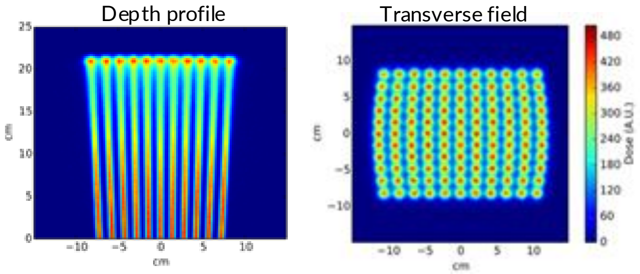

LDRD

High Gradient mm-Wave Linac for Very High Energy Electron Therapy

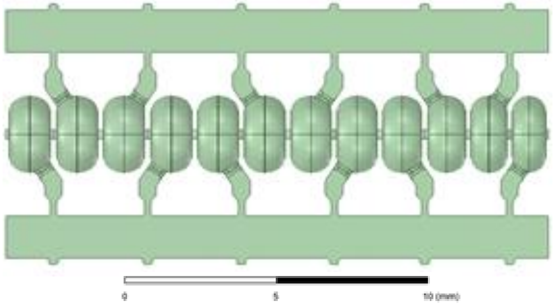

Medical Accelerator R&D at SLAC

Meeting the demand for high dose rate FLASH capability

D.O.E. Accelerator Stewardship Program

3D High S
Hadr

High Energy Compact Cryogenically Cooled Linac System for Very-High-Energy-Electron Radiation Therapy

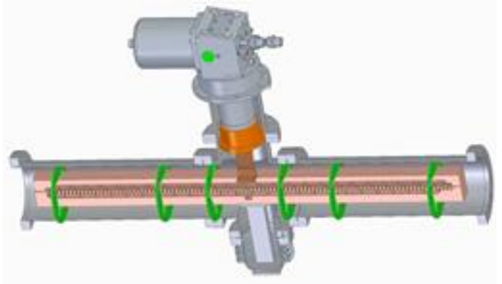

Program Objectives:

- Deliver 100 MeV electron beam from 1 m accelerator at dose rate of ≥40 Gy/s
- Accelerator design and power supply must be compatible with clinical infrastructure
- Prototype installed at Stanford Medical within 3 years

SLAC
LDRD

High Grad
Very High

Getting to FLASH VHEE capability

Cryogenic accelerator tests at X-band

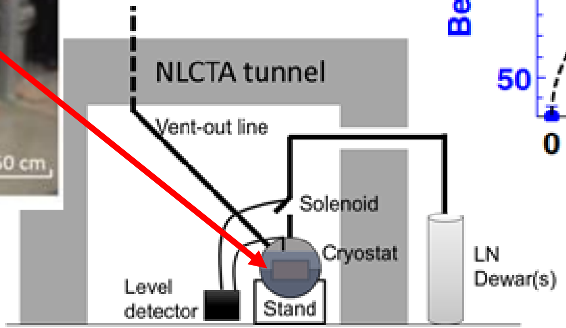

Liquid nitrogen cryostat on XTA beamline

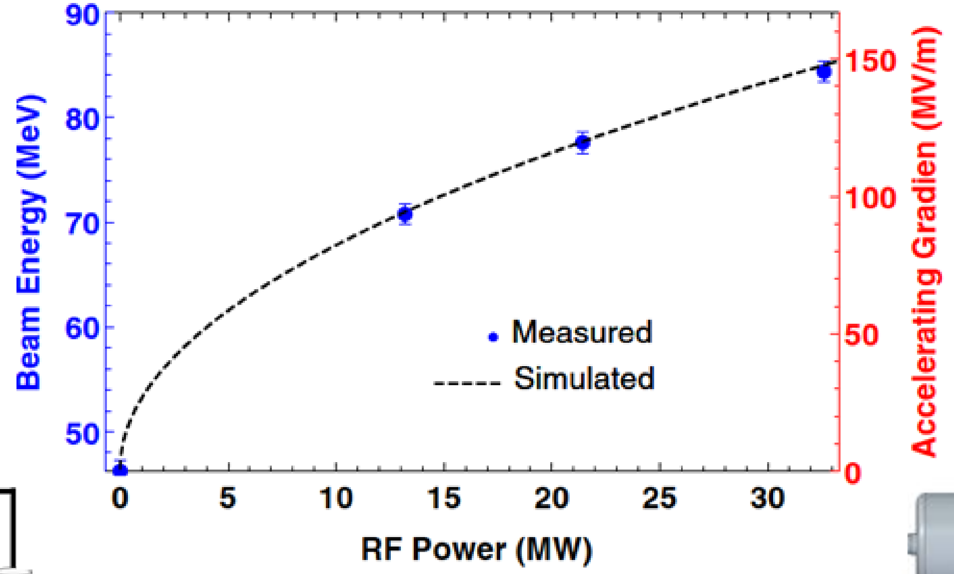

Successfully demonstrated up to 150 MeV/m gradient

Applying same approach for a 1 m structure with a single stage cold head (~250 W cooling power)

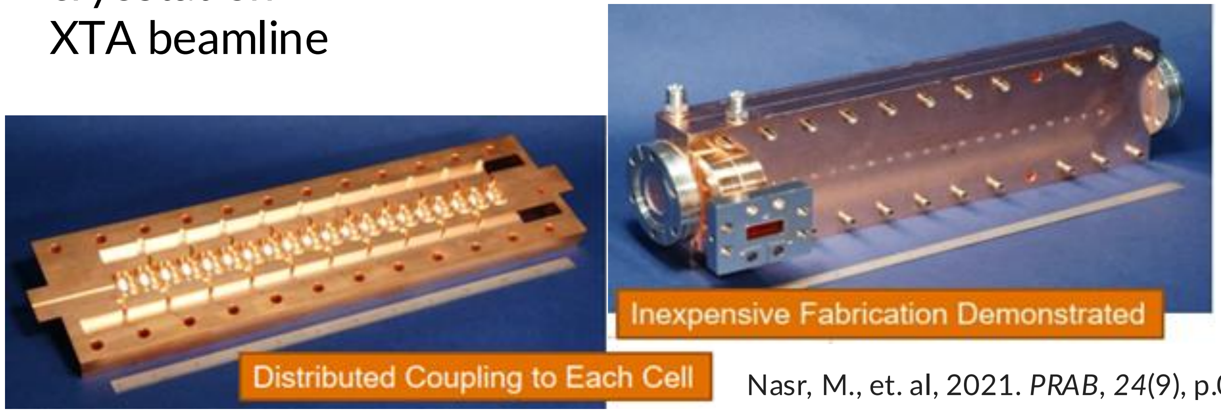

Nasr, M., et. al, 2021. *PRAB*, *24*(9), p.093201.

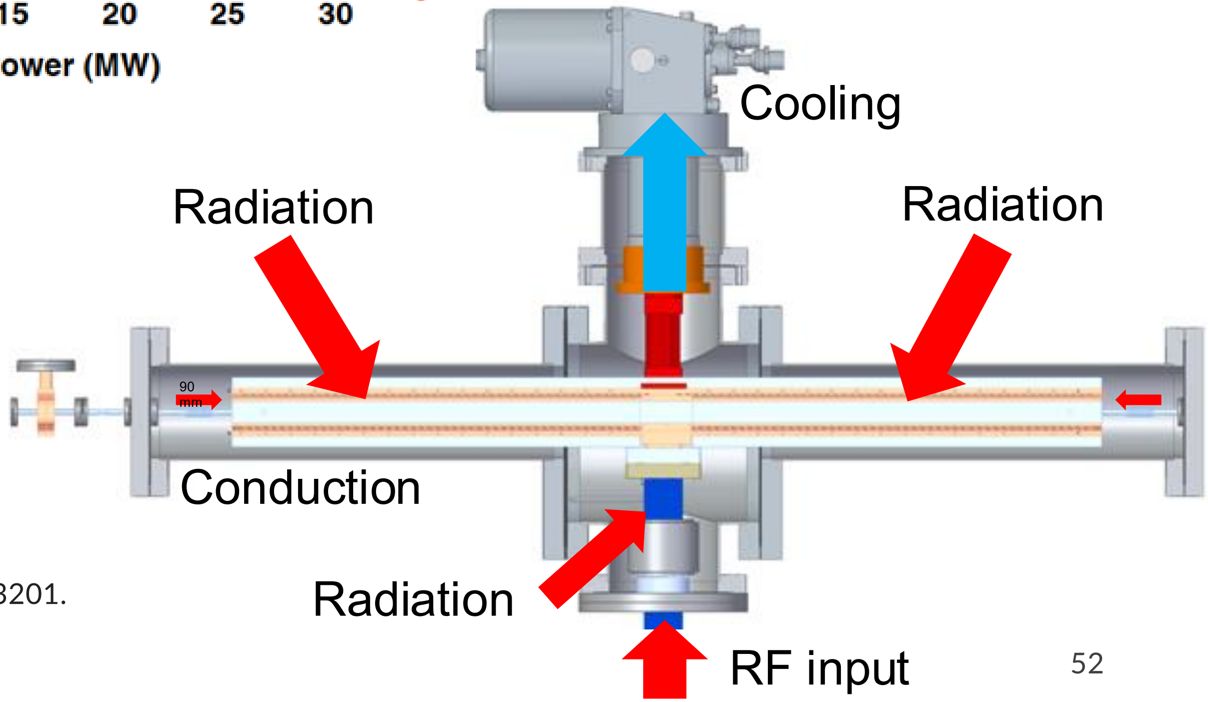

Medical Accelerator R&D at SLAC

Meeting the demand for FLASH capability

D.O.E. Accelerator Stewardship Program

High Energy Compact Cryogenically Cooled Linac System for Very-High-Energy-Electron Radiation Therapy

3D High Speed RF Beam Scanner for Hadron Therapy of Cancer

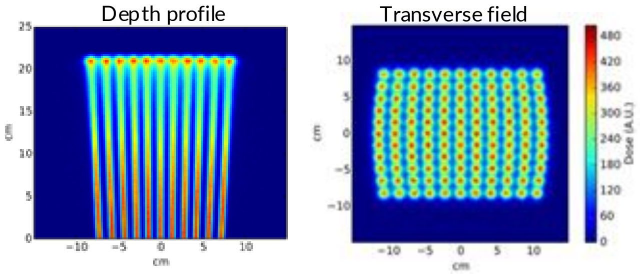

LDRD

Program Objectives:

Design component technology to cover 4 L volume with >20 Gy/L/s

- Energy modulator providing +/- 30 MeV
- Deflector providing +/- 100 mrad
- System length ≤ 2 m

RF Energy Modulator for fast layer switching

Distributed coupling linac allows flexible phasing

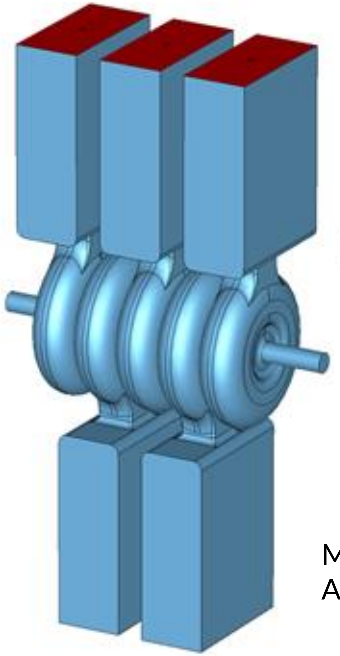

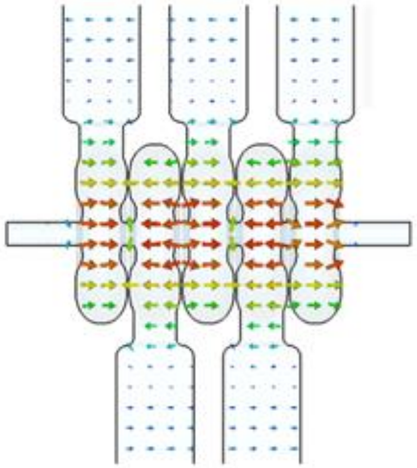

Modeling in ANSYS-HFSS

Parameter	Value
Frequency	2.856 GHz
Beam aperture (diameter)	1.05 cm
Phase advance per cell	160°
Quality factor Q_0	11936
External quality factor Q_{ext}	11911
Shunt impedance r_s	54.8 MΩ/m
r_s/Q	4.6 kΩ/m
Average gradient E_a	$15\ \mathrm{MV/m} \cdot \sqrt{P/(100\ \mathrm{kW})}$
E_{peak}/E_a	2.26
$H_{peark} Z_0/E_a$	1.25
Pulsed heating temp.	$0.53°\mathrm{C} \cdot [P/(100\ \mathrm{kW})]\sqrt{t_p(\mu s)}$

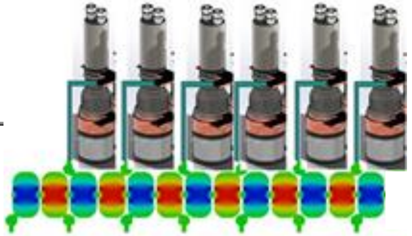

Franzi et al., LCWS 2018

10 kW avg input
Initial Temp: 22°C
Max Temp Rise: 33.5°C

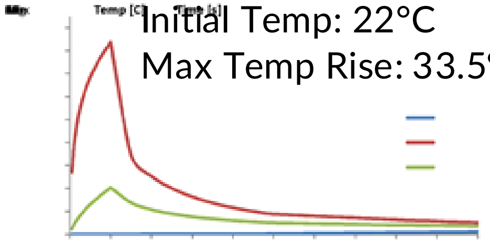

1 m structure with 400 kW per cell reaches 30 MV/m gradient for nonrelativistic protons (β ~.5)

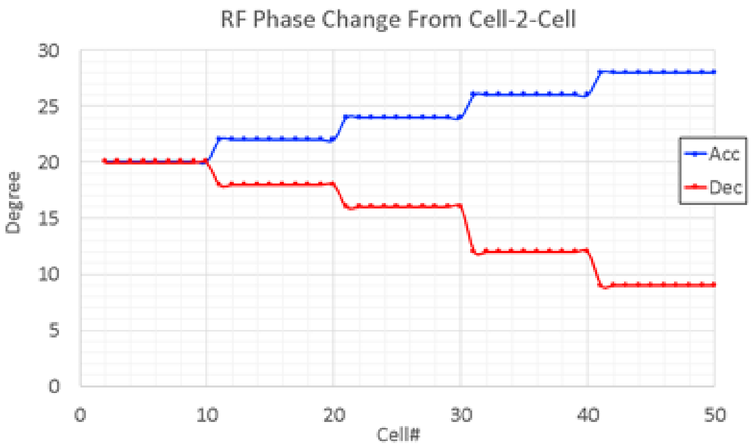

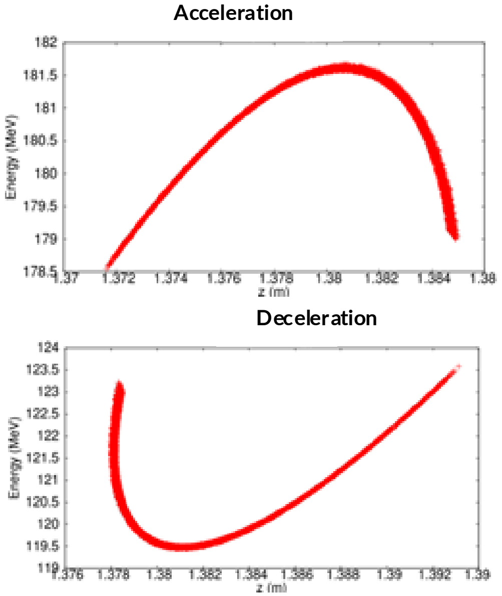

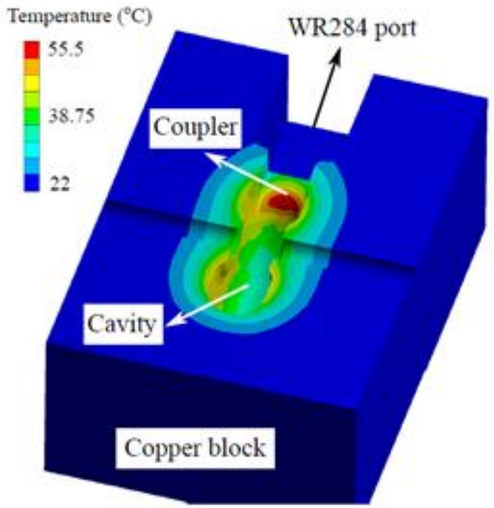

Synergy with HEP accelerator development

Linac designs for EIC and C^3 address challenges for proton energy modulator

Proton energy modulator prototype provides informative results for high gradient C-band work

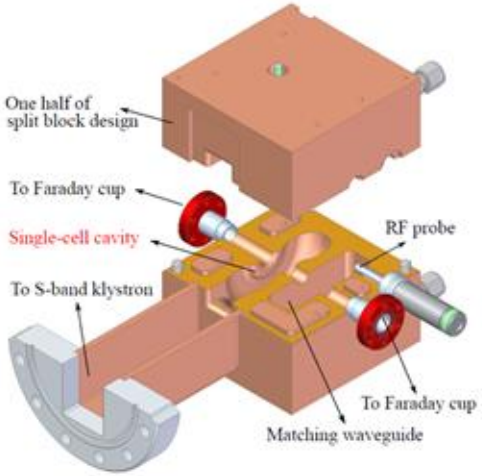

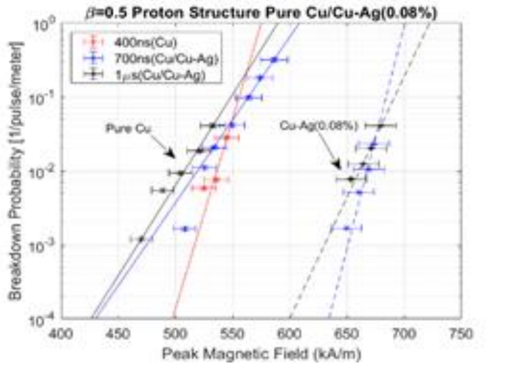

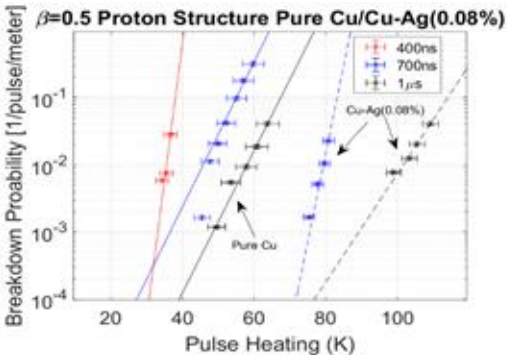

M. Zuboraj, IPAC'22 Proceedings preprint

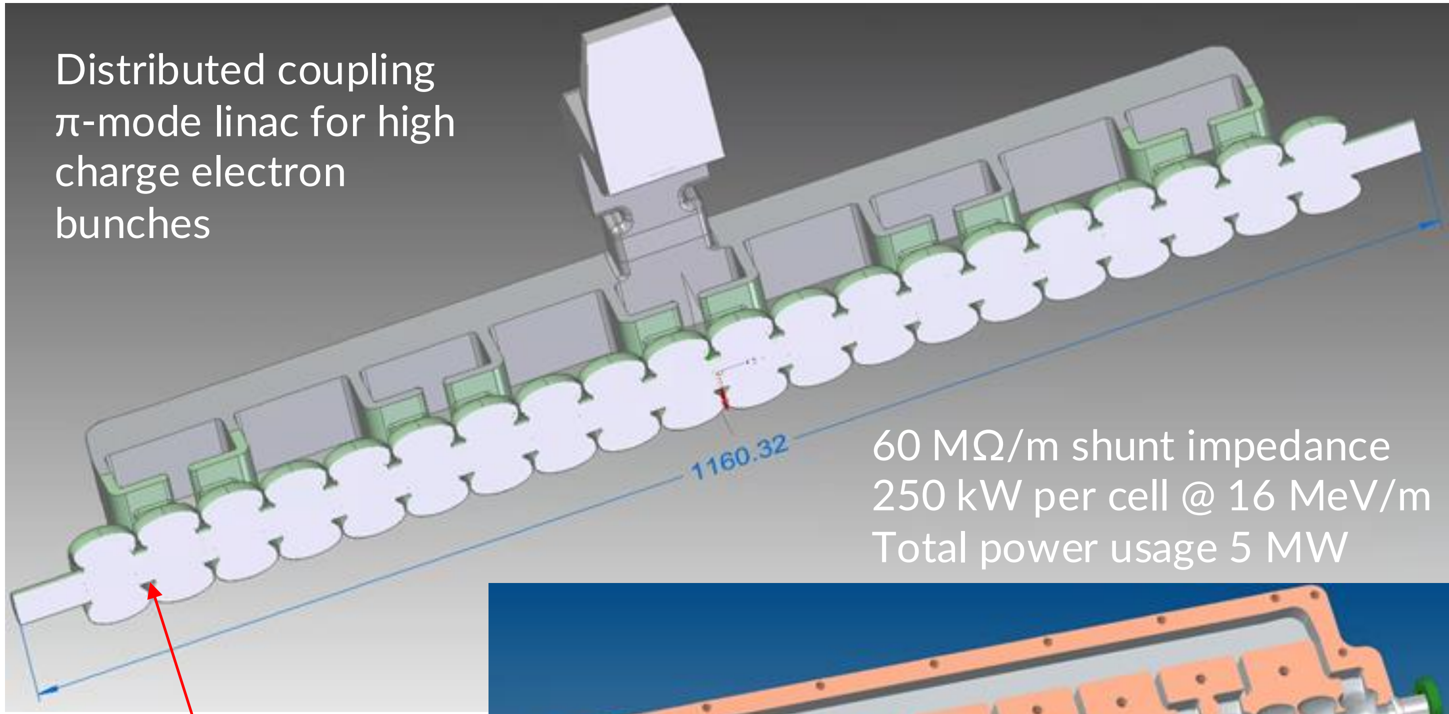

Distributed coupling π-mode linac for high charge electron bunches

60 MΩ/m shunt impedance
250 kW per cell @ 16 MeV/m
Total power usage 5 MW

Large iris aperture

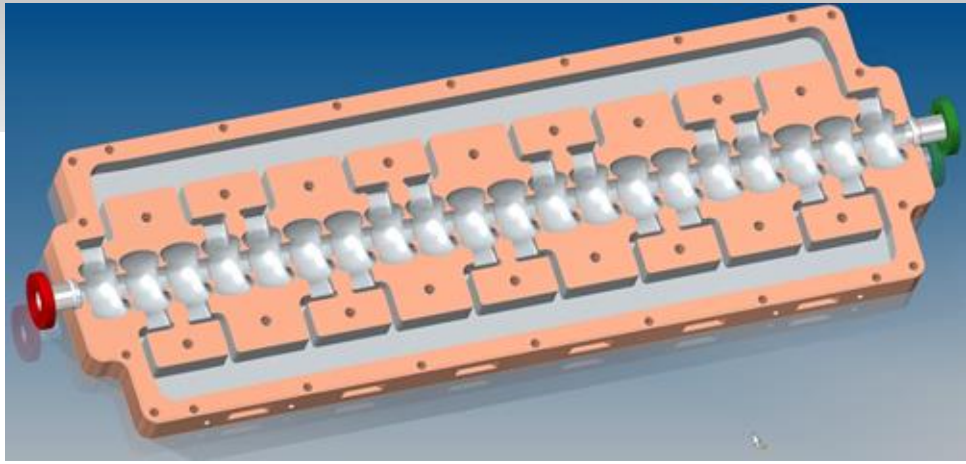

RF deflector for pencil beam scanning

TE_{11}–like cavity for high transverse shunt impedance inspired by LHC crab cavities

- Design goal: 100 mrad deflection
- Posts protruding into pillbox determine cell polarization
- Additional cells with wider irises
- Up to 48 mrad kick in 10 cell structure at 40 K

6 cell structure for 15 mrad kick

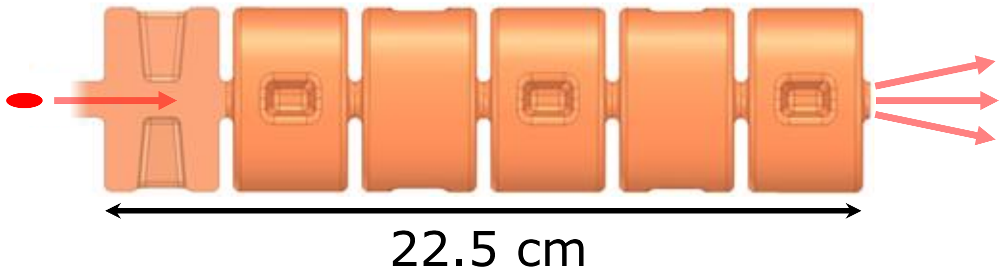

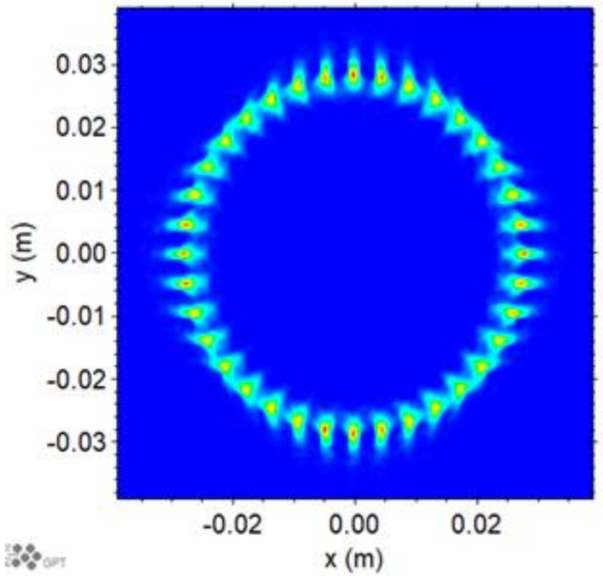

Density plot of beamlet distribution
- 2 m downstream of deflector entrance
- Cumulative 36 shots (10° interval)

Design parameters	
Frequency	2.856 GHz
Cell period, d	37.5 mm
Q	6996
shunt impedance	66.8 MΩ/m
Dissipated power	800 kW
Integrated V_y	1.415 MV
Kick	37.73 MeV/m

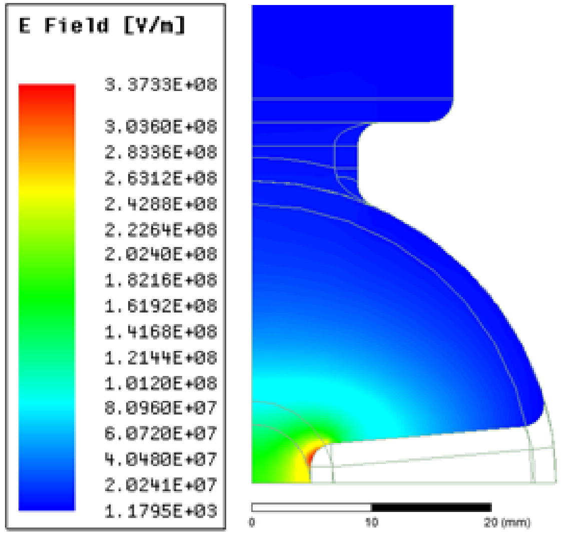

Boost with PMQ's?

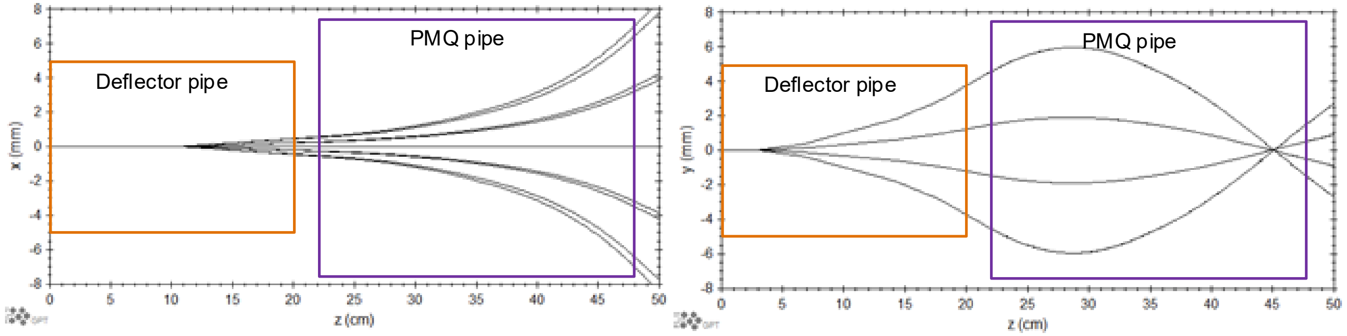

Magnifying the RF steering with PMQ

PMQ for C^3 can be tested for deflector, benchmarking performance of cryogenic equipment

Enhance transverse proton steering from RF deflector with permanent magnet quadrupole

Electron Energy Corporation (EEC) design for compact (47 kg), tunable, cryogenic PMQ

Specs: 2 Halbach cylinders, 12 cm each, 202 T/m gradient

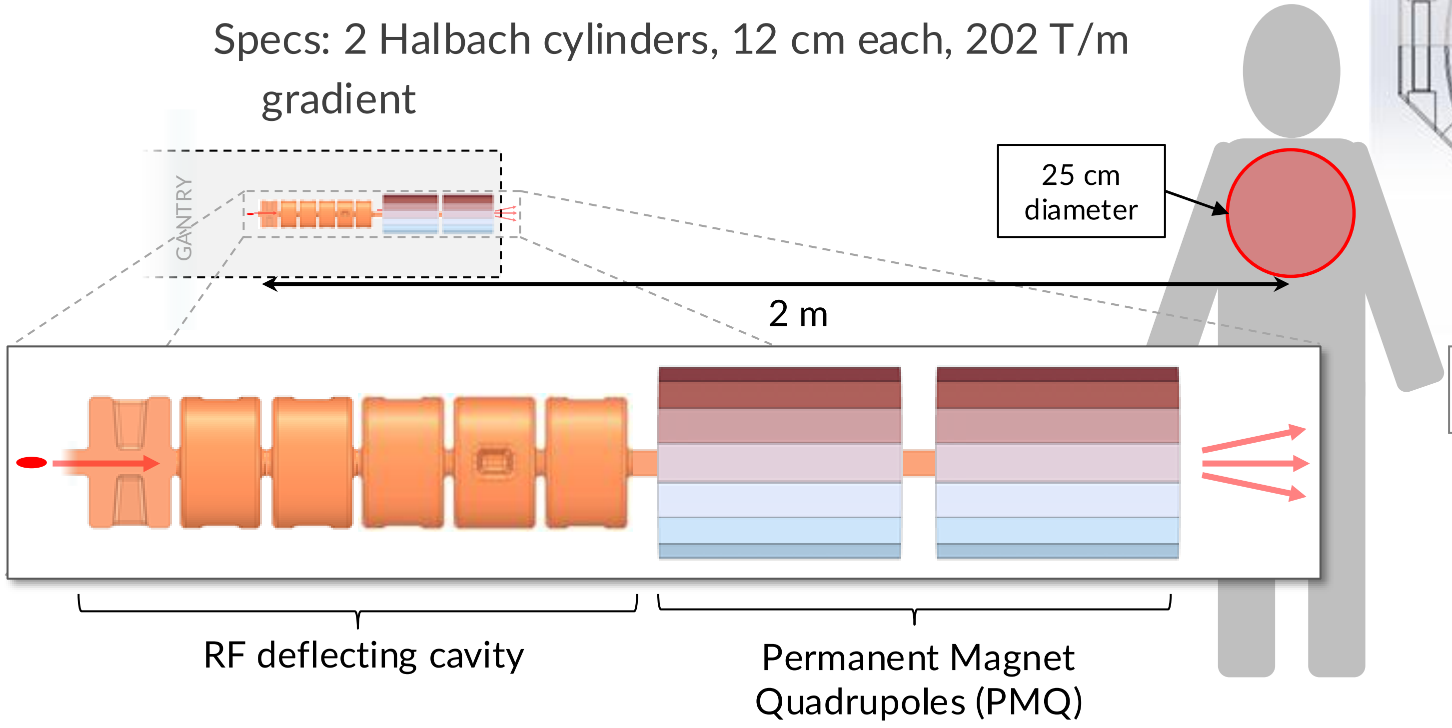

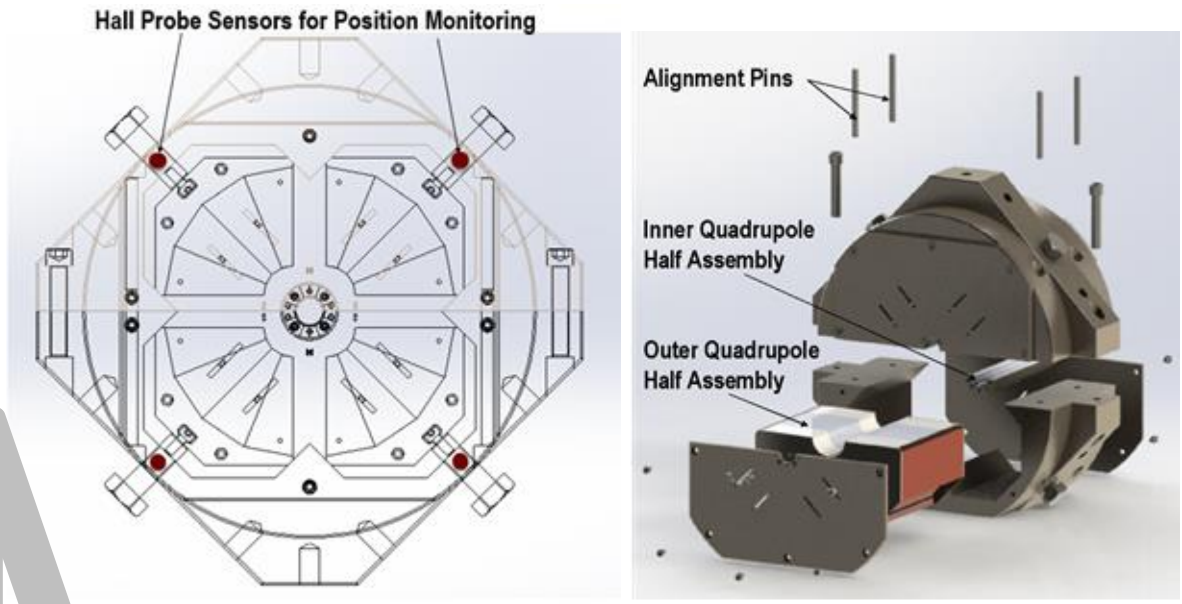

May contain trade secrets or commercial or financial information that is privileged or confidential and exempt from public disclosure. A paragraph containing trade secret or commercial or financial information is marked with brackets [ ].

Cryomodule schematic for C^3

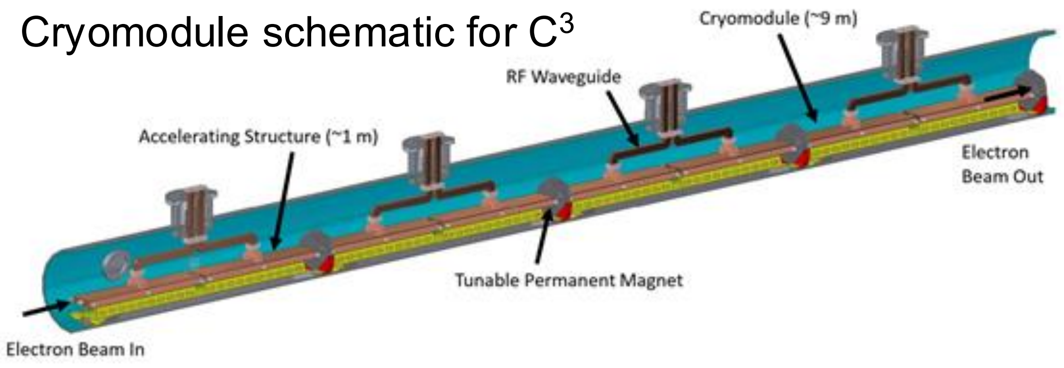

Partnering with clinicians to study efficacy

Dose Deposition Study (J. Mendez, UCSF)

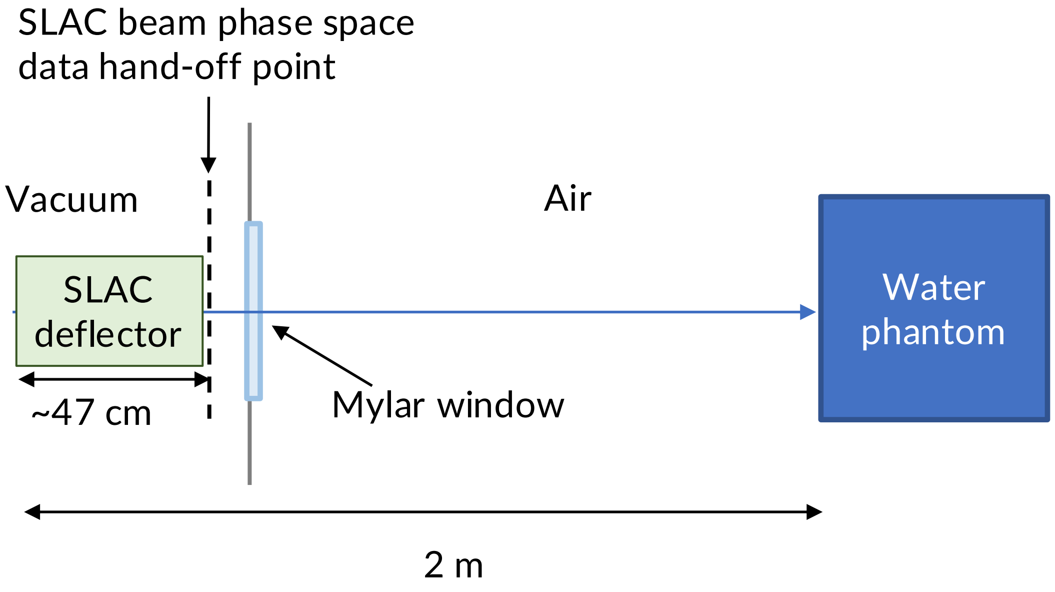

Stanford MEDICINE | Radiation Oncology

UCSF Department of Radiation Oncology

Northwestern Medicine

LOMA LINDA UNIVERSITY School of Medicine

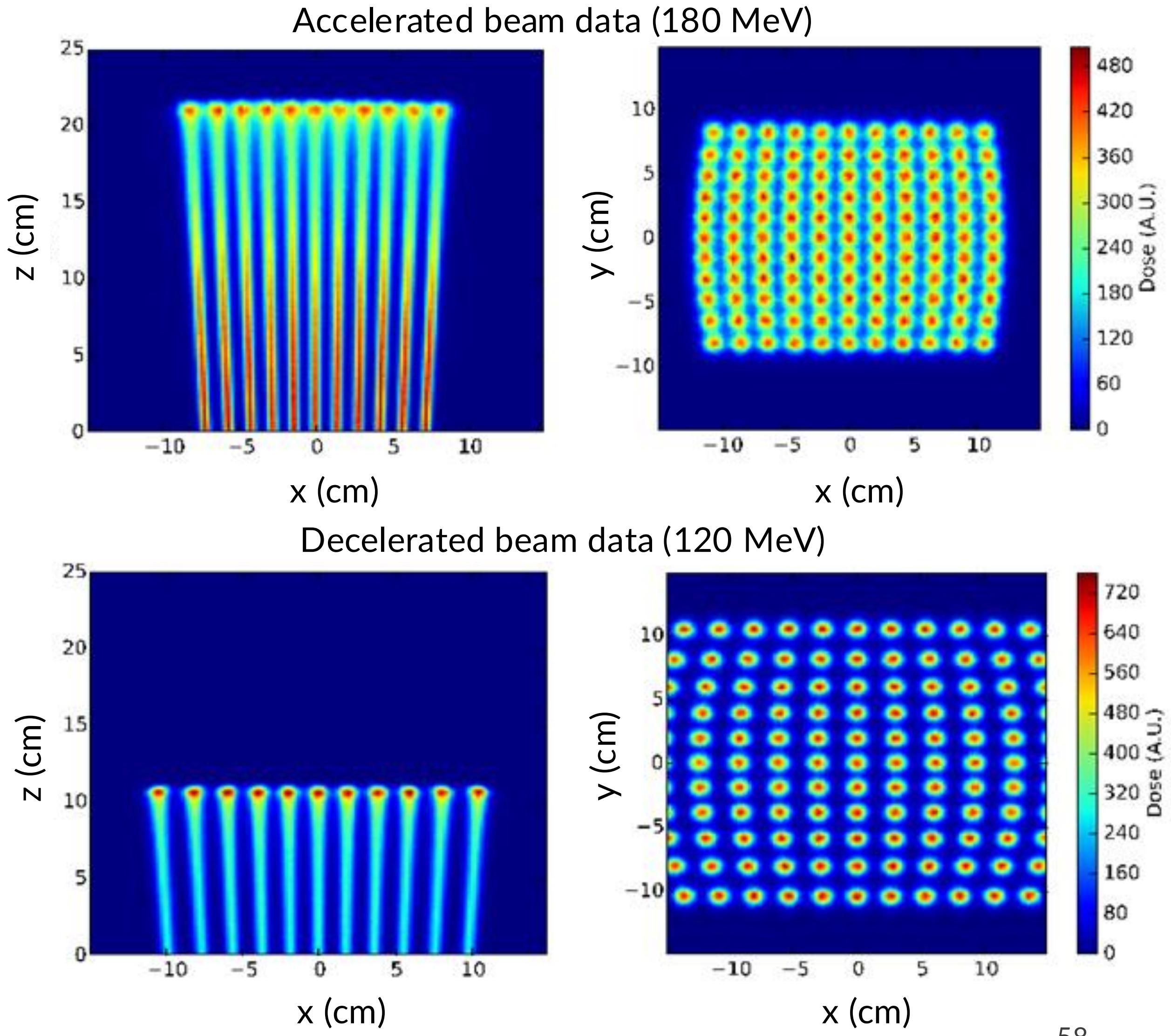

Conclusion

Distributed coupling provides a versatile platform for optimizing rf accelerators

Cold-copper provides distinct advantages for applications requiring compactness and high gradient

COLD will play a central role in scaling of this technology to higher energy

Future work on structures could improve efficiency or relax alignment tolerances

Opportunities to consider more exotic – hybrid NCRF/SRF – could further improve the performance of linacs

Technology industrialization proceeding in parallel through applications -> for example medical

Questions?

Backup

RF Sources Available vs. Near Term Industrial Efforts

RF sources and modulators capable of powering CCC-250 commercially available

Plan to leverage significant developments in performance (HEIKA) of high power rf sources – requires industrialization

Los Alamos NATIONAL LABORATORY EST. 1943

New 50 MW peak power C-band klystron installed in September 2019

BVEI X-band 50 MW 57% COM Prototype

SLAC BAC Prototype
S-band Retrofit +10% efficiency, 73 MW

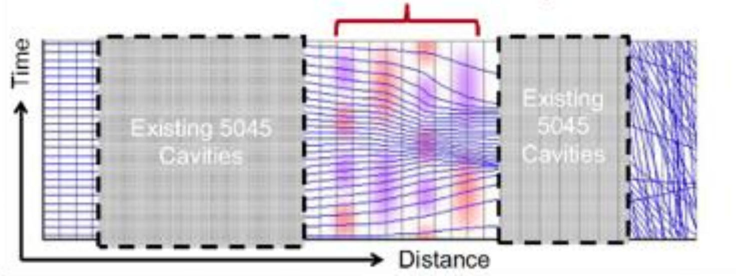

Near Term Industry

20-MW X-band Klystron

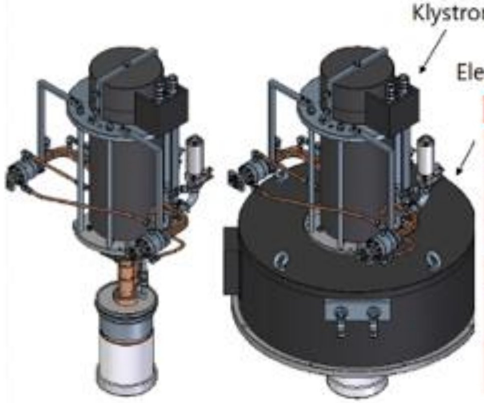

Perveance : 1.25

Parameter	Sim. Target	Design result
Beam voltage[kV]	265 (<290)	265
Beam current [A]	170.3 (<195)	170.3
Output power [MW]	>23	24.3
Efficiency [%]	>51	53.8
Drive power [W]	~120 (<400)	120
Max. electric field strength [kV/mm]	<64.5 (at 1.5 μs)	60.4
Stability	No reflected electrons	OK

* Actual efficiency is estimated to be 46 - 48%.

Canon
CANON ELECTRON TUBES & DEVICES CO., LTD.

Two tubes have been built and tested up to 20MW

High Efficiency Klystrons

Please See I. Syratchev's Talk for Many Great Examples from Designs to Prototypes

Retro-fit High Efficiency 50 MW, 12 GHz klystron (CERN/CPI).

Saturated efficiency & RF power

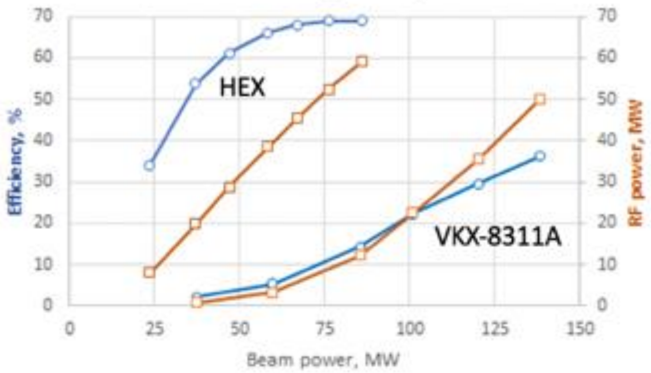

- Re-used solenoid.
- Increased life time (> factor 2)
- Reduced modulator power (~ factor 2)
- Increased power gain (10 dB)
- Reduced solenoidal field

Prototype fabrication is under negotiation within CPI/INFN/CERN collaboration.

I. Syratchev, CLIC PM #41, 13.12.2021

3D Particle-in-Cell (PIC) simulations

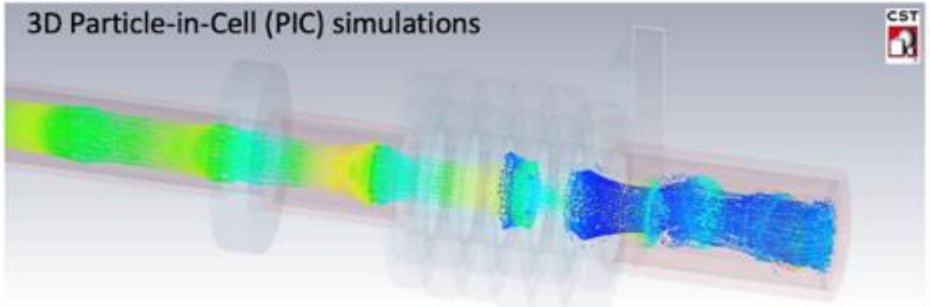

	VKX-8311A	HEX COM_M (CERN/CPI)
Voltage, kV	420	420
Current, A	322	204
Frequency, GHz	11.994	11.994
Peak power, MW	49	59
Sat. gain, dB	48	59
Efficiency, %	36.2	69
Life time, hours	30 000	85 000
Solenoidal magnetic field, T	0.6	0.37
RF circuit length, m	0.316	0.316

https://indico.cern.ch/event/1101548/contributions/4635964/attachments/2363439/4034986/CLIC_PM_13_12_2021.pdf

Makes a Unit of This Distributed Feed (n_0: Number of Networks to be Cascaded in Each Manifold)

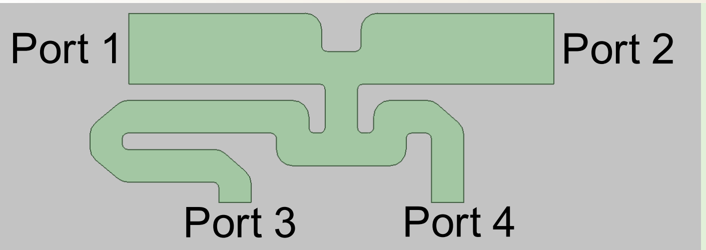

Port 3 feeds n^{th} cavity at ϕ_{c_n} phase.

Port 4 feeds $(n+1)^{th}$ cavity at $\phi_{c_{n+1}} = \phi_{c_n} - 135° \times 2 = \phi_{c_n} + 90°$ phase.

$$S = -\frac{1}{2n_0+1}\begin{pmatrix} 1 & 2n_0 & -\sqrt{2n_0} & -i\sqrt{2n_0} \\ 2n_0 & 1 & \sqrt{2n_0} & i\sqrt{2n_0} \\ -\sqrt{2n_0} & \sqrt{2n_0} & \frac{1}{2}\left(2n_0 - 1 + e^{i\phi}(2n_0+1)\right) & \frac{i}{2}\left(2n_0 - 1 - e^{i\phi}(2n_0+1)\right) \\ -i\sqrt{2n_0} & i\sqrt{2n_0} & \frac{i}{2}\left(2n_0 - 1 - e^{i\phi}(2n_0+1)\right) & -\frac{1}{2}\left(2n_0 - 1 + e^{i\phi}(2n_0+1)\right) \end{pmatrix}.$$

Here, ϕ is an arbitrary phase factor.

- A compact four-port network is designed to achieve S_{11}, S_{12}, S_{13} and S_{14}. Then ϕ is determined as, [Shumail]

$$\phi = Arg[-(S_{33} + iS_{34})] = Arg[-iS_{43} - S_{44}].$$

- For tuning purpose, the reflection coefficient at ports 3 or 4 of a detuned cavity should be $e^{i\theta}$ where $\theta = -(\phi + k\pi)/2$ and k is an odd integer.

- The guide length l_c (for ports 3 and 4) to the plane where cavity presents a reflection coefficient of -1 when detuned, is determined as:

$$l_c = \frac{m\pi - \theta}{4\pi}\lambda_g.$$

Here, m is an odd integer and λ_g is guide wavelength of port 3 and 4.

HOM Detuning and Damping

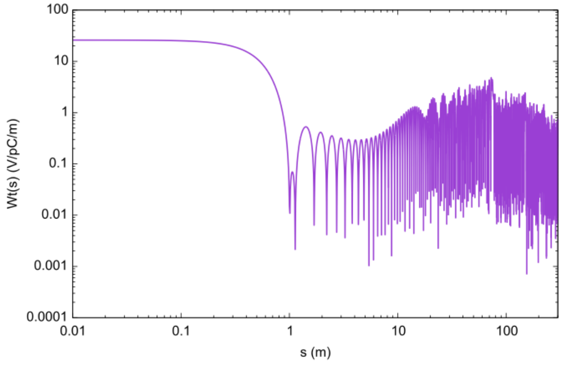

Effect of detuning

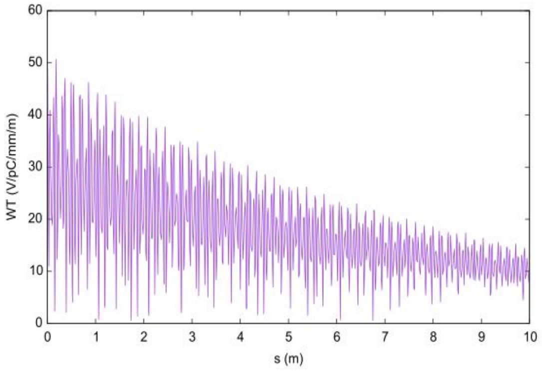

Effect of damping

Past Work on RDDS Structure Wakefield Damping

Round Damped Detuned Structure (RDDS)

RDDS structure
HOM couples to manifold
via slots cut into disk

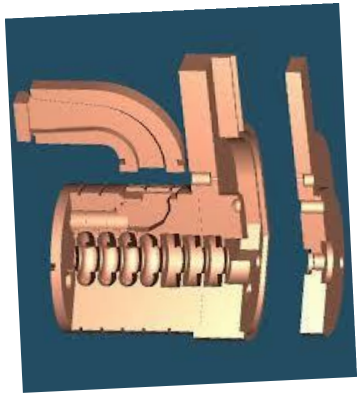

Manifold matched to
external HOM load

Wakefield profile for
Detuned Structure and
Damped Detuned
Structure

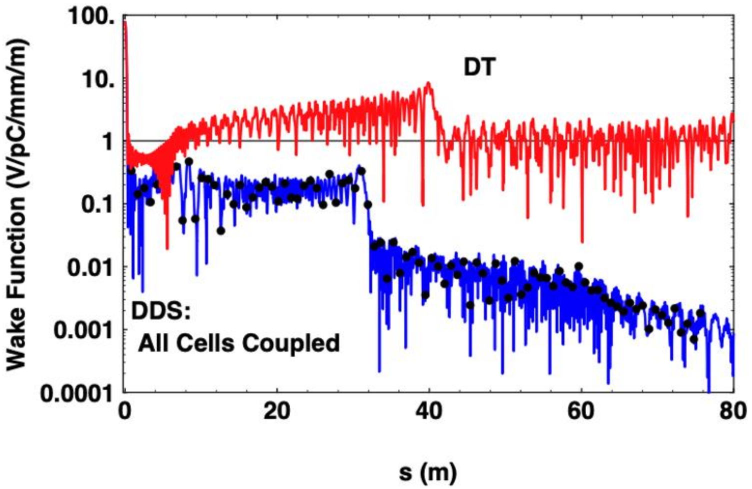

NLC X-Band Traveling Wave Structure Detuning

NLC RDDS structure

- 206 cells
- Gaussian detuning vis aperture (1st band) and disk thickness (6th band)

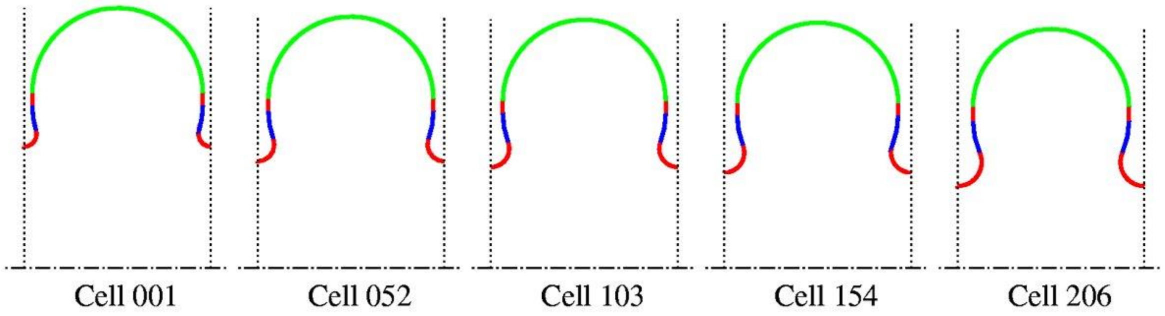

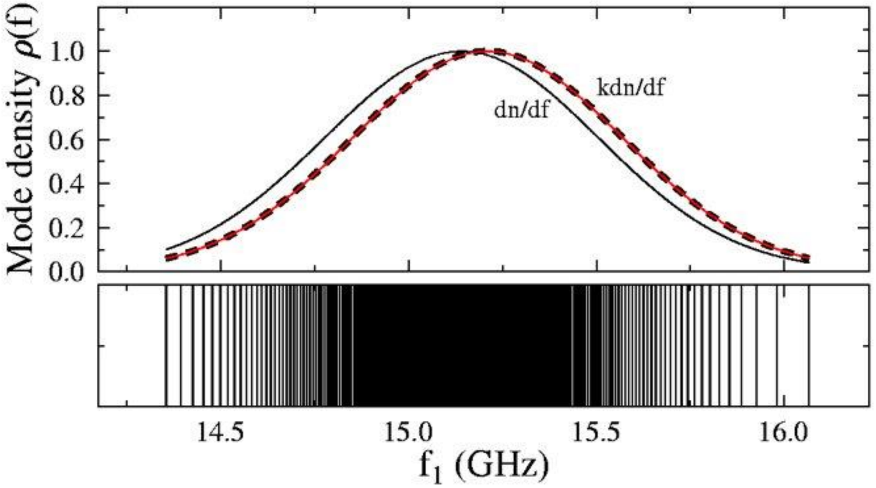

Dipole mode spectrum (1st band)

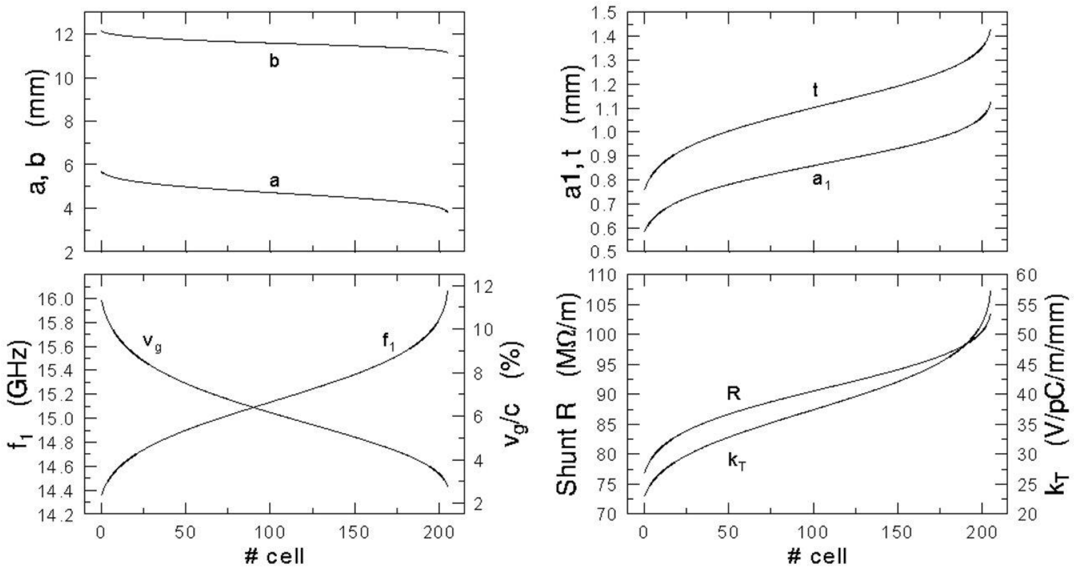

Cell dimension for HOM detuning

C-Band 135/deg Dipole detuning via Iris Radius “a” – Not effective

Cell-to-cell phase advance: 135 deg

- Cell length: 19.682 mm
- Detuning using iris “a”

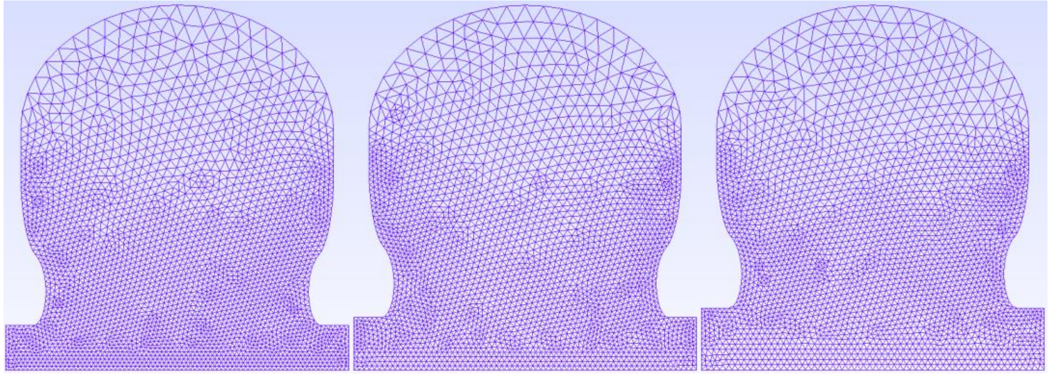

a=2.55mm
R=129 Mohm/m

a=3.00mm
R=122 Mohm/m

a=3.55mm
R=114 Mohm/m

(vg/c=0.056%)

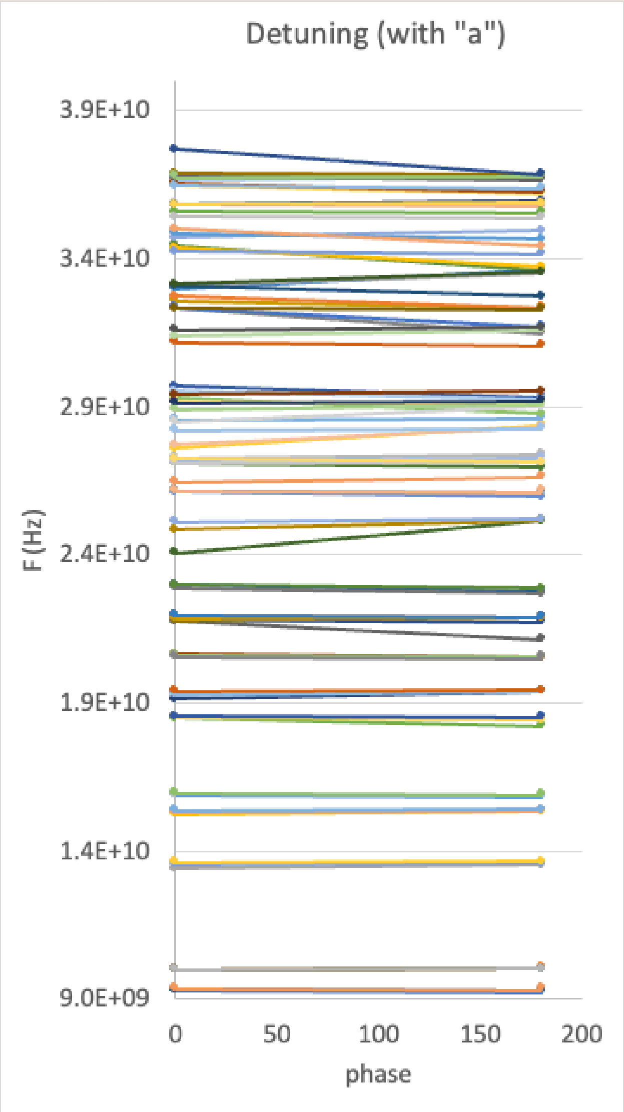

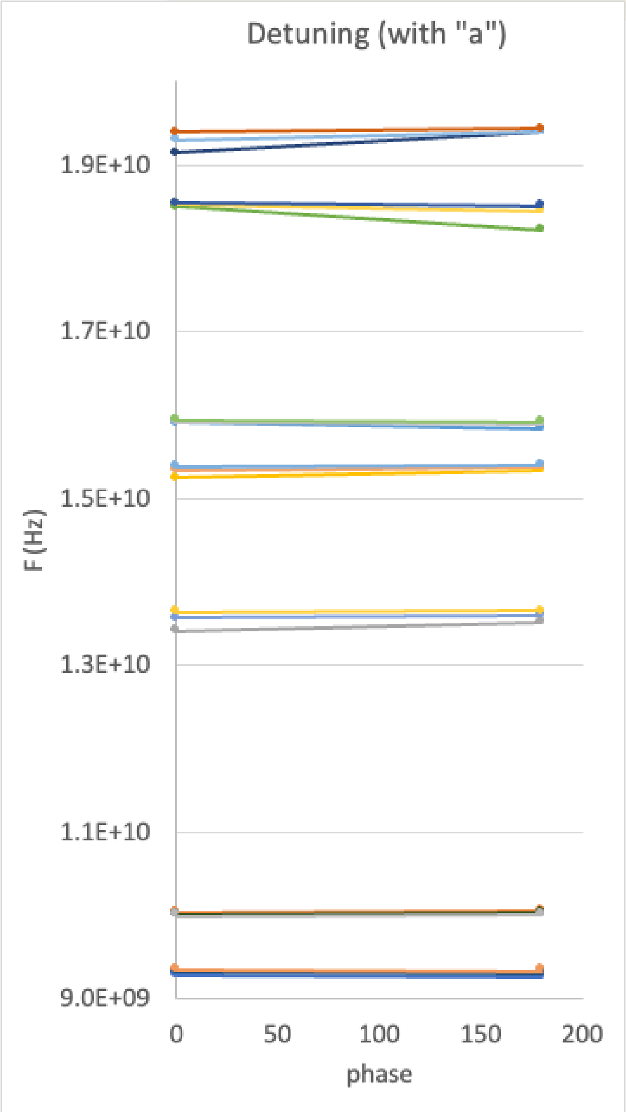

C-Band 135/deg Dipole detu

- Cell length: 19.682 mm
- Detuning using iris "thickness"

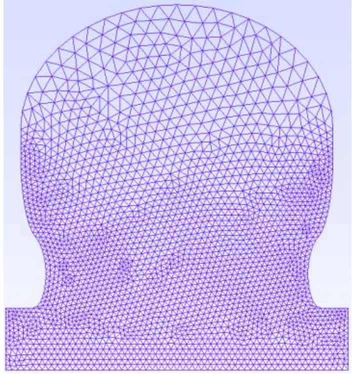

Gap1
R=113.67 Mohm/m

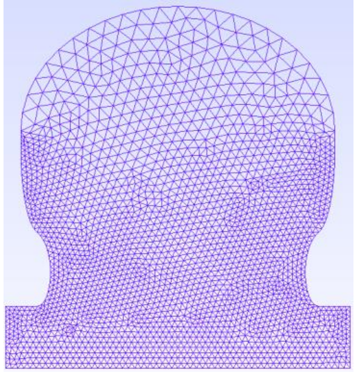

Gap1-0.5mm
R=114.32 Mohm/m

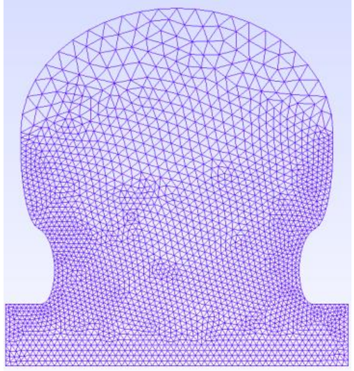

Gap1-1mm
R=114.38 Mohm/m

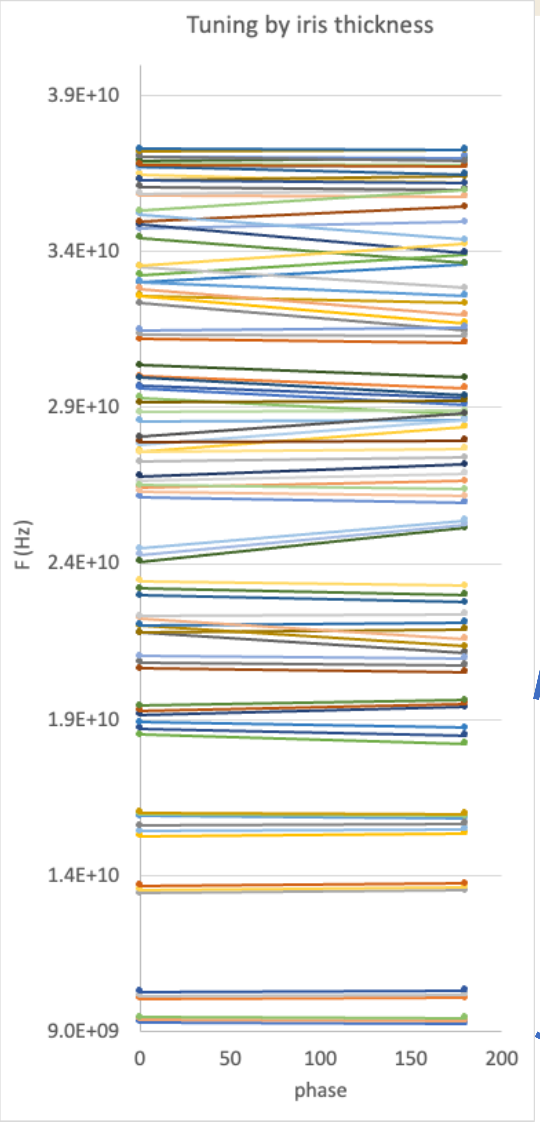

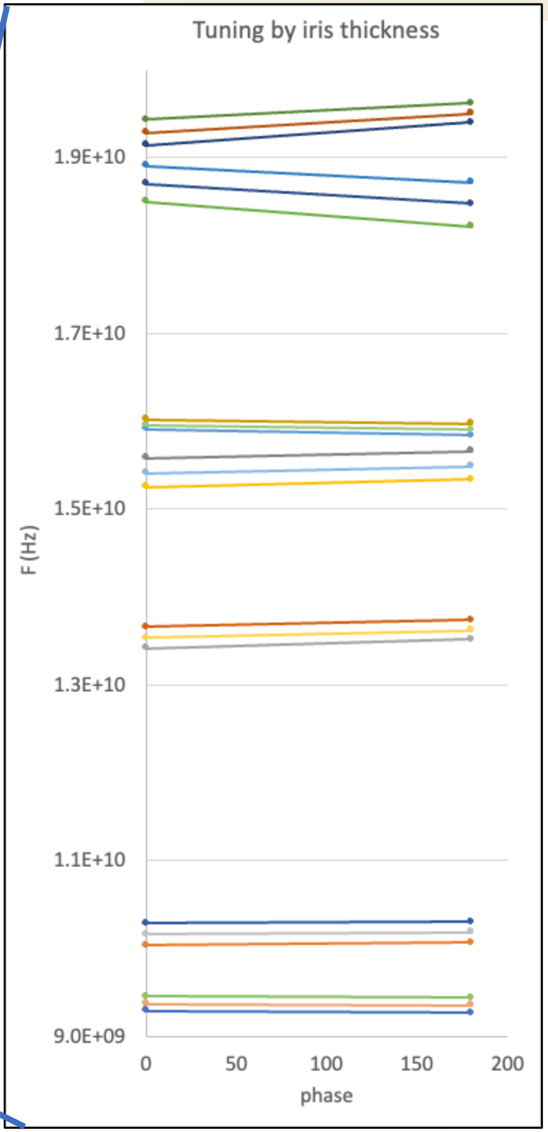

- Detuning effective
- Need to explore effect of profile details on different HOM bands

Gaussian Detuned Spectrum

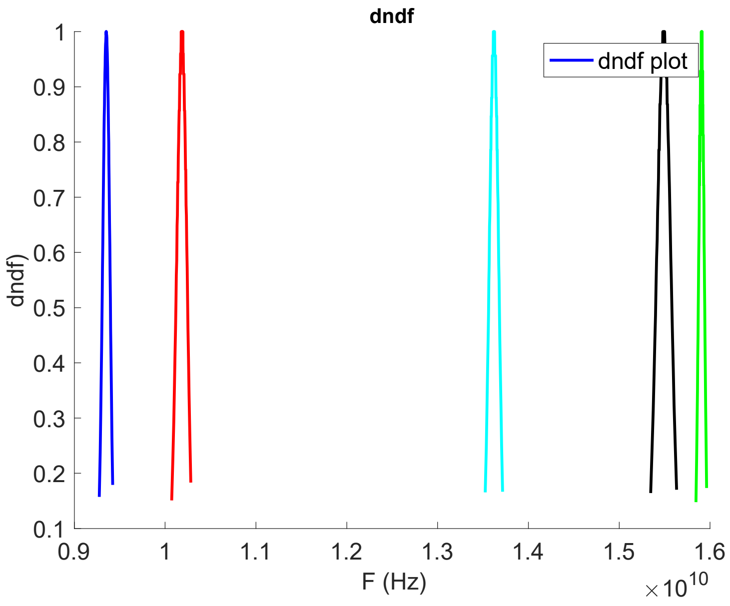

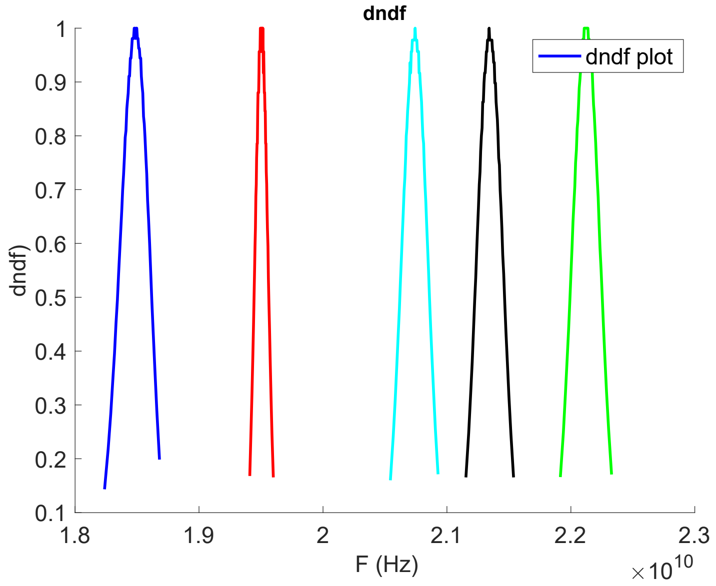

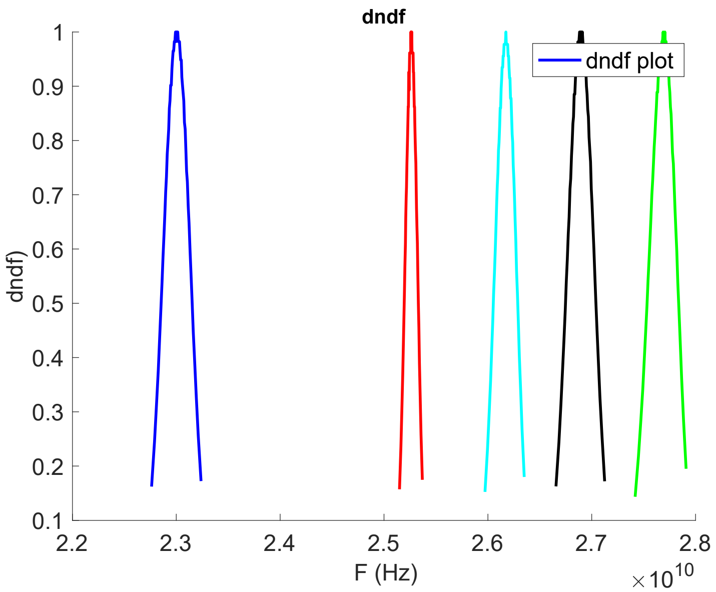

TE11 beam pipe cutoff

- A=3.55 mm
- Fc=24.74 GHz

56-Cell Structure Tapered HOM Mode

- Band 1 (9.3 GHz)

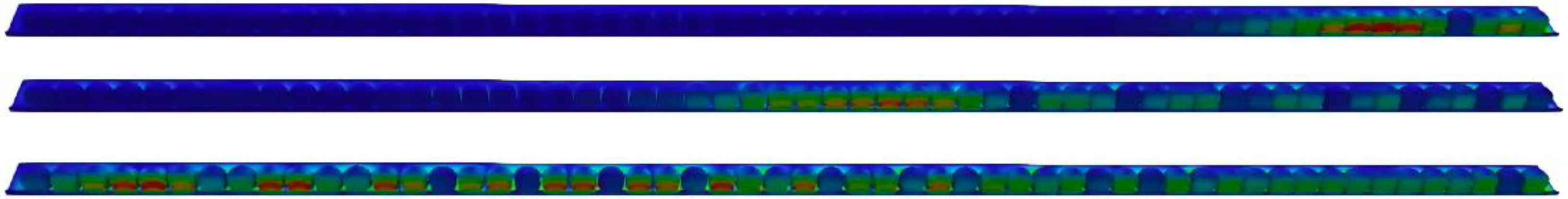

- Band 2 (10.0 GHz)

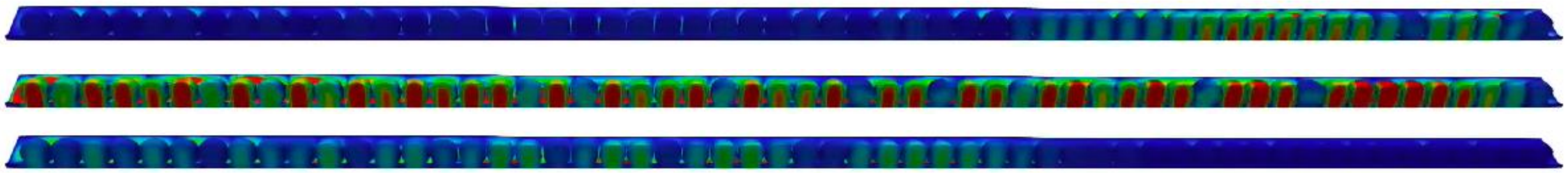

- Band 3 (13.6 GHz)

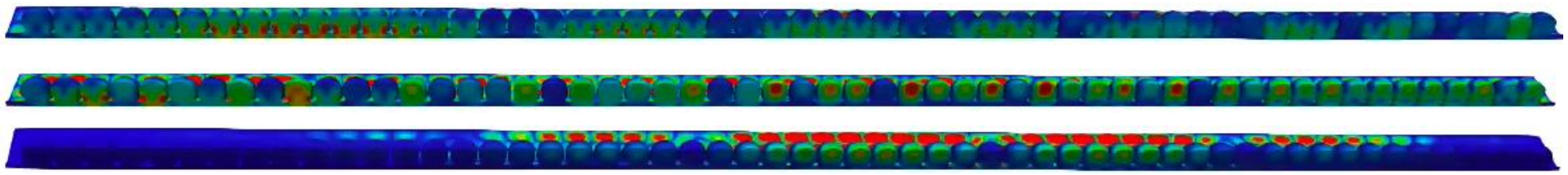

56-Cell Structure T

- Band 1 (9.3 GHz)

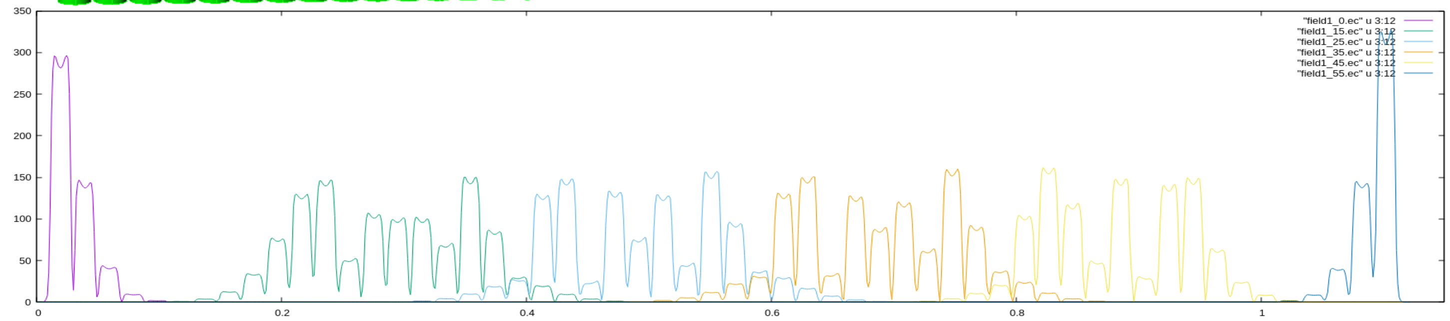

- Band 2 (10.0 GHz)

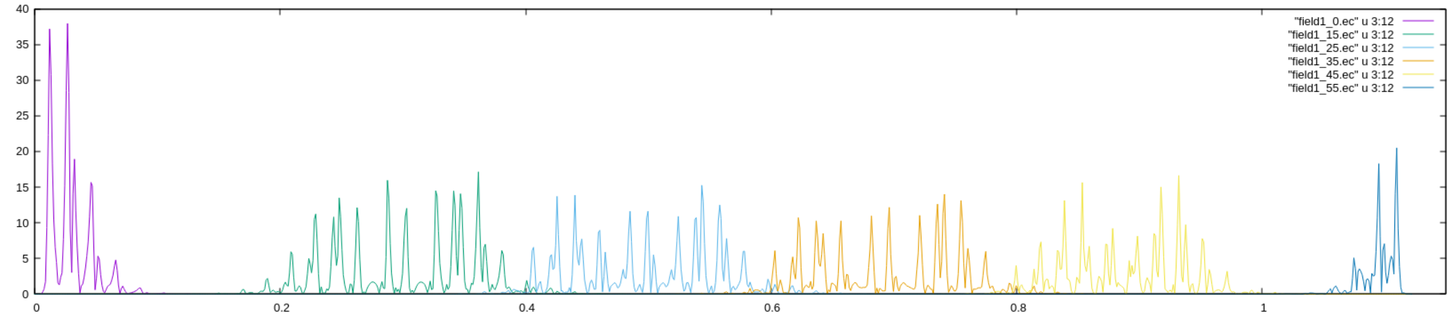

- Band 3 (13.6 GHz)

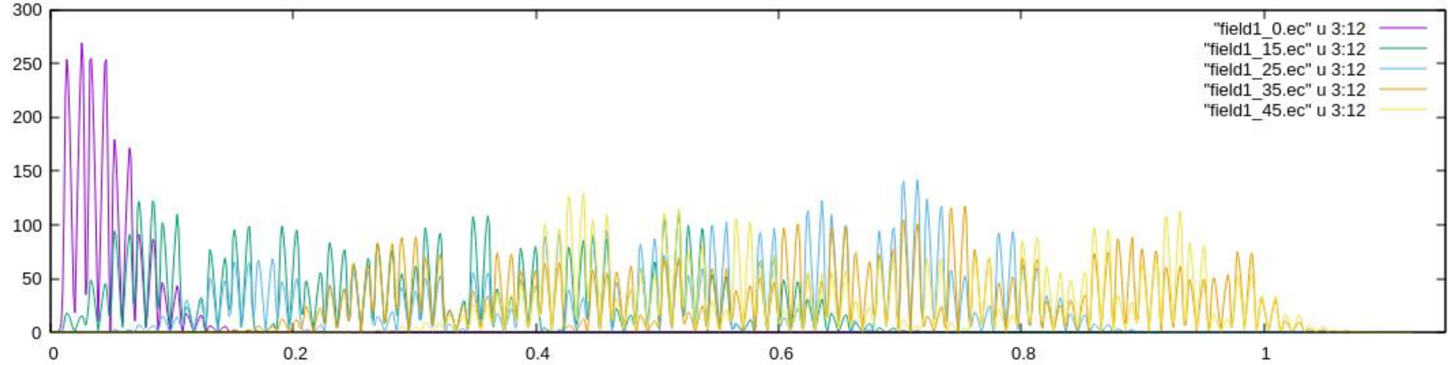

0.5mm slot
Conductivity on slot surface: 1e6

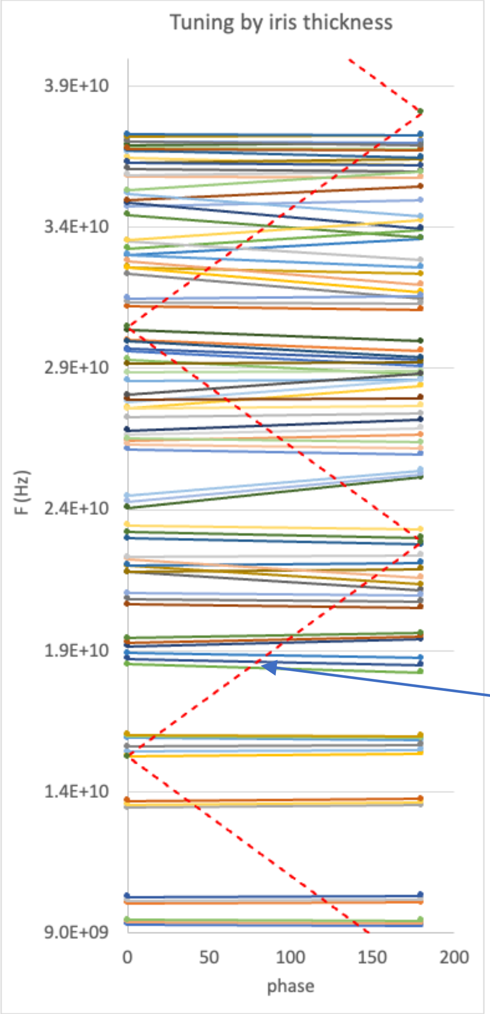

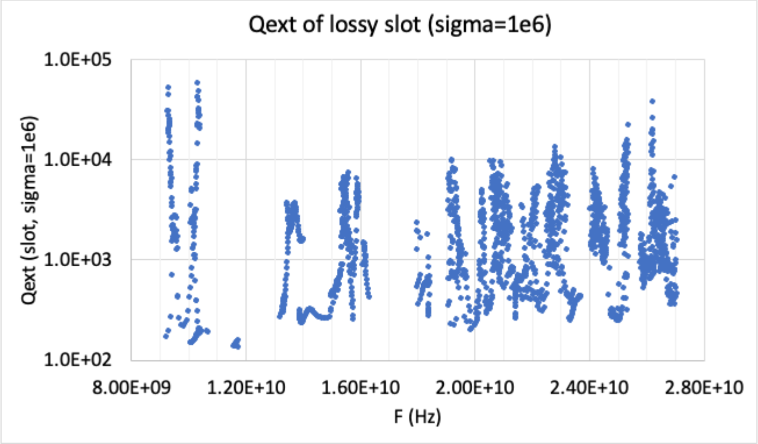

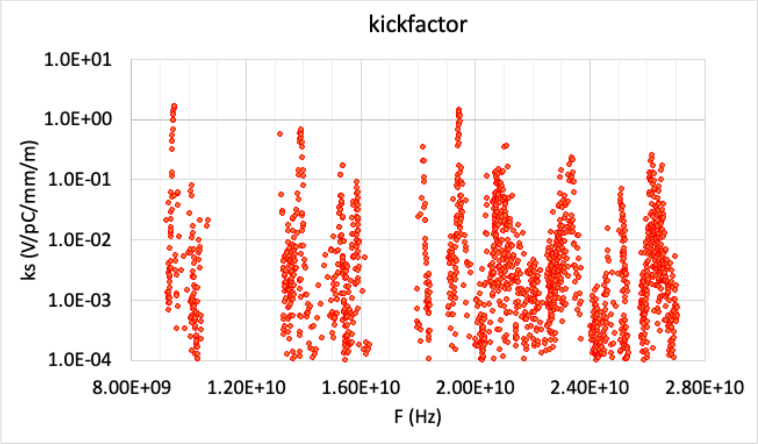

Mod synchronize with beam
interact stronger with beam

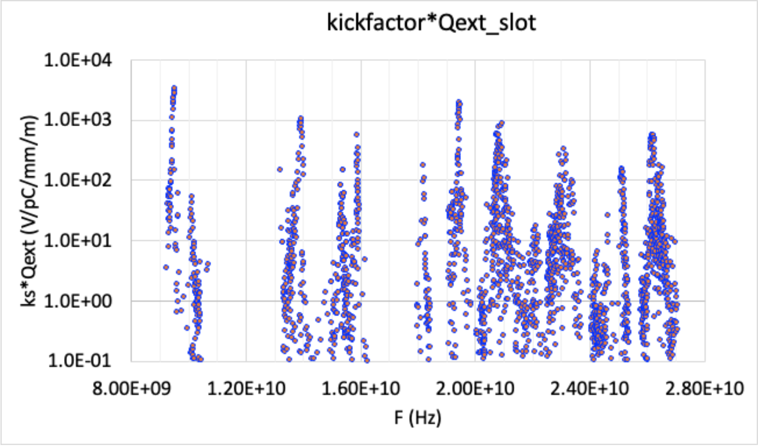

Using Tapered Slot Could Further Improve Damping

180 deg/cell Structure HOM Damping with Tapered Lossy Slot – Dongsung Kim

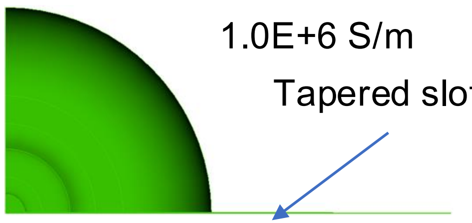

Slot surface conductivity (Ni-Cr)

1.0E+6 S/m

Tapered slot

Linear taper: slot height: from 300 micron to 100 micron

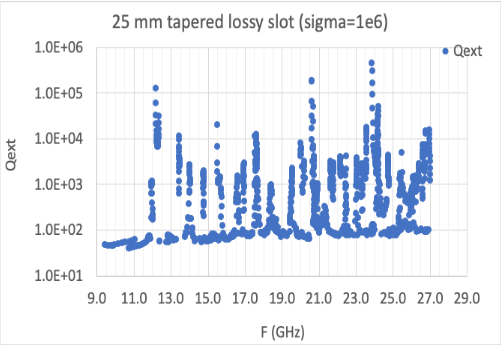

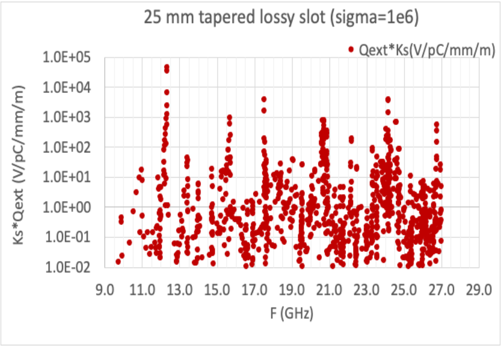

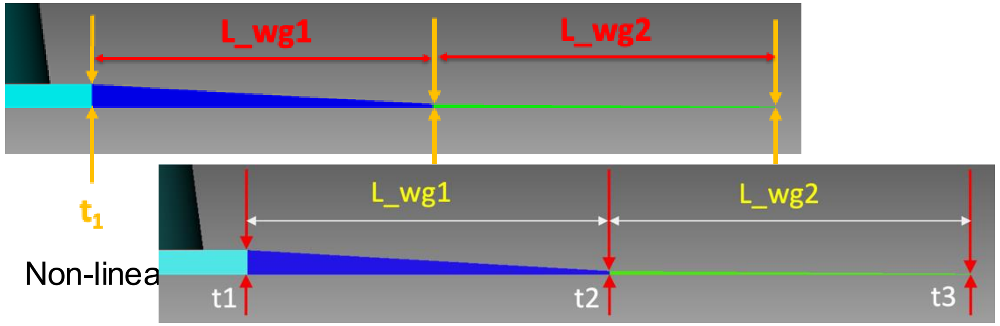

Non-linea

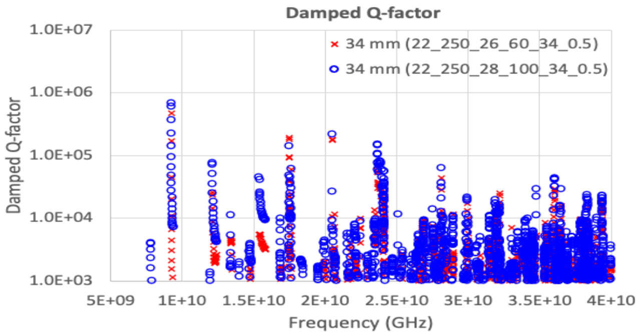

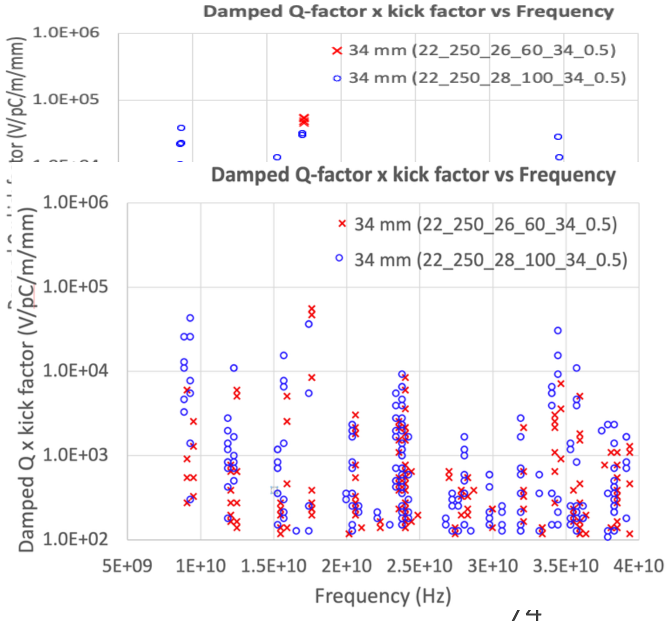

- Need understand more detail
  - Lossy materials at cold temperature (77K)
  - Coating or thin layers brazing on to structure

Compact RF pulse compression

Powering the FLASH-VHEE linac

Utilizing a commercial power source to ensure wider accessibility

Achieving necessary peak power through RF pulse compression

K200 Solid State Modulator System from ScandiNova

- 11.424 GHz
- Peak power 6 MW

	Unit	Klystron	
RF Peak Power	MW	6	
RF Average Power	KW	10	
Modulator Peak power	MW	20.1	
Modulator Average power	kW	49.5	
Operational Voltage range	kV	193	
Operational Current range (incl 10% mar	A	115	
PRF range (min/max)	Hz	1	400
Pulse length (top)	µs	0.1	4.0
Top flatness (dV)	< +/- %	1.00	
Rate of rise (min/max)	kV/µs	100	150
Amplitude stability	< +/- %	0.01	
Trig delay	µs	~1.2	
Pulse to Pulse time jitter	ns	<±5	
Pulse width time jitter	ns	<±8	

Single cavity spherical resonator design enabled pulse compression for up to 6-fold higher peak power

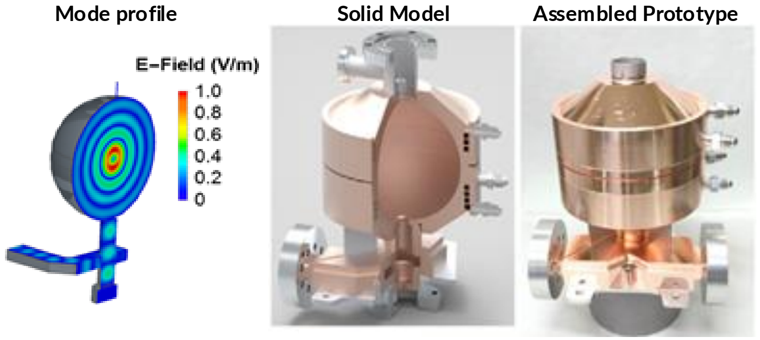

Franzi, M., Wang, J., Dolgashev, V., & Tantawi, S. (2016). Compact rf polarizer and its application to pulse compression systems. *Physical Review Accelerators and Beams*, 19(6), 062002.

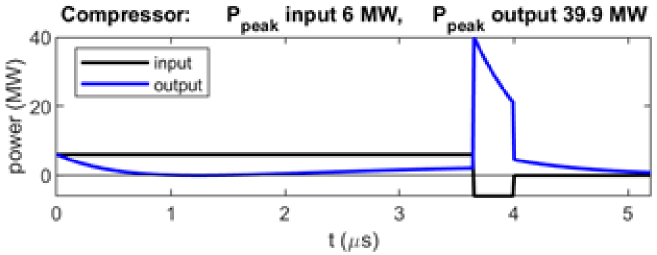

HE_{11} Corrugated Cylinder Circularly Polarized SLED

C. Nantista, Z. Li

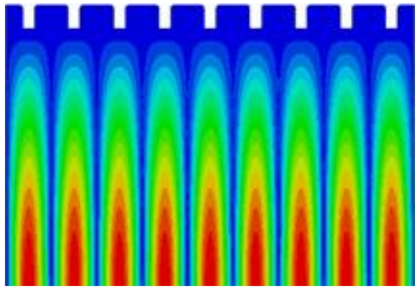

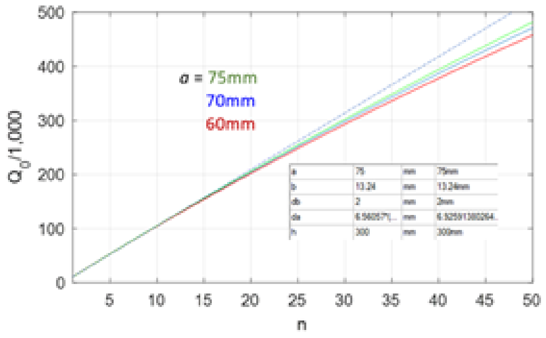

- nominal design has a diameter of 6.4509″ and L = 23.976″ (n = 46) promises a quality factor of Q0 = ~450,000
- Currently investigating optimal coupling

Broad Impact and Reach of Accelerator Physics

5G Telecommunications (AT&T)

ta consumption with mobile
vices continues to grow rapidly
ansformational opportunities: rural
edicine/
uc., emerg.
rvices,
art grid, IoT